UNIVERSITA' DEGLI STUDI DI MILANO-BICOCCA

Scuola di Dottorato di Scienze

Dottorato di Ricerca in Biotecnologie Industriali

XXVI Ciclo

Effects of methanol on the activity and structure of lipase enzymes

Francesco Sasso

Tutor: Prof.ssa Marina Lotti

Anno Accademico 2012/2013

Dottorato di Ricerca in Biotecnologie Industriali XXVI Ciclo

Dottorando: Francesco Sasso
Matricola: 715944

Tutor: Prof.ssa Marina Lotti
Coordinatore: Prof. Marco Vanoni

Università degli Studi di Milano-Bicocca
Piazza dell'Ateneo Nuovo, 1, 20126, Milano

Dipartimento di Biotecnologie e Bioscienze
Piazza della Scienza 2, 20126, Milano

Table of contents

Abstract

The search for alternative fuels has gained much attention because of the rapid depletion of fossil fuels, their rising prices and environmental concerns. Biodiesel, monoalkyl esters of vegetable oils or animal fats, is a potential substitute for petroleum-based diesel. It exhibits several advantages over diesel fuel such as low toxicity, high biodegradability, lower emission of particulate matter and its derivation from renewable energy sources. The process commonly used to produce commercial biodiesel is the chemical alkaline catalysis to convert vegetable oils or fats and methanol (MeOH) to fatty acid methyl esters (FAME). However, this process is energy consuming and produces high amount of alkaline waste water. This motivates the current interest toward biocatalysis. Among enzymes, lipases convert vegetable oils to FAME in highly selective reactions carried out in mild, environmentally-favorable conditions. Different lipases have been described suitable for biodiesel production. The enzymatic approaches have become more and more attractive but their industrial exploitation is impaired by relatively high costs, partly due to the short operational life of catalysts. A major cause of low lipases performance is the inhibition by methanol. Although many scientific publications proved that the activity of several free and immobilized lipases is severely affected by methanol, none of them addresses the causes of inactivation. These investigations focused on how to override the inhibition rather than to explain why inhibition occurs.

In the present work we investigated the molecular and kinetic effects of methanol on lipases already used or potentially applicable/interesting for the industrial production of biodiesel.

Firstly, we set up a novel method based on analytical Fourier Transform Infrared Spectroscopy (FTIR) to detect and quantify the total methyl esters and fatty acids present in complex mixtures. The FTIR approach allows to monitor simultaneously transesterification and hydrolysis reactions catalyzed by lipase

enzymes and exhibits several advantages over the traditional analytical methods: rapid, inexpensive, accurate, requiring very limited sample preparation and simple statistical analysis of the spectroscopic data. This method was validated through the comparison with data obtained by gas chromatography, a conventional technique commonly employed for the determination of methyl esters. Our FTIR method is based on the determination of the intensity of two different peaks, proportional to the total methyl ester and oleic acid amounts present in the mixture (**Paper I**).

The study of the inactivation effects exerted by methanol was carried out on two different lipases, the *Burkholderia glumae* lipase (BGL) and the *Candida antartica* lipase B (CALB), in two different reaction systems.

First of all we investigated the influence of methanol on the catalytic activity and conformation of BGL, a lipase known in literature to be tolerant to methanol. To this aim, 24-hours transesterification reactions of triolein and methanol, at 37°C and different oil:MeOH molar ratios, ranging from 1:1 up to 1:6, were carried out. MeOH is thus present from lower to higher amounts than required by the reaction stoichiometry (1:3). We found that the highest catalytic activity is reached in the presence of ~70% v/v MeOH, corresponding to a molar ratio 1:5, while for higher molar ratios the yield decreases dramatically. On the other hand, hydrolysis is proportional to the water content. In parallel, a structural study of the impact of MeOH on BGL structure and conformation was performed by means of mass spectrometry (MS), circular dichroism (CD), and intrinsic fluorescence spectroscopy. Under the conditions providing the highest reaction yield, we found that the enzyme stability is perturbed, leading to gradual protein unfolding and finally to aggregation (**Paper II**).

Morevorer, we investigated the effect of methanol and water activity on CALB, one of the most commonly employed lipases for the industrial production of biodiesel, mainly in its immobilized form (Novozym 435).

We obtained a model of the molecular mechanism of CALB deactivation exerted by methanol. Experimental data from the enzymatic alcoholysis

reaction of vinyl acetate (VA) by methanol in the presence of toluene were fitted to a kinetic model. Reactions at constant VA (15.2% v/v), methanol concentrations ranging from 0.7% up to 60% v/v and at three different water activity values (0.02, 0.05, 0.09) were performed. CALB shows the highest activity at MeOH concentrations as low as 0.7% followed by a sharp decrease at higher concentrations. For MeOH concentrations higher than 10% the activity was constant. Water activity does not influence the decrease of lipase activity induced by MeOH.

Experimental results were adapted to a kinetic model and combined to molecular dynamics simulations of CALB in toluene–methanol–water mixtures. Thus, a thermodynamic model of the lipase activity was established, which indicates that methanol acts as a competitive inhibitor of the enzyme (**Paper III**).

Riassunto

A causa del rapido esaurimento dei combustibili fossili, dell'aumento dei prezzi e dei problemi ambientali connessi al loro utilizzo, la ricerca di combustibili alternativi sta attirando un crescente interesse. Il biodiesel, una miscela di monoalchil esteri di oli vegetali o grassi animali, è un potenziale sostituto del gasolio ottenuto da petrolio. Esso, infatti, presenta diversi vantaggi rispetto al convenzionale combustibile diesel: bassa tossicità, alta biodegradabilità, minore emissione di particolato atmosferico, ottenimento da fonti di energia rinnovabili. La reazione di produzione del biodiesel è una transesterificazione di trigliceridi di origine vegetale o animale con alcoli a catena corta (metanolo o etanolo) e il processo comunemente impiegato è la catalisi chimica in condizioni alcaline. Questo processo, però, prevede un alto consumo energetico e produce una notevole quantità di acque di scarico alcaline che devono essere opportunamente trattate. Tali problematiche hanno spostato l'interesse verso la biocatalisi, che prevedere l'utilizzo di enzimi come catalizzatori di reazioni altamente selettive e condotte in condizioni blande e poco inquinanti. Le lipasi sono gli enzimi più adatti a catalizzare la transesterificazione di oli vegetali in esteri monoalchilici di acidi grassi a lunga catena. La stechiometria della reazione prevede l'utilizzo di metanolo (MeOH) in rapporto molare 3:1 rispetto all'olio. Il MeOH, però, è spesso causa dell'inattivazione del biocatalizzatore per motivi che non sono ancora compresi a fondo.

In questo lavoro sono stati studiati gli effetti prodotti dal metanolo su lipasi già impiegate o potenzialmente utilizzabili/di interesse per la produzione industriale di biodiesel.

Preliminarmente, è stato messo a punto e validato un nuovo metodo analitico di Spettroscopia a Infrarossi in Trasformata di Fourier (FTIR) per rilevare e quantificare la presenza di metil esteri ed acidi grassi in miscele di reazione complesse. Questo metodo, più semplice e rapido della più comune tecnica

di gas cromatografia (GC), è stato applicato per monitorare reazioni enzimatiche di transesterificazione e idrolisi in cui metil esteri ed acidi grassi sono prodotti/substrati di reazione. Il metodo si basa sulla rilevazione del picco a 1435 cm^{-1} in derivata seconda dello spettro FTIR, la cui intensità è direttamente proporzionale alla quantità di metil esteri. Al contempo è possibile monitorare l'idrolisi dei trigliceridi misurando l'assorbimento a 1709 cm^{-1}, lunghezza d'onda al quale assorbe l'acido oleico (**Paper I**).

L'indagine sugli effetti di inattivazione causati dal metanolo è stata realizzata su due diverse lipasi, da *Burkholderia glumae* (BGL) e *Candida antartica* (CALB), in due diversi sistemi di reazione.

Innanzitutto, è stata studiata l'influenza del metanolo sulla attività catalitica e sulla conformazione di BGL, enzima noto per essere tollerante al metanolo. Sono state allestite miscele di reazione a diversi rapporti molari trioleina:MeOH (da 1:1 a 1:6), in cui MeOH è presente in quantità sia maggiore che inferiore rispetto alla stechiometria 1:3 richiesta dalla reazione. Il massimo di attività catalitica è stato rilevato in presenza di ~70% di metanolo, corrispondente ad un rapporto molare trioleina:MeOH 1:5, mentre per rapporti molari superiori la resa cala drasticamente. L'idrolisi, invece, è risultata proporzionale al contenuto di acqua presente nella miscela di reazione.

Parallelamente, è stata condotta una indagine sull'impatto del metanolo su struttura e conformazione dell'enzima. In particolare, è stata analizzata la struttura secondaria e terziaria di BGL in presenza di concentrazioni variabili di alcool utilizzando le tecniche di spettrometria di massa, spettroscopia di dicroismo circolare e fluorescenza intrinseca. Nel saggio di transesterificazione, nelle condizioni in cui BGL esprime il massimo di attività catalitica, ovvero in presenza del 50-70% di alcool in fase acquosa, il MeOH stesso influenza la stabilità dell'enzima provocandone una graduale denaturazione e successiva aggregazione (**Paper II**).

Infine, è stato razionalizzato l'effetto del metanolo e il ruolo dell'attività dell'acqua sulla attività catalitica di CALB. Questo enzima è uno dei più

impiegati nella produzione industriale di biodiesel, principalmente nella forma immobilizzata (Novozyme 435).

E' stato proposto un meccanismo molecolare dell'inattivazione da metanolo applicando i dati sperimentali ad un modello cinetico ed effettuando simulazioni di dinamica molecolare. Le condizioni sperimentali più adeguate a quelle simulate con metodi computazionali corrispondono ad una reazione di metanolisi di vinilacetato (VA) che produce metilacetato e vinil alcool. Le reazioni sono state realizzate a VA costante, con un range di concentrazione di MeOH da 0.7% a 60% v/v, a tre diversi valori di attività dell'acqua (a_w): 0.02, 0.05 e 0.09. Per ciascuna a_w saggiata, la velocità iniziale di CALB è massima alla più bassa concentrazione di MeOH impiegata, diminuisce drasticamente all'aumentare del MeOH, e si mantiene costante a concentrazioni di alcool superiori al 10%. E' emerso, invece, che l'attività dell'acqua non ha effetto sulla diminuzione di attività catalitica indotta da MeOH.

Questi risultati sperimentali sono stati adattati ad un modello cinetico e combinati alle simulazioni di CALB in miscele ternarie toluene/MeOH/VA. Ne è stato ottenuto un modello termodinamico del comportamento di CALB da cui emerge che il MeOH agisce sull'enzima come un inibitore competitivo (**Paper III**).

1. Introduction

1.1 Definition and relevance of biodiesel

Biodiesel is defined as a mixture of mono alkyl esters of long-chain fatty acids (FAAE) derived from vegetable oils or animal fats, for use in compression–ignition (diesel) engines. This specification refers to pure (100%) biodiesel and not to blends with other diesel fuels (US National Biodiesel Board, 2008). Its energy content and the physical and chemical properties are similar to conventional diesel fuel, allowing its use either on its own or mixed with conventional diesel in any diesel engine, without requiring any modifications either to the ignition system or to the fuel injector. Indeed, to date biodiesel is the only alternative fuel directly suitable to the use in existing engines. In addition, it possesses better lubricant properties which enhance engine yield and extend engine life (Vasudevan and Briggs, 2008). Biodiesel can be pumped, stored and handled using the same infrastructures, devices and procedures usually employed for conventional diesel fuel. In fact, as biodiesel does not produce explosive vapors and has a relatively high flash point (close to 150 °C), transportation, handling and storage are safer than with conventional diesel (Al-Zuhair, 2007).

In recent years there has been increasing interest in developing biodiesel as an alternative to fossil fuels, mainly in the automotive sector, because of its compatibility with current available engines. This interest is due to the following reasons:

(1) Environmental concerns related to climate change and the reduction of contaminant emissions. Major advantages of using biodiesel are: (a) it is a quasi-neutral fuel with respect to CO_2, since the only emissions are those previously fixed by photosynthesis; (b) it does contain smaller amount of the major atmospheric contaminants presents in conventional diesel, such as: particles in suspension, CO, polycyclic aromatic hydrocarbons, unburned

hydrocarbons and especially sulphur, SOx (Korbitz, 1999); (c) it is highly biodegradable and only slightly toxic in soils or aquatic environments (Lapinskiené *et al*., 2006); (d) biodiesel can be produced by recycling waste vegetable oils (i.e. frying–kitchen oils or refinery processed oils), allowing a valorization of these residues.

(2) The rise in fossil fuel prices. According to calculations, locally produced biofuels are not feasible without any subsidy. However, steadily rising oil prices over USA $80/barrel suggest that biofuels may be economically viable in the medium term (Henniges and Zeddies, 2006). Nowadays, prices are around $100/barrel. In addition, other factors favoring feasibility are: (a) tax rules based on an international agreement for environmental protection. Tax rules include differential rates depending on the oilseed used, where they are grown, and whether they are produced by large agribusiness or family farmers; (b) the optimization and genetic improvement of certain oleaginous plants (Akoh *et al*., 2007), or microalgae with high lipid contents (Xu *et al*., 2006; Li *et al*., 2007; Haag, 2007; Chisti, 2007, 2008); (c) the development of more efficient processes in the production, recovery and purification of biodiesel, especially those based on green alternatives (i.e. substrates and catalysts fermented from renewable sources, making the biodiesel production fully environmental friendly) such as enzymatic biodiesel.

(3) The diversification of energy sources to guarantee supply, especially in the European countries that barely dispose of fossil fuel sources. The renewable features of biodiesel refers to the fact it can be produced indefinitely, while current fossil fuel reserves will be exhausted in decades at current consumption rates (Vasudevan and Briggs, 2008).

(4) The need for a market for agricultural production surpluses (soybean in the U.S, rapeseed oil or sunflower oils in EU). Biofuels create added value and provide employment in rural areas (Henniges and Zeddies, 2006).

The European Union has arguably been the global leader in biodiesel production. Biodiesel production in the United States also increased dramatically in the past few years. A rapid expansion in production capacity is

being observed not only in developed countries such as Germany, Italy, France, the United States but also in developing countries such as China, Brazil, Argentina, Indonesia, and Malaysia.

The global biodiesel market is estimated to reach 37 billion gal by 2016, growing at an average annual rate of 42%. Europe will continue as the major biodiesel market for the next decade or so, closely followed by the US market (Sims 2007).

1.2 Analytical methods to quantify FAME

There are many analytical methods which are employed for biodiesel analysis and for the quantification of FAME in complex mixtures. The most common ones are: gas chromatography with flame ionization detector (GC-FID) (Knothe, 2006; Freedman *et al*., 1986), gas chromatography with mass spectrometry detector (GC-MS) (Mittelbach, 1993), high pressure liquid chromatography (HPLC) with UV, atmospheric pressure chemical ionization (APCI detectors) or evaporative light-scattering detector (ELSD detectors) (Holcapek *et al*., 1999), gel-permeation chromatography (GPC) (Darnoko *et al*., 2000), size-exclusion chromatography (SEC) (Arzamendi *et al*., 2006), thin-layer chromatography (TLC) (Cvengros and Cvengrosova, 1999), near-infrared spectroscopy (NIR) (Knothe, 1999), nuclear magnetic resonance (NMR) (Gelbard *et al*., 1995), viscosimetry (De Filippis *et al*., 1995), and Fourier transform infrared spectroscopy (FTIR). All these methods have drawbacks, which hinder their practical use, such as in the biodiesel manufacturing plant. For example, GC is a very good method to determine the compositions of biodiesel, monoglycerides, diglycerides, and triglycerides. However, it requires several sample processing steps, such as derivatization, and the use of reagents such as N,O-bis(trimethyisilyl)trifluoroacetamide (BSTFA) and N-methyl-N-trimethylsilyltrifluoroacetamide (MSTFA). Also, the use of an internal standard is needed to obtain accurate results in the case of GC, GC-MS, and HPLC. The

time required for analysis is quite long in most cases, and the method is sample-destructive. Similarly for HPLC analysis, costly chemical reagents are required for separation of sample compounds. HPLC also involves the use of very sophisticated and costly detectors, such as APCI, MS, and ELSD. Thin layer chromatography (TLC) is a cheap analytical technique but is not reliable. Its accuracy is low, and also, it is sensitive to humidity. NMR is a very good technique for biodiesel analysis, but again, it is a very costly instrumentation to use and maintain on a daily basis in a production or blending unit. Recently, methods based on infrared (IR) spectroscopy in the mid- and near-IR spectral regions have been developed; however, they require complex statistical analysis of the spectroscopic data (Monteiro *et al*., 2008; Zagonel *et al*., 2004; Richard *et al*., 2011). In addition to these limitations, skilled and costly labor is required to apply these techniques. Hence, their wide use in biodiesel plants units is a point of concern for manufacturers and distributors.

1.3 Chemical *versus* enzymatic transesterification approach

The direct usage of vegetable oils as biofuel in diesel engines is not technically possible because of their: (i) high viscosity; (ii) low stability against oxidation (and the subsequent reactions of polymerization), and (iii) low volatility, with formation of a relatively high amount of ashes due to incomplete combustion. Therefore, vegetable oils must be processed so as to acquire the properties necessary to be directly used in current diesel engines. The possible processes are pyrolysis (or cracking), microemulsion and transesterification (Ma and Hanna, 1999). As the first two are cost intensive processes and yield a low quality biodiesel, the most usual method to transform oil into biodiesel is transesterification. This consists of the reaction between triacylglycerols (contained in the oils) and an acyl acceptor. The acyl-group acceptor may be a carboxylic acid (acidolysis), an alcohol (alcoholysis) or another ester (interesterification). Only alcoholysis and interesterification are of interest to

produce biodiesel. Moreover, FAAE can be obtained also by esterification of fatty acids with alcohols (**Figure 1**).

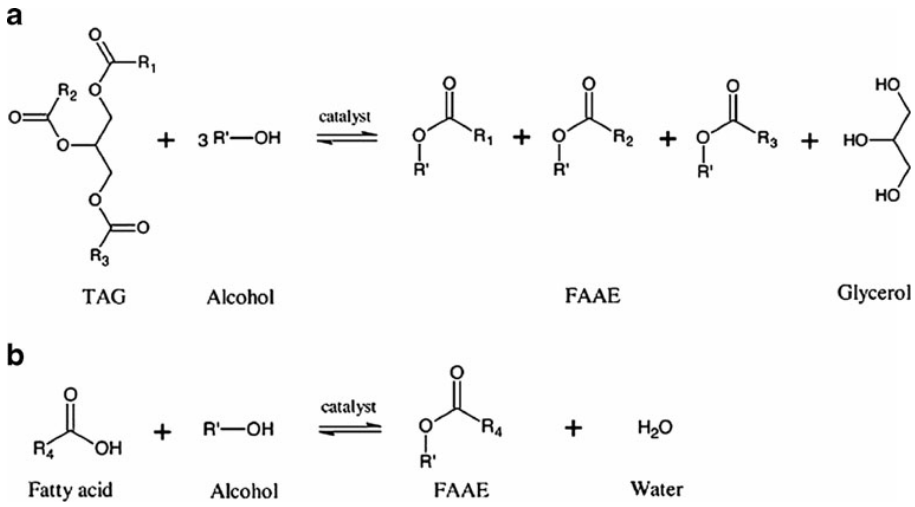

Figure 1. Synthesis of FAAE. **a)** Transesterification of TAG and short-chain alcohols leading to FAAE and glycerol. **b)** Esterification of fatty acid and short-chain alcohol leading to FAAE and water R_{1-4} acyl residues, R alcohol moiety ($R=CH_3$ for methanol; $R=CH_2CH_3$ for ethanol). From (Zhang *et al*., 2012).

Alcohols are the most frequently used acyl-acceptors, particularly methanol and, to a lower extent, ethanol (EtOH). Other alcohols can be used, e.g. propanol, butanol, isopropanol, tert-butanol, branched alcohols and octanol, but the cost is much higher. Regarding the choice between methanol and ethanol, the former is cheaper, more reactive and the fatty acid methyl esters are more volatile than those of the fatty acid ethyl esters (FAEE). However, ethanol is less toxic and it can be considered more renewable because it can be easily produced from renewable sources by fermentation. In contrast, methanol is mainly produced from non-renewable fossil sources, such as natural gas. Regarding their characteristics as fuels, FAME and FAEE show slight

differences; for example, FAEE have slightly higher viscosities and slightly lower cloud and pour points than the corresponding FAME (Bozbas, 2008).

The transesterification of triacylglycerols can be carried out by different catalytic processes (Marchetti *et al*., 2007; Demirbas, 2008), or in supercritical conditions (Demirbas, 2007). The catalyst used may be classified as: (1) alkaline catalyst (sodium hydroxide, potassium hydroxide, sodium methoxide); (2) acid catalyst (sulphuric acid, phosphoric acid, hydrochloric acid, sulfonic acid); (3) enzymatic catalyst (lipases); (4) inorganic heterogeneous catalyst (solid phase catalyst).

In the alkaline process sodium hydroxide or potassium hydroxide is used as a catalyst and methanol (or ethanol) as acyl acceptor. Initially, during the process, alcoxy is formed by reaction of the catalyst with alcohol and the alcoxy is then reacted with any vegetable oil to form biodiesel and glycerol. Due to its density, glycerol settles at the bottom and biodiesel can be decanted. This is the most efficient and least corrosive process; moreover the reaction rate is reasonably high, even at low temperature (60 °C) and using a stoichiometric excess of alcohol. The risk of free acid or water contamination and soap formation makes the separation process difficult (Ma and Hanna, 1999; Fukuda *et al*., 2001; Barnwal and Sharma, 2005). The second conventional way of producing biodiesel is using an acidic catalyst. Any mineral acid can be used to catalyze the process; the most commonly used acids are sulphuric acid and sulfonic acid. Although yield is high, the acids, being corrosive, may damage the equipment and the reaction rate was also observed to be low (Freedman *et al*., 1984).

Nowadays, the most common industrial approach is alkaline transesterification, where raw material with a high water or FFA content needs pretreatment with an acidic catalyst in order to esterify FFA (Freedman *et al*., 1984; Kaieda *et al*., 1999; Zhang *et al*., 2003). Pretreatment is necessary to reduce soap formation during the reaction and to simplify the extensive handling for separation of biodiesel and glycerol, together with removal of catalyst from alkaline wastewater (Meher *et al*., 2006; Mittelbach, 1990). The amount of wastewater

from a traditional biodiesel plant is around 0.2 ton per ton biodiesel produced (Suehara *et al*., 2005). Therefore, wastewater treatment represents an economical and environmental concern.

Contrary to the inorganic catalysts, biochemical catalysts, i.e. enzymes, developed quickly in the past decade. The advantages of biochemical catalysis are: (a) milder conditions, implying less energy consumption; (b) flexibility in the choice of feedstocks, including waste oils with a high acidity; (c) easy separation of immobilized enzymes from the reaction mixture; (d) lower pollution emission and environment-friendly process (Shah *et al*., 2004; Nelson *et al*., 1996; Kumari *et al*., 2007). Moreover, contrary to alkaline catalysts, enzymes do not form soaps and can esterify both FFA and TAGs in one step, without the need of a subsequent washing step. Thus, enzymes are an interesting resource for industrial-scale production, since they can reduce production costs. This is especially the case when using materials with high FFA content, such as rice bran oil (Lai *et al*., 2005), inedible *Madhuca indica* oil (Kumari *et al*., 2007) or second-generation raw materials, like spent oils, animal fat and similar waste fractions.

Figure 2 and **Figure 3** compare the difference in downstream operation required for alkaline and enzymatic processes.

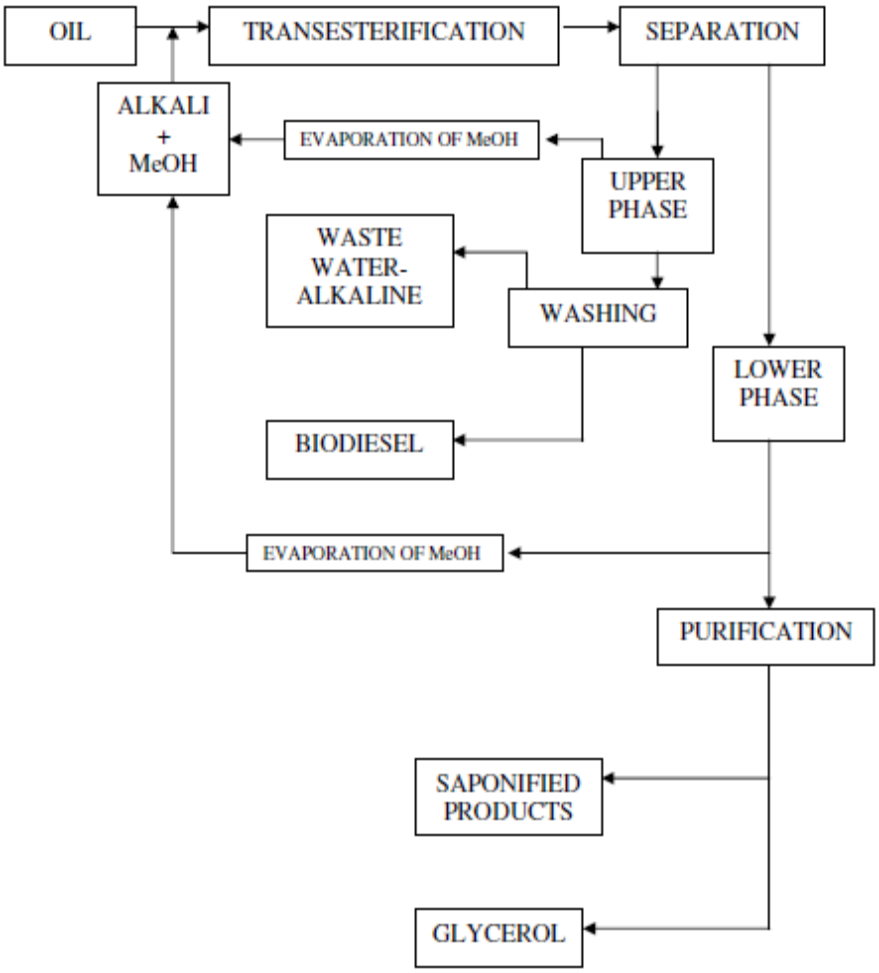

Figure 2. Production of biodiesel by alkali process. From (Ranganathan *et al*., 2008).

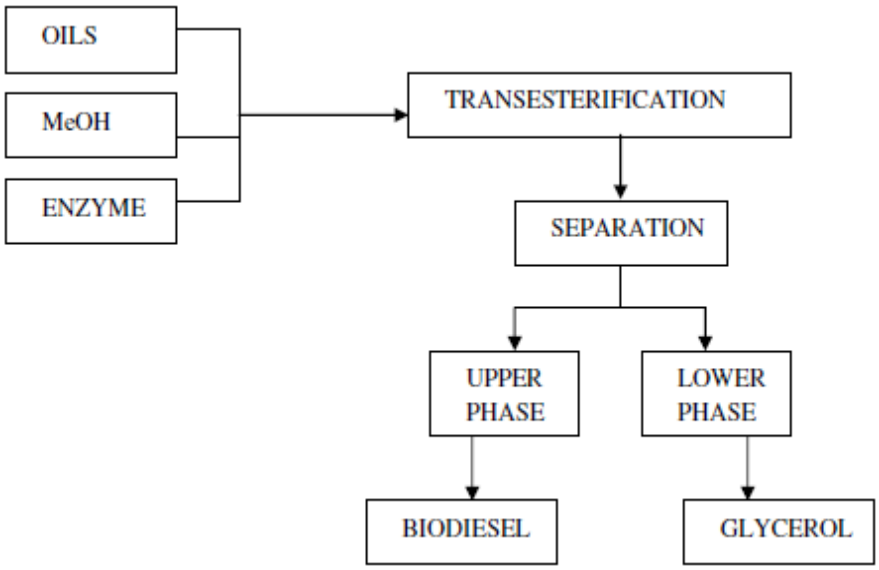

Figure 3. Enzymatic production of biodiesel. From (Ranganathan *et al*., 2008).

Enzymatic technology for biodiesel production has recently started to be applied at the industrial scale. Recently, in China was established the first industrial-scale plant employing lipase as the catalyst for the production of 20,000 t/year of biodiesel (Du *et al*., 2008). Although this approach is promising and is gaining more attention in biodiesel production, there are several drawbacks:

- low reaction rate (Zhang *et al*., 2003);
- enzyme inactivation due to methanol (Chen and Wu, 2003; Salis *et al*., 2005; Shimada *et al*., 1999);
- cost of catalysts (1,000 US$ per kg compared to 0.62 US$ for sodium hydroxide) (Fukuda *et al*., 2001; Haas *et al*., 2006; Jaeger and Eggert, 2002; Ma and Hanna, 1999; Meher *et al*., 2006; Shimada *et al*., 1999);
- loss of activity, typically within 100 days of operation.

These are the key issues to be addressed to make feasible the use of lipases for the industrial production of biodiesel.

1.4 Molecular mechanism of lipase-catalyzed transesterification

Though lipases differ widely in their primary sequences, their active site is conserved and built up by the three amino acids serine, aspartate and histidine, which form the catalytic triad. The three-dimensional structure of all lipases follow a common motif, the α/β-fold of hydrolases, that in lipases consist of eight mostly parallel β-sheets surrounded on both sides by α-helices (Bornscheuer and Kazlauskas, 1999). The triad and several oxyanion-stabilizing residues are thought to compose the active center of lipases. In most lipases, a short α-helical segment, termed "lid", shields the active site and is responsible for the phenomenon of "interfacial activation" that occurs upon interaction of the enzyme with the lipid-water interface (Verger, 1997). The lid interacts directly with substrate molecules and is therefore important also for substrate specificity.

Figure 4 shows the molecular mechanism of the lipase-catalyzed transesterifaction reaction which involves the catalytic triad.

The histidine residue attracts the hydrogen atom of the hydroxyl group of serine building an oxygen anion. The latter attacks a carbonyl atom of TAG resulting in the tetrahedron intermediate I. The proton of histidine is transferred to the separating diacylglycerides (DAG), yielding an acyl enzyme intermediate. After that, the serine ester interacts with the alcohol molecule. First, the nitrogen atom of the histidine attracts the hydrogen atom of the alcohol producing an alkoxide anion ($R\text{-}O^-$). Then, this alkoxide anion attacks the carbonyl carbon atom of the serine ester yielding the tertrahedron intermediate II. In the last step, the FAAE molecule and the free enzyme are released (Al-Zuhair 2007; Röttig *et al*., 2010).

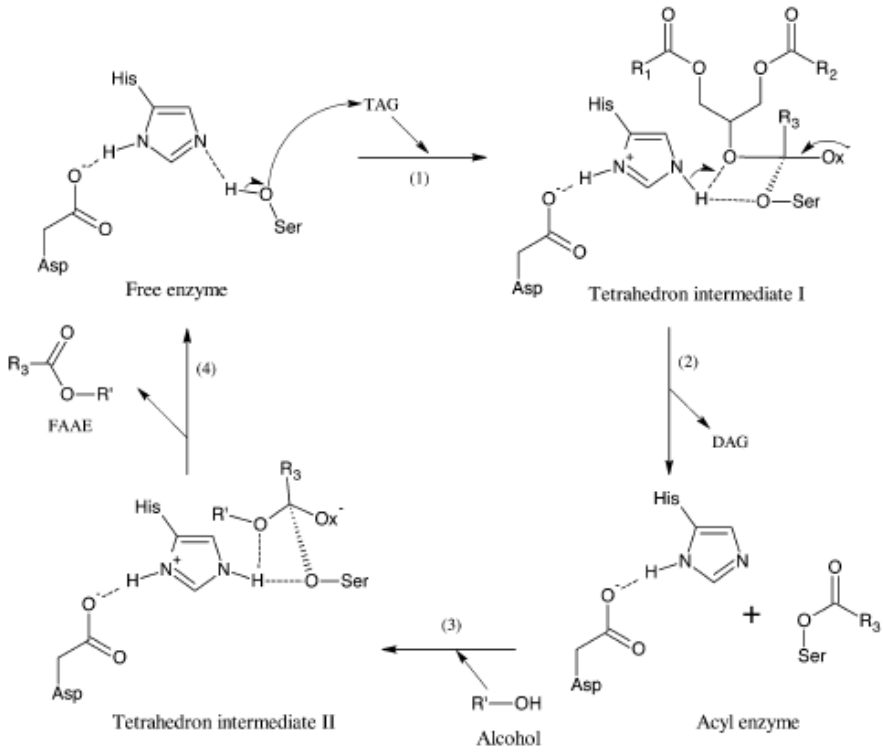

Figure 4. Mechanism of lipase catalyzed-transesterification. R_1– R_3 long-chain acyl moieties, R' short-chain alkyl moiety of the alcohol, His histidine, Ser serine, Asp aspartic acid, Ox oxygen atom. From (Röttig *et al*., 2010).

1.5 Transesterification with lipases: key factors

Crucial factors affecting productivity of enzymatic biodiesel synthesis are shown in **Figure 5**. To achieve the economic viability, the suitable raw materials and lipase preparation have to be chosen. The biocatalyst can be modified to improve stability and catalytic efficiency. These steps are followed by selection of organic solvent, optimization of molar substrates ratio, temperature, water activity, pH of enzyme microenvironment (the so named subparameters).

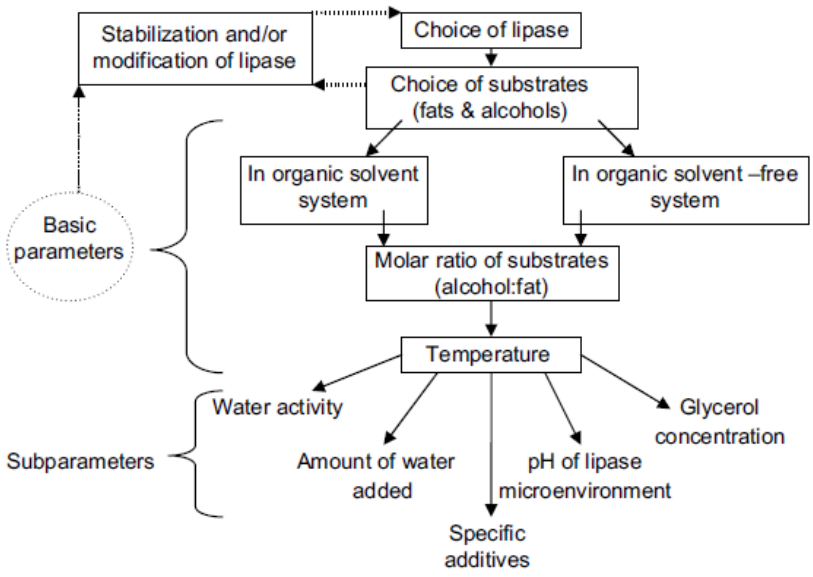

Figure 5. Crucial parameters affecting the yield of enzymatic synthesis of biodiesel. From (Antczak *et al*., 2009).

1.5.1 Starting oils

Biodiesel is produced by methanolysis (for FAME) of the oils and fats from various origin. Theoretically, any form of oils and fats from animals, plants or even microorganisms can be used as feedstock for biodiesel production. Currently the main feedstock are classified into three categories: (1) oil from plants, such as soybean (Lv *et al*., 2008; Silva *et al*., 2007), jatropha (Shah *et al*., 2004; Tamalampudi *et al*., 2008), palm (Halim *et al*., 2009; Sim *et al*., 2009; Talukder *et al*., 2006), cottonseed, sunflower etc (Dizge *et al*., 2009a,b; Soumanou and Bornscheuer, 2003; Wu *et al*., 2007); (2) animal fat, such as tallow (Da Cunha *et al*., 2009), lard and grease etc. (Lee *et al*., 2002; Ngo *et al*., 2008) and (3) waste cooking and industrial oil (Dizge *et al*., 2009a,b; Lara Pizarro and Park, 2003). Every country develops biodiesel feedstock according to its national conditions (Min and Zhang, 2006). The United States mainly use genetically modified soybean oil as raw material, while the European Union

and Canada use rapeseed oil. Some South-eastern Asian countries such as Malaysia and Indonesia produce biodiesel from palm oil. Although China is a large agriculture country, the food supply system is still a big problem. In order to follow the principle of never competing with grain land, China's recent production is based on waste cooking oil. Jatropha oil will become another choice for China due to some unique advantages. In fact, Jatropha tree can grow on waste land with a minimum water and fertilizer demand, and the oil is non-edible because of the presence of some antinutritional factors such as toxic phorbol esters (Jegannathan *et al*., 2008; Shah *et al*., 2004). Other non-food oil sources such as micro-algae oil and microbial oil also have significant potential since they have short production cycles and can be produced by fermentation using inexpensive sources, such as CO_2 or waste water (Um and Kim, 2009; Xue *et al*., 2006, 2008).

1.5.2 Choice of lipase

Lipases for biodiesel production from TAG should be non-regio-specific, so that all tri-, di- and mono-glycerides can be converted to FAAE.

In terms of regioselectivity, i.e. the position of scissile ester linkage, lipases have been divided into three types:

- sn-1,3-specific (hydrolyze ester bonds in positions R_1 or R_3 of TAG);
- sn-2-specific (hydrolyze ester bond in position R_2 of TAG);
- nonspecific (do not distinguish between positions of ester bonds to be cleaved).

Substrate specificity of lipases consists in their ability to distinguish structural features such as the length of acyl chains, the number, position, and configuration of double bonds, the presence of branched groups, as well as the nature of the acyl source: free acid, alkyl ester, glycerol ester, etc (Marangoni, 2002). In reactions of triacylglycerols and alcohols, lipases distinguish the length and type of FA contained in TAG and the length of

alcohol. For instance, *Burkholderia glumae* lipase shows a significant preference towards long chain fatty acids and, for chains with the same length, towards saturated ones (Aires-Barros *et al*., 1994).
Lipases from bacteria and fungi are the most commonly used for transesterification of TAG. In general, the best performing enzymes are able to attain conversions above 90%, while reaction temperatures vary between 30 and 50 °C. Reaction time also varies greatly: for example, from a minimum of 8 hours for immobilized *Pseudomonas cepacia* lipase transesterifying Jatropha oil with ethanol to 90 h for the same free enzyme transesterifying soybean oil with methanol.

1.5.3 Free *versus* immobilized lipases

Most industrial processes use immobilized enzymes since they are more stable than free ones and can be used repeatedly without complex separation procedures. Immobilization of an enzyme on a carrier increases the enzyme stability towards temperature, chemicals and allows ease handling and recovery of the enzyme. There are different methods of enzyme immobilization: adsorption, entrapment, cross-linking, microencapsulation, covalent binding (**Figure 6**). The most common carriers for lipase immobilization are kaolinite, fiber cloth, hydrotalcite, macroporous resins, silica gel. The main drawbacks of immobilization are the internal and external mass transfer limitations and the costs of the carrier.
Several lipases employed for biodiesel production have been immobilized. The best known example is Novozym 435, which is *Candida antarctica* lipase immobilized on a macroporous acrylic resin. Other examples are: *Burkholderia glumae* lipase immobilized on celite-545 (Shah *et al*., 2004), *Candida rugosa* and *Rizhopus oryzae* lipases immobilized on silica gel (Lee *et al*., 2010), *Pseudomonas cepacia* lipase immobilized on celite and on sol-gel ceramic polymer (Noureddini *et al*., 2004).

Novozym 435 has been used for the methanolysis of different oil sources giving yields higher than 90 % (Li *et al*., 2006, Shimada *et al*., 1999, Kose *et al*., 2002). Moreover, the lipase catalyst could be used for more than 100 days without decrease of the activity (Shimada *et al*., 1999).

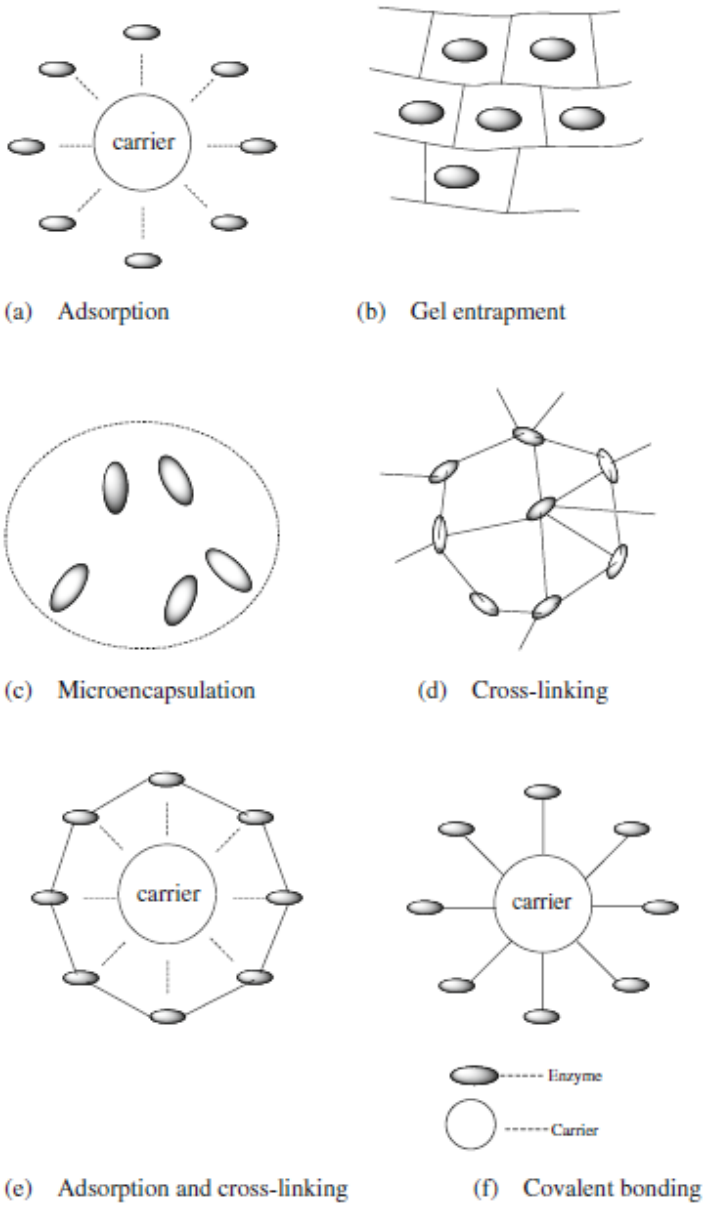

Figure 6. Methods of enzyme immobilization. From (Zhang *et al*., 2012).

Recently, new materials have been explored as potential carriers for lipases immobilization. Gold spherical nanoparticles represent a promising carrier and can be conveniently functionalized to bind enzymes (Colombo *et al*., 2012). Vorhaben *et al*. (2010) immobilized CALB lipase on porous polypropylene (Accurel MP 1000) treated with oxygen plasma. The plasma treatment allowed high immobilization yield and the lipase retained high activity and could be recycled several times without significant loss of performance.

Xie and Ma (2009) used magnetic Fe_3O_4 nanoparticles treated with (3-aminopropyl)triethoxysilane as immobilization carrier and bound covalently lipase from *Thermomyces lanuginosa* to the amino-functionalized magnetic nanoparticles by using glutaraldehyde as a coupling reagent. Thus, the immobilized lipase converted soybean oil to biodiesel with a yield over 90% and could be recycled several times.

1.5.4 Use of organic solvents

At the very beginning, solvent-free systems were proposed for biodiesel production. In such systems, methanol has poor solubility in oil feedstocks, and it forms droplets causing local over dosage that has some negative effect on lipase activity. Therefore, stepwise methanol addition was recommended to produce biodiesel through enzyme catalysis in solvent-free system (Shimada *et al*., 1999). Through a three-step methanol addition, 98.4% conversion of oil to its corresponding methyl esters could be achieved with immobilized *C. antarctica* lipase. In the process glycerol is produced as a by-product. Glycerol is very hydrophilic and insoluble in oils, so it is easily adsorbed onto the surface of the immobilized lipase, leading to negative effects on activity and operational stability (Soumanou and Bornscheuer 2003). How to impair the negative effects caused by methanol and glycerol are key points in the production of biodiesel in solvent-free system with immobilized lipase. A way to overcome this problem consists in the use of an organic solvent as reaction medium. This strategy has

multiple advantages: organic solvents can ensure a homogeneous reaction mixture alleviating the problems with having the reactants in two phases; they reduce the viscosity of the reaction mixture thus increasing the diffusion rates and limiting mass transfer problems around the enzyme; moreover, for immobilized enzymes, non-polar solvents might maintain residual water around the enzyme, locally increasing the water activity and thus stabilizing the protein. In general, enzymes can maintain high catalytic activity in organic solvents, which are rather hydrophobic (usually LogP>3) and show low catalytic activity in organic solvents with LogP<2 (Soumanou and Bornscheuer 2003; Lara and Park 2004). Actually, with hydrophobic organic solvents (petroleum ether, n-hexane etc), methanol and glycerol still have poor solubility in the system. So, the negative effects caused by these molecules cannot be eliminated, and lipase still exhibits poor operational stability in such reaction media.

For this reason, attention has been focused on hydrophilic solvents. For instance, *tert*-butanol, a relatively hydrophilic organic solvent (LogP=0.35), can allow rather high activity and good stability of enzymes, and has been developed as a novel reaction medium for lipase-mediated methanolysis. Both methanol and glycerol are soluble in *tert*-butanol medium, so the negative effects on lipase performance can be totally avoided. This solvent has been shown to stabilize the activity of Novozym 435 (Chen and Wu, 2003; Li *et al*., 2006; Royon *et al*., 2007), since no loss of lipase activity was observed after being repeatedly used for 200 cycles. For this reason, *tert*-butanol medium has been employed in the pilot plant being tested in China (Du *et al*., 2008).

1.5.7 Influence of water on transesterification reaction in solvent-free systems

Protection of the water surrounding the lipases is important for optimal conformation of the enzyme, and removal of the water can lead to both

reversible and irreversible changes in the protein structure (Miller *et al*., 1988; Yamane, 1987).

In low water systems, there is a minimum and optimum water level required for providing enough conformational flexibility (Lu *et al*., 2009). As the water content increases, hydrolysis starts competing with transesterification and the equilibrium shifts towards hydrolysis. An additional feature of this process is that fatty acids produced by hydrolysis would again be converted to fatty acid methyl esters. However, this esterification reaction is also favored by low water conditions.

The optimal water activity for the enzymatic transesterification reaction system is specific for any given lipase (Kaieda *et al*., 2001; Linko *et al*., 1995; Tan *et al*., 2006; Zhang *et al*., 2002, 2005; Lu *et al*., 2008).

The water content in reaction mixtures can be expressed as water activity (a_w) or percentage concentration (%). In non-aqueous media the degree of medium hydration is frequently expressed as a_w, defined as a ratio of vapor pressure over the standard state partial vapor pressure of pure water (p=pH_2O). Water activity of a given reaction system is a function of water activities of individual components of this system and its value defines the amount of water which is not bound in the system and can be evaporated. It was found that the optimum water activity, corresponding to the highest activity of enzyme was characteristic of both the enzyme and reaction medium composition.

Water concentration in reaction mixture is usually assayed by the Karl-Fischer method (expressed as percentage content) and it is one of the most important factors that influence the lipase-catalyzed transesterification rate and the yield of biodiesel synthesis (Iso *et al*., 2001; Nie *et al*., 2006). Numerous studies revealed that addition of a small amount of water to enzyme-catalyzed reaction mixture increased the rate of fatty acid esters synthesis (Shah and Gupta, 2007; Kaieda *et al*., 2001); exciding amounts of water shift the equilibrium of the reaction towards hydrolysis (**Figure 7**).

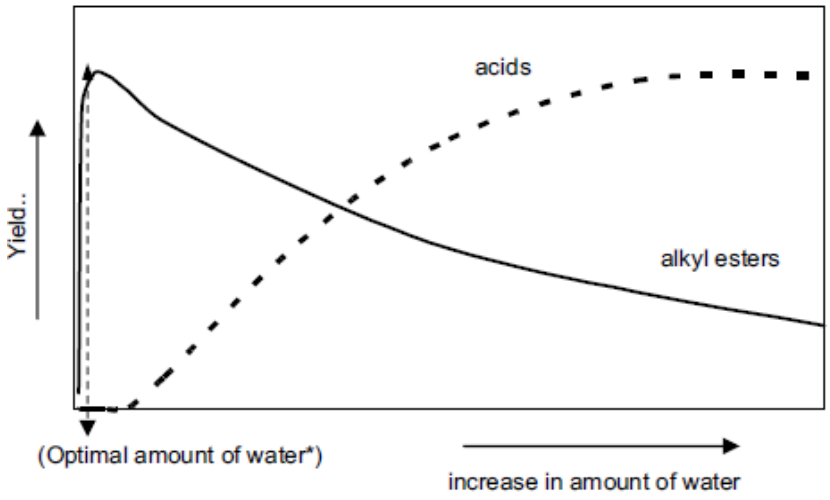

Figure 7. The effect of water concentration in reaction mixture on the yield of products of enzymatic transesterification (alkyl esters) and hydrolysis (acids). The optimum water concentration depends on the type of lipase preparation and reaction mixture composition. From (Antczak *et al.*, 2009).

1.6 Effects of methanol on lipases transesterification activity

As stated before, to optimize the production costs, the alcohols used for industrial biodiesel production must be cheap, as methanol and ethanol. The most used acyl-acceptor is methanol, since it is cheaper than ethanol. The stoichiometry of the transesterification reaction requires 3 moles of methanol for each mole of TAG. The molar excess of methanol over fatty acids contained in TAG increases the transesterification yield but it can also inhibit and inactivate the enzyme, in particular when the alcohol is insoluble in the reaction mixture. This effect has also been reported for ethanol, although to lower extent. In general, the optimum molar ratio of alcohol used for enzymatic biodiesel synthesis has to be determined separately for each alcohol–fat–lipase system.
Shimada *et al*. (2002) observed the irreversible inactivation of *C. antarctica* lipase by methanol and ethanol when alcohol:oil molar ratio was higher than

1:2. In order to explain this behavior, the Authors investigated the solubility of methanol in vegetable oil (a mixture of soybean and rapeseed oils) and they found that the solubility of MeOH was 1/2 of the stoichiometric amount. Being aware that proteins are generally unstable in short-chain alcohols, such as MeOH and EtOH, the authors concluded that low methanolysis (ethanolysis) is due to the inactivation of lipases by contact with insoluble MeOH, which exists as droplets in the oil (**Figure 8**). Actually, MeOH was completely consumed in methanolysis of vegetable oil with <1/3 molar equivalent of MeOH using immobilized *C. antarctica* lipase, but the methanolysis was decreased significantly by adding >1/2 molar equivalent of MeOH. In addition, the activity did not resume in subsequent reaction with 1/3 molar equivalent of MeOH, showing that the immobilized lipase was irreversibly inactivated by contact with insoluble MeOH in the oil.

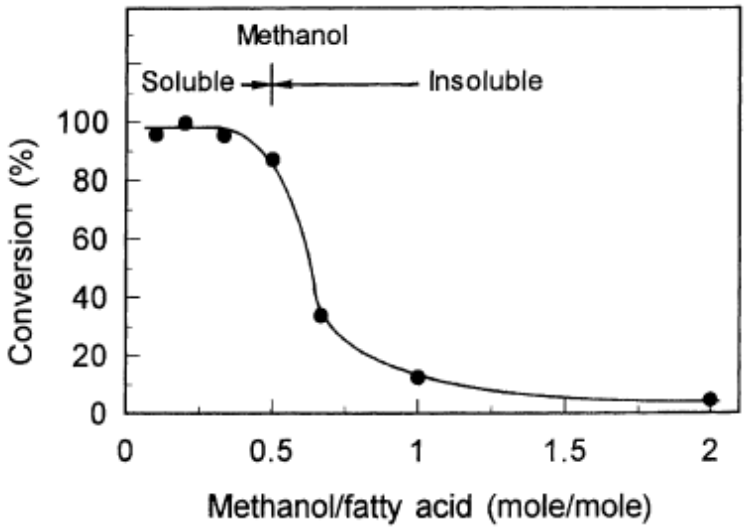

Figure 8. Methanolysis of vegetable oil with different amounts of MeOH using immobilized *C. antarctica* lipase (Novozym 435; Novozymes, Bagsvaerd, Denmark). The conversion is expressed as the amount of MeOH consumed through the ester conversion of the oil. From (Shimada *et al*., 2002).

Lipases from *Pseudomonas spp*. display more resistance towards methanol inhibition and have a higher optimum molar ratio of methanol to oil. Noureddini *et al*. (2005) found at 8.2:1 mole alcohol to oil that a *P. cepacia* lipase gave highest ester yield out of nine lipases tested for methanolysis of soybean oil.

Important to underline is that the observation of methanol inhibition can be masked if using very high enzyme loadings, that is 50 wt. % immobilized enzyme based on oil weight.

A solution to minimize alcohol inhibition is a stepwise addition of the alcohols, which was introduced and successfully performed by Shimada *et al*. (1999) and Watanabe *et al*. (1999) (**Figure 9**). On the negative side, maintaining methanol concentration at a very low level by stepwise addition is not an appropriate approach for the large-scale production of biodiesel.

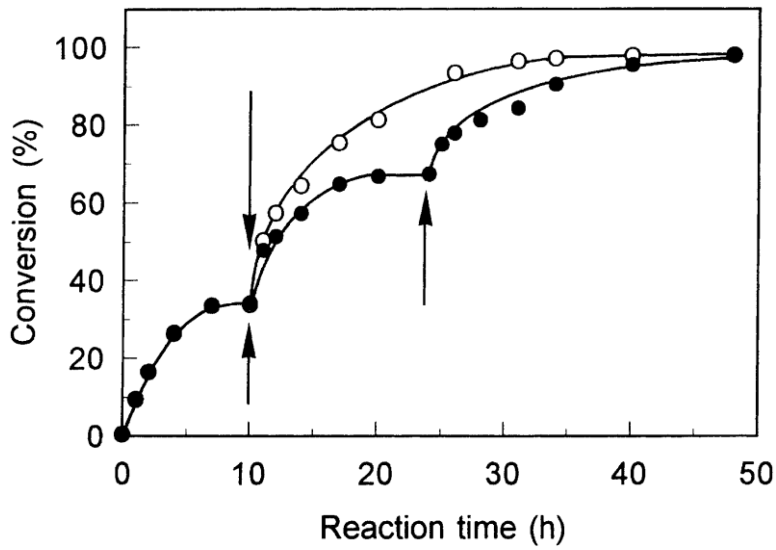

Figure 9. Three-step batch methanolysis of waste oil (black points) and vegetable oil (white points) with *C. antarctica* lipase. The reactions were started at 30°C with shaking (130 oscillations/min) in a 30 g mixture of oil, 1/3 molar equivalent of MeOH for the stoichiometric amount, and 4 wt.% immobilized lipase. Arrows indicate the addition of 1/3 molar equivalent of MeOH. From (Shimada *et al*., 2002).

Alternative strategies have been employed to overcome the methanol deactivation of lipases: (i) organic solvents have been used to improve the solubility of methanol, (ii) methanol has been replaced by methyl acetate, (iii) salts-saturated solutions and silica-gel based controlled release system for methanol have also been applied. However, these techniques have some inherent problems. The methanolysis in organic solvent such as hexane is relatively slower. Although a noticeable increase in reaction rate using *tert*-butanol has been reported, a large molar excess of methanol (methanol to oil ratio 6:1) is required to obtain a higher biodiesel yield. When methanol is replaced by methyl acetate, the byproduct triacetylglycerol makes difficult the product purification. Furthermore, methyl acetate is more expensive than methanol. Finally, the presence of salt-saturated solution or silica-gel causes difficulties in downstream separation.

1.7 Lipase engineering to improve the tolerance to methanol

Genetic engineering is a powerful tool potentially useful to prevent the inactivation caused by methanol. However, to date there are only a few examples of lipase engineering to improve their performances in the process of biodiesel production.

Park *et al*. (2012) reported an effective rational design scheme to improve CALB enzyme stability in methanol. Experiments of directed evolution already showed that mutants with improved stability contain a more intertwined/interlaced net of hydrogen bonds involving polar or charged amino acids from solvent-exposed coil or loop regions. CALB variants designed according to this information showed enhanced stability in the presence of methanol, thus indicating that the hydrogen bonding between the enzyme surface and water molecules is crucial for the enzyme stability in a water-miscible organic solvent. Stabilized variants, however, were tested in hydrolysis reactions only.

Dror *et al*. (2013) applied, in parallel, random and structure-guided mutagenesis on an unexplored lipase gene from *Geobacillu stearothermophilus* T6. A high-throughput colorimetric screening assay was used to evaluate lipase activity after an incubation period in high methanol concentrations. Both protein engineering approaches were successful in evolving two variants with elevated half-life values in 70% methanol. *In-silico* modeling analysis suggests that: (i) the enhanced stability of one variant is a result of new hydrogen bonds; (ii) a single-amino acid substitution of the other variant facilitates a closed lid conformation which limits both the methanol and substrate excess into the active site.

More recently, Korman *et al*. (2013) employed directed evolution to improve the thermostability and the tolerace to methanol of a *Proteus mirabilis* lipase, a particularly promising catalyst for biodiesel synthesis as it produces high yields of methyl esters and can be easily produced in *Escherichia coli*. To screen for mutants with improved methanol and heat tolerance, the authors developed a rapid colony assay for stability screening.

The mutant thus obtained, called Dieselzyme, was a variant with 13 mutations, and it had greatly improved thermal stability, with a 30-fold increased thermostability and dramatically increased methanol tolerance, showing a 50-fold longer half-inactivation time in 50% aqueous methanol. Compared to the wild-type enzyme, a crystal structure of Dieselzyme 4 reveals additional hydrogen bonds and salt bridges, suggesting again that polar interactions may become particularly stabilizing in the reduced dielectric environment of the oil and methanol mixture used for biodiesel synthesis.

2. Experimental work

This section contains publications and some preliminary results. A global overview of the topic and discussion of results will be given at the beginning of each main section, leaving experimental details to full papers.

The main sections will be organized like following:

2.1 A new analytical method to monitor the enzymatic transesterification
    2.1.1 **Paper I** Natalello *et al*., 2013
2.2 Effects of methanol on the activity and structure of two lipases
    2.2.1 **Paper II** Santambrogio *et al*., 2013
    2.2.2 Effects of methanol on the initial rate of methanolysis of vinyl acetate by BGL (Preliminary results)
    2.2.3 **Paper III** Kulschewski *et al*., 2013
    2.2.4 Effects of methanol on CALB structure in presence of toluene (Preliminary results)
2.3 Immobilization of BGL on polypropylene membranes treated with oxygen plasma (Preliminary results)

2.1 A new analytical method to monitor the enzymatic transesterification

As discussed in the introduction, nowadays there are already many analytical methods to monitor transesterification and biodiesel production, such as gas chromatography (GC), high-pressure liquid chromatography, nuclear magnetic resonance (NMR), and Fourier transform infrared spectroscopy (FTIR). Each method has some drawbacks: time required for each analysis and lack of processivity, need of internal standards, complexity of sample preparation, high cost of devices and consumable, complexity of statistical analysis of data etc.

In the first part of the PhD work, a new analytical method based on FTIR to quantify FAME in complex mixtures was developed. Differently from other classical approaches, this method allows to monitor both the transesterification and the side reaction of hydrolysis, which occurs in presence of water, TAG, methanol and lipase catalyst. Moreover, the method is simple, rapid, inexpensive and accurate, requiring fast sample preparation and simple analysis of the spectroscopic data.

This FTIR method might be applied for the analysis of FAME in biodiesel production plants. In fact, such a fast and simple analytical technique might satisfy the need for a cost-effective, rapid screening to set up the best transesterification conditions, and routinely to monitor the process.

2.1.1 Paper I

Enzymatic transesterification monitored by an easy-to-use Fourier transform infrared spectroscopy method

A Natalello, F Sasso, F Secundo (Biotechnology Journal 2013, *8*, 133-138)

Enzymatic transesterification monitored by a new easy-to-use Fourier transform infrared spectroscopy method

Biotechnol J 2013 Jan; 8(1): 133-138

Antonino Natalello[1,2,] *, Francesco Sasso[1], and Francesco Secundo[3]

[1] Department of Biotechnology and Biosciences, University of Milano-Bicocca, Piazza della Scienza 2, 20126 Milan (I).

[2] Consorzio Nazionale Interuniversitario per le Scienze Fisiche della Materia (CNISM), UdR Milano-Bicocca, Milan (I).

[3] Istituto di Chimica del Riconoscimento Molecolare, CNR, Via Mario Bianco 9, Milan, (I).

*Corresponding Author:
Antonino Natalello
Phone +39 02 64483461, Fax +39 02 64483565
e-mail: antonino.natalello@unimib.it

Key-words: Biodiesel, Biocatalysis, Fourier transform infrared spectroscopy; Lipase; Second derivative IR spectra.

Abbreviations: ATR, Attenuated total reflection; BCL, *Burkholderia cepacia* lipase; BGL, *Burkholderia glumae* lipase; CRL1, *Candida rugosa* lipase 1; FTIR, Fourier transform infrared spectroscopy; GC-FID, gas chromatography-flame ionization detection; IR, infrared; IU, international unit of enzyme activity; NMR, nuclear magnetic resonance

Abstract

Transesterification of triglycerides with short chain alcohols is the key reaction in biodiesel production, in addition to other applications in chemical synthesis. However, it is crucial to optimize reaction conditions to make enzymatic transesterification a cost effective and competitive process. In this work, a new easy Fourier transform infrared (FTIR) spectroscopic approach for monitoring the transesterification reaction is reported and compared with a gas-chromatographic method. The concentration of the total methyl esters in the reaction mixture is determined from the peak intensity at ~1435 cm^{-1} in the second derivatives of the FTIR absorption spectra using a calibration curve obtained by simple linear regression. Interestingly, we found that the use of the FTIR second derivatives allows an accurate determination of the methyl esters without the interference of free fatty acids. Moreover, information on substrate hydrolysis can be obtained within the same measurement by the IR absorption at ~1709 cm^{-1}. We applied this approach to monitor methanolysis and hydrolysis reactions catalyzed by commercial lipases. While the *Candida rugosa* lipase activity undergoes methanol inhibition already at 1:2 of triglyceride:methanol ratio, the *Burkholderia cepacia* lipase reaches the maximum yield with the triglyceride:methanol ratio of 1:5. Therefore, the FTIR approach reported in this work represents a rapid, inexpensive, and accurate method to monitor enzymatic transesterification, requiring very limited sample preparation and a simple statistical analysis of the spectroscopic data.

Practical Application

We reported here an easy, rapid, and accurate FTIR approach to quantify methyl ester content and hydrolysis side-products obtained upon alcoholysis and hydrolysis of triglycerides by lipase to produce biodiesel.

The method could also be used to monitor the chemical synthesis of biodiesel. More in general, the method could be applied to study the activity of enzymes by monitoring the intensity of peaks associated to product synthesis or substrate depletion, in the absorbance or either in the second derivatives of the FTIR absorption spectra.

Interestingly, the FTIR analysis required small sample volume, very limited sample preparation and simple statistical analyses of the spectroscopic data. Moreover, the method could be optimized for on-line analyses.

1. Introduction

There is a growing interest in lipases for their applications in a variety of biotechnological processes, as the synthesis of biopolymers, biodiesel, agrochemicals, and flavor compounds [1]. In particular, the lipase-catalyzed transesterification of triglycerides with simple alcohols represents a promising approach for biodiesel production [2]. However, the commercialization of biodiesel obtained through lipase catalysis is strongly restricted by the cost of the enzymatic process that is not competitive compared to the chemical catalysis. Several lipases and reaction conditions have been tested with different oil substrates and alcohols. These researches indicated the crucial role of the reaction conditions in determining the final yield of fatty acid esters [2]. An efficient setup of the transesterification conditions requires accurate and rapid analytical tools for the analyses of the reaction products. There are already many methods to monitor transesterification and biodiesel production, such as gas chromatography (GC), high-pressure liquid chromatography, nuclear magnetic resonance (NMR), and Fourier transform infrared spectroscopy (FTIR) [3]. However, each method has some drawbacks. For instance, NMR is very costly to use and maintain; GC is relatively time consuming as it often requires long time for sample preparation and analysis, in addition to the need of an internal standard. Also methods based on infrared spectroscopy in the mid and near IR spectral regions have been developed; however, they require complex statistical analysis of the spectroscopic data [3-5]. In this work, a new easy FTIR approach is reported to monitor transesterification and hydrolysis catalyzed by three commercial lipases, from *Burkholderia glumae* (BGL), Candida rugosa (CRL1) and Burkholderia cepacia (BCL). In particular, we show here that the total methyl ester content can be determined through the peak intensity at ~1435 cm^{-1} in the second derivatives of the IR absorption spectra, without the interference of free fatty acids. This FTIR approach allows a rapid, inexpensive,

and accurate monitoring of enzymatic transesterification, requiring very limited sample preparation and a simple statistical analysis of the spectroscopic data.

2. Materials and methods

Materials

The enzymes used in this work were *Burkholderia glumae* lipase (BGL) 437707 from CalBioChem (San Diego, CA, USA), *Candida rugosa* lipase (CRL1) L8525 from Sigma-Aldrich (St Louis, MO, USA) and *Burkholderia cepacia* lipase (BCL) 62309 from Sigma-Aldrich. Methanol, p-nitrophenyl laurate, triton X-100, ammonium acetate, methyl oleate, oleic acid, pure triolein (≥ 97%) and triolein ~ 65% in triglyceride mixture were from Sigma-Aldrich. In particular, triolein ~ 65% is provided in mixture with other triglycerides, mainly composed of palmitic acid, linoleic acid, and other fatty acids present in lower amount.

Preparation of enzyme solutions

BGL (2.5 mg), BCL (100 mg), and CRL1 (70 mg) were dissolved in 1 ml of deionized water. The mixtures were mixed vigorously and centrifuged at 11200 x *g* for 5 min. The supernatants or appropriate dilutions thereof were used as the enzyme solutions.

Activity assay

Lipase activities were determined by measuring the increase in absorbance at 410 nm produced by the release of *p*-nitrophenol during the hydrolysis of 10 mM *p*-nitrophenyl laurate (dissolved in isopropanol) in 10 mM ammonium acetate pH 7.2 and 0.5% Triton X-100, at ~ 25°C. The reactions were triggered when 1 µM lipase was added to 100 µl of substrate solution, in a final volume of 1 ml. Hydrolysis was followed for 2 min. One unit was defined as the amount of enzyme which releases 1 µmol of *p*-nitrophenol/min under the test conditions. Measurements were performed in triplicate. Specific activity of BGL, BCL and CRL1 were around 1000, 300 and 90 U/mg protein respectively.

Methanolysis of triolein

Lipases were investigated for their ability to catalyse the methanolysis reaction in mixtures with different methanol contents. Transesterification reactions catalysed by BGL were performed with pure triolein (≥97%), while those catalysed by BCL and CRL1 were performed with triolein mixture (~ 65%). As substrates for the reaction, triolein (0.388 g) and methanol were mixed in 1.5-ml screw-cap vials and 9 µl enzyme solution containing 10 IU BGL, 3 IU BCL or 1.4 IU CRL1 was added. Different amounts of methanol (14.2-85.3 mg) were used in order to satisfy tryglicerides:methanol molar ratios ranging from 1:1 up to 1:6. Deionized water was added to reach the final volume of 550 µl.

The reaction mixtures were incubated at 37 °C under agitation in a BIO RS-24 rotator (Biosan, Riga, Latvia) at 30 rpm for 24 hours, then centrifuged at 11200 x *g* for 1 minute in order to separate the organic and aqueous phases. The organic phase was analysed for its content of methyl esters (methanolysis product) by FTIR spectroscopy and GC analysis.

GC Analysis

For GC analysis, 30 µl of the organic phase and 150 µl of hexane with 2% dodecane solution were mixed in 1.5-ml screw-cap vials. Dodecane was used as internal standard.

The methyl-oleate content in the organic phase from reaction mixtures was analyzed on an Agilent gas chromatograph ("6850 Network GC System" Model), equipped with a flame ionization detector (FID), a MEGA-WAX capillary column 25m×0.32mm, and a split injection system with a 1:100 ratio. Injector and detector temperatures were kept at 250°C. The oven was initially maintained at 100°C for 1 min, heated up to 150°C at a 10°C min^{-1} rate, then heated up to 250°C at a 15°C min^{-1} rate and kept constant at 250°C for 3min. Hydrogen was used as the carrier gas at a 0.8 mL min^{-1} flow rate. The "Chemstation for GC System" software was used to automatically integrate the peaks areas. The retention times for hexane, dodecane and methyloleate were 0.95, 1.4, 9.7 min respectively.

FTIR spectroscopy

FTIR absorption spectra of standard and reaction mixtures were collected in attenuated total reflection (ATR) by the Varian 670-IR (Varian Australia, Mulgrave, Australia) spectrometer equipped with a nitrogen cooled mercury cadmium telluride detector. In particular, 5 μL of the sample were deposited on the one reflection diamond element of the ATR device (Golden Gate, USA) and the spectrum was collected under the following conditions: 2 cm-1 spectral resolution, 25 kHzscan speed, 512 scan coadditions, and triangular apodization [6].

The minimum sample amount required for the ATR measurements (5 μL in our case) can be determined monitoring the infrared absorption at increasing sample volumes until a constant intensity is reached. Under these conditions, the use of an ATR device guaranties a constant penetration depth at a specific wavenumber. Indeed, the penetration depth depends on the refractive index of the ATR element and of the sample, on the wavelength of the radiation and on the angle of incidence of the beam [6].

The second derivatives of the FTIR spectra were obtained after the Savitsky-Golay smoothing of the absorption spectra using the Resolutions-PRO software (Varian Australia, Mulgrave, Australia).

3. Results and Discussion

Setup and validation of the method

The key process in biodiesel production is the transesterification of triglycerides in the presence of short-chain alcohols, such as methanol, resulting in mono-alkyl esters (biodiesel) and glycerol as end products. This reaction can be catalyzed chemically or enzymatically by lipases. Even if biodiesel can be considered the best renewable substitute for fossil diesel fuel, its commercial use is strongly limited by the production costs, which are even higher in the case of the enzymatic processes. Therefore, in recent years a great effort has been devoted to the development of more cost effective processes and, in particular, to the optimization of transesterification conditions. To this goal, it would be desirable to have analytical methods able to monitor accurately

the transesterification reaction in an easy, rapid, and cheap way. With this aim, in this work we explored the possibility to develop a new FTIR approach that, besides being rapid and easy to operate, does not require heavy statistical analysis of the spectroscopic data. To identify the infrared marker bands of the process, we started our investigations measuring the mid infrared spectra of a model triglyceride substrate, containing 65% of triolein, and of methyl-oleate that is the product of triolein transesterification with methanol. These spectra are reported in Fig. 1, which also shows the IR spectrum of oleic acid, a possible and undesirable side-product generated by the substrate hydrolysis. In the C=O stretching region (1800-1700 cm^{-1}), the oleic acid displayed a peak around 1709 cm^{-1} that appeared well separated from that of triolein and methyl oleate, respectively occurring at ~ 1743 cm^{-1} and ~ 1741 cm^{-1}. The different peak positions between fatty acid ester and free fatty acid has been already exploited to develop FTIR approaches for monitoring lipase catalyzed hydrolysis, as for instance reported in [7, 8]. The small downshift of the C=O stretching mode from triglycerides (at ~1743 cm^{-1}) to methyl esters (at ~1741 cm^{-1}) can be potentially used to follow the transesterification reaction. However, the very limited spectral difference in this IR region requires, necessarily, the application of multivariate analyses of the spectroscopic data [4]. In Fig. 1 are also reported the absorption spectra of the three compounds in the 1490-1390 cm^{-1} spectral region, where only methyl-oleate displayed an intense and sharp peak at 1435 cm^{-1}, due to the CH_3 deformation mode [9]. Interestingly, triolein spectrum is characterized by a shoulder at the same peak position, making it possible to use the ~1435 cm^{-1} band as a transesterification marker. Indeed, the above spectral region has been successfully exploited for biodiesel analyses coupling FTIR spectroscopy with nonlinear classical last square analysis [9]. These authors validated the accuracy and prediction capability of their approach by biodiesel-oil mixtures of known concentration, therefore without the possible interference of free fatty acids. However, as can be seen in Fig. 1A, oleic acid displayed a broad absorption around 1435 cm^{-1} that might interfere with the methyl ester determination by the infrared absorption of the reaction mixture at this peak position. To isolate the contribution of methyl esters from that of free fatty acids, we performed the second

derivative of the absorption spectra taking advantage of the very different IR band width characteristic of the two compounds. Indeed, it is well known that the intensity of the negative peaks in the second derivative is proportional to the original intensity but inversely proportional to the square of the half-width in the measured spectrum [10]. From this inverse proportionality it is expected that the second derivative greatly enhances the relative contribution of sharp components (as that of methyl esters) and strongly reduces that of broad bands (as that of triglycerides and free fatty acid) of the measured absorption spectrum. In fact, in the second derivative spectra triolein and oleic acid displayed similar and very low intensity around 1435 cm^{-1}, where methyl oleate, instead, showed a high peak intensity (Fig. 1B), making this peak of potential interest for monitoring transesterification reactions even in the presence of free fatty acids. Indeed, free fatty acids can be present in the reaction mixture as they are side-products generated by the enzyme-catalyzed triglyceride hydrolysis. Moreover, several potential substrates for biodiesel production have also high content of free fatty acid, as the recycled restaurant grease.

All these results indicate that the ~1435 cm^{-1} peak can be taken as a marker band of methyl esters, thanks to the lack of interference of free fatty acids in the second derivate spectra.

To verify if there is a linear relationship between the methyl ester concentration and the ~1435 cm^{-1} peak height in the second derivative spectra, standard samples of known concentrations of the single components have been measured. In Fig. 2, the absorption and the second derivative spectra are reported for samples containing increasing concentrations of methyl oleate, from 0% (v/v) to 100% (v/v) in triolein (~65 in triglycerides mixture). The intensity of the ~1435 cm^{-1} peak displayed a linear correlation with methyl oleate concentration not only in the absorption spectra (Fig. 2A and data not shown) but also in the second derivative spectra, as indicated in Fig. 2C. The suitability of the simple linear regression, derived from standard data, to evaluate methyl ester content has been assessed by measuring test samples containing a known concentration of methyl oleate. Obviously, these test samples were not included in the data used for the straight-line calibration curve. This procedure has been performed

with three independent calibration curves and using four sets of three test samples for each curve. An example of this analyses is reported in Fig. 2D. In particular, the concentration determined by second derivative FTIR spectra of the samples of known concentration (actual value) was found to have an average accuracy of 1%. Moreover, the analysis of each sample by three independent straight-line calibration curves determined the methyl ester content with standard deviation ≤ 1% (data not shown). These analyses demonstrated that the method is accurate and reliable.

On the bases of these promising outcomes, our FTIR approach has been tested for the analysis of lipase-catalyzed transesterification reactions using, as reference method, gas chromatography-flame ionization detection (GC-FID) [3]. The FTIR and GC-FID analyses were compared for BGL-catalyzed transesterification of pure triolein (~99%) in the presence of methanol, at different triglyceride and alcohol molar ratio. Methyl ester amounts estimated with the two techniques were found differing from less than 3% (Supporting Information).

Monitoring triglyceride transesterification by second derivative FTIR spectroscopy

The FTIR method described in the previous paragraph has been here applied to follow the transesterification reactions catalyzed by BCL, BGL, and by CRL1. The lipase-catalyzed reactions were done as described in Materials and Methods and, after 24 hour incubation at 37°C, an aliquot of the reaction mixture has been centrifuged. Five microliters of the organic phase have been then deposited on the ATR plate and the infrared spectrum was collected. We should note that this procedure is relatively fast compared to other approaches, since each FTIR spectrum is collected in less than 10 minutes and a very limited sample preparation is required (for instance, no extraction or dilution in suitable solvent, no sample derivatization, and no internal standard addition are needed). Moreover, after the measurement of the standard solution, the calibration curve is obtained by simple linear regression; therefore, without the use of complex statistical analyses.

In a first set of experiments, the BCL-catalyzed conversion of the model triglyceride substrate, containing 65% of triolein, has been investigated at different

triglyceride:methanol molar ratios from 1:1 to 1:6. The FTIR absorption spectra collected at the end of the reactions are reported in Fig. 3A in the 1770-1670 cm^{-1} region, where the absorption of the C=O stretching mode of esters and free fatty acids occurs. Fig. 3B represents the second derivatives of the absorption spectra in the 1500-1420 cm^{-1} spectral region. The intensity of the 1435 cm^{-1} peak in the second derivative spectra was used to evaluate the total methyl ester content (Fig. 3C) by the straight-line calibration curve (Fig. 2C), obtained as described in the previous paragraph. Indeed, this peak allows to detect methyl esters without considering the specific acyl chain of the fatty acid esters. For BCL-catalyzed methanolysis, we found that the methyl ester yield increased with the triglyceride:methanol ratio up to 5:1, reaching a methyl ester concentration of about 45 % (v/v), while, for higher methanol concentrations, this yield was found to decrease rapidly.

The absorption around 1709 cm^{-1} (Fig. 3A) has been then considered to evaluate the hydrolysis of the substrate (Fig. 3D). As expected, the free fatty acid content in the final reaction mixture decreased with the triglyceride:methanol ratio, from around 15% (v/v) at 1:1 to a very low content at 1:6 (Fig. 3D), as estimated by comparison with the standard solutions containing from 0 to 20% (v/v) of oleic acid. The possibility to directly detect free fatty acids, interfering with the evaluation of the absorption intensity at ~1435 cm^{-1}, further underlines the usefulness of our FTIR approach. Indeed, the free fatty acids contribution does not affect the analyses performed using the second derivative peak intensity of the ~1435 cm^{-1} band, indicated in the previous paragraph as a marker of methyl esters. A similar trend to that obtained for BCL (Fig. 3) was obtained for BGL (data not shown).

When the same analyses were performed for CRL1-catalyzed transesterification of triolein and methanol, a more marked methanol inhibition (of the enzymatic activity) was observed. Indeed, the yield in methyl esters decreased with the increase of triglyceride:methanol ratio. At the end of reaction, the content of methyl esters was ~16.5% (v/v) for 1:1 triglyceride:methanol ratio, but it dropped to less than 4% (v/v) for 1:4 ratio (Fig. 3C). Also the substrate hydrolysis was observed to decrease rapidly with increased methanol concentrations (Fig. 3D).

The reported examples illustrate a new application of FTIR technique to rapidly monitor transesterification and hydrolysis reactions, from the same measurement of the same samples. The application of our analytical method allowed to compare three commercial preparations of microbial enzymes and indicated that CRL1 activity undergoes methanol inhibition already at 1:2 triglyceride:methanol ratio, while BCL and BGL reach the maximum yield with the triglyceride:methanol ratio of 1:5. Actually, lipases from Pseudomonas have been found to be more resistant to methanol inhibition and to have a higher optimum of oil:methanol molar ratio compared to other lipases, including that from *Candida rugosa* [11, 12].

Therefore, in the case of BCL a higher fraction of methanol, in respect to the stoichiometry of methanolysis, can be exploited to overcome the possible presence of free fatty acids and of water that promotes the competitive hydrolysis of the substrate.

In the case of CRL1-catalized transesterification, the stepwise addition of the stoichiometrically appropriate amount of methanol might allow to overcome the methanol inhibition effects , as it has been found for other lipases [13].

4. Concluding Remarks

We presented a new, easy, and rapid FTIR approach to monitor transesterification reactions. In this method, the methyl esters content in the reaction mixture is determined from the peak intensity at 1435 cm^{-1} in the second derivate FTIR spectrum, using a simple linear regression analysis. Therefore, this procedure doesn't require complex statistical analyses of the data and additional software. Noteworthy, we found that the use of the second derivative spectra allows an accurate and reproducible determination of the methyl ester content without the interference of free fatty acids, which instead affect the analysis of the absorption spectra in the spectral region of interest. This is an important point, since fatty acids are side-product generated by the enzymatic hydrolysis of triglycerides and since they are also present in several potential substrate for biodiesel production. Moreover, information on transesterification (second derivative peak intensity at 1435 cm^{-1}) and substrate

hydrolysis (absorption at 1709 cm^{-1}) is simultaneously obtained within the same measurement.

We exemplified the method studying the triglyceride methanolysis and hydrolysis catalized by different commercial lipases, which displayed different sensitivities to methanol inhibition.

In this way, the FTIR approach reported in this work can be applied to monitor enzymatic transesterification and to setup the reaction conditions leading to the highest yield in methyl esters and the lowest amount of side-products (free fatty acids).

Acknowledgements

This work was partly supported by a grant ASTIL- Cooperazione Scientifica e Tecnologica Internazionale by Regione Lombardia to the project "Diesel-Biotech".

The authors acknowledge Marina Lotti, Silvia M. Doglia, Rita Grandori , and Stefania Brocca (University of Milano-Bicocca) for the helpful discussions.

The authors declare no commercial or financial conflict of interest.

References

[1] Jaeger, K. E., Eggert, T., Lipases for biotechnology. *Curr Opin Biotech* 2002, *13*, 390-397.

[2] Bajaj, A., Lohan, P., Jha, P. N., Mehrotra, R., Biodiesel production through lipase catalyzed transesterification: An overview. *Journal of Molecular Catalysis B-Enzymatic* 2010, *62*, 9-14.

[3] Monteiro, M. R., Ambrozin, A. R. P., Liao, L. M., Ferreira, A. G., Critical review on analytical methods for biodiesel characterization. *Talanta* 2008, *77*, 593-605.

[4] Zagonel, G. F., Peralta-Zamora, P., Ramos, L. P., Multivariate monitoring of soybean oil ethanolysis by FTIR. *Talanta* 2004, *63*, 1021-1025.

[5] Richard, R., Li, Y., Dubreuil, B., Thiebaud-Roux, S., Prat, L., On-line monitoring of the transesterification reaction between triglycerides and ethanol using near infrared spectroscopy combined with gas chromatography. *Bioresource Technol* 2011, *102*, 6702-6709.

[6] Griffiths, P. R., de Haseth, J. A., *Fourier Transform Infrared Spectrometry*, Wiley-Interscience, New York 1986.

[7] Walde, P., Luisi, P. L., A Continuous Assay for Lipases in Reverse Micelles Based on Fourier-Transform Infrared-Spectroscopy. *Biochemistry* 1989, *28*, 3353-3360.

[8] Snabe, T., Petersen, S. B., Application of infrared spectroscopy (attenuated total reflection) for monitoring enzymatic activity on substrate films. *Journal of Biotechnology* 2002, *95*, 145-155.

[9] Mahamuni, N. N., Adewuyi, Y. G., Fourier Transform Infrared Spectroscopy (FTIR) Method To Monitor Soy Biodiesel and Soybean Oil in Transesterification Reactions, Petrodiesel-Biodiesel Blends, and Blend Adulteration with Soy Oil. *Energ Fuel* 2009, *23*, 3773-3782.

[10] Susi, H., Byler, D. M., Resolution-Enhanced Fourier-Transform Infrared-Spectroscopy of Enzymes. *Method Enzymol.* 1986, *130*, 290-311.

[11] Noureddini, H., Gao, X., Philkana, R. S., Immobilized Pseudomonas cepacia lipase for biodiesel fuel production from soybean oil. *Bioresource Technol* 2005, *96*, 769-777.

[12] Soumanou, M. M., Bornscheuer, U. T., Lipase-catalyzed alcoholysis of vegetable oils. *Eur J Lipid Sci Tech* 2003, *105*, 656-660.

[13] Shimada, Y., Watanabe, Y., Sugihara, A., Tominaga, Y., Enzymatic alcoholysis for biodiesel fuel production and application of the reaction to oil processing. *Journal of Molecular Catalysis B-Enzymatic* 2002, *17*, 133-142.

Figures and legends

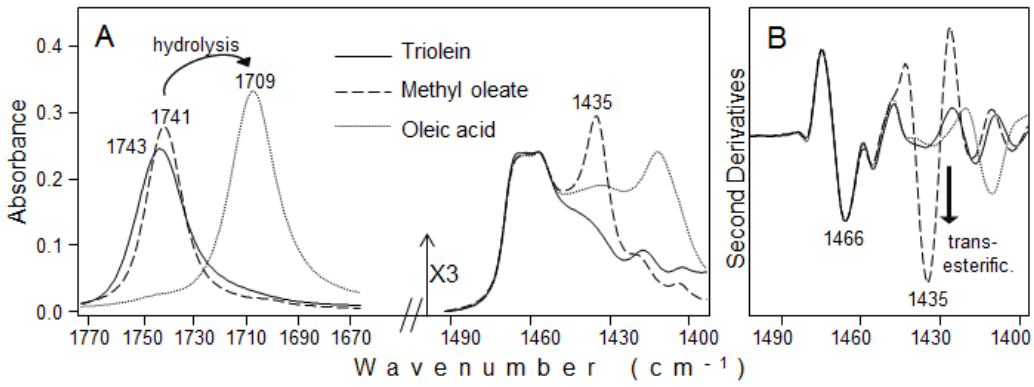

Figure 1. Fourier transform infrared spectra of triglycerides, methyl esters and free fatty acids.

(A) The FTIR absorption spectra of a triglyceride mixture (containing 65% of triolein), of methyl oleate, and of oleic acid are reported in the C=O stretching (1670-1770 cm^{-1}) and in the 1400-1490 cm^{-1} spectral regions. The different peak position of the C=O stretching in esters and free fatty acids can be exploited to follow the substrate hydrolysis. The spectra in the 1400-1490 cm^{-1} IR region are given in an expanded absorption scale.

(B) Second derivatives of the absorption spectra reported in (A). The 1435 cm^{-1} component can be taken as marker band of methyl ester formation. Spectra are normalized at the CH_2 scissoring peak at 1466 cm^{-1} to compensate for possible differences in the sample amount.

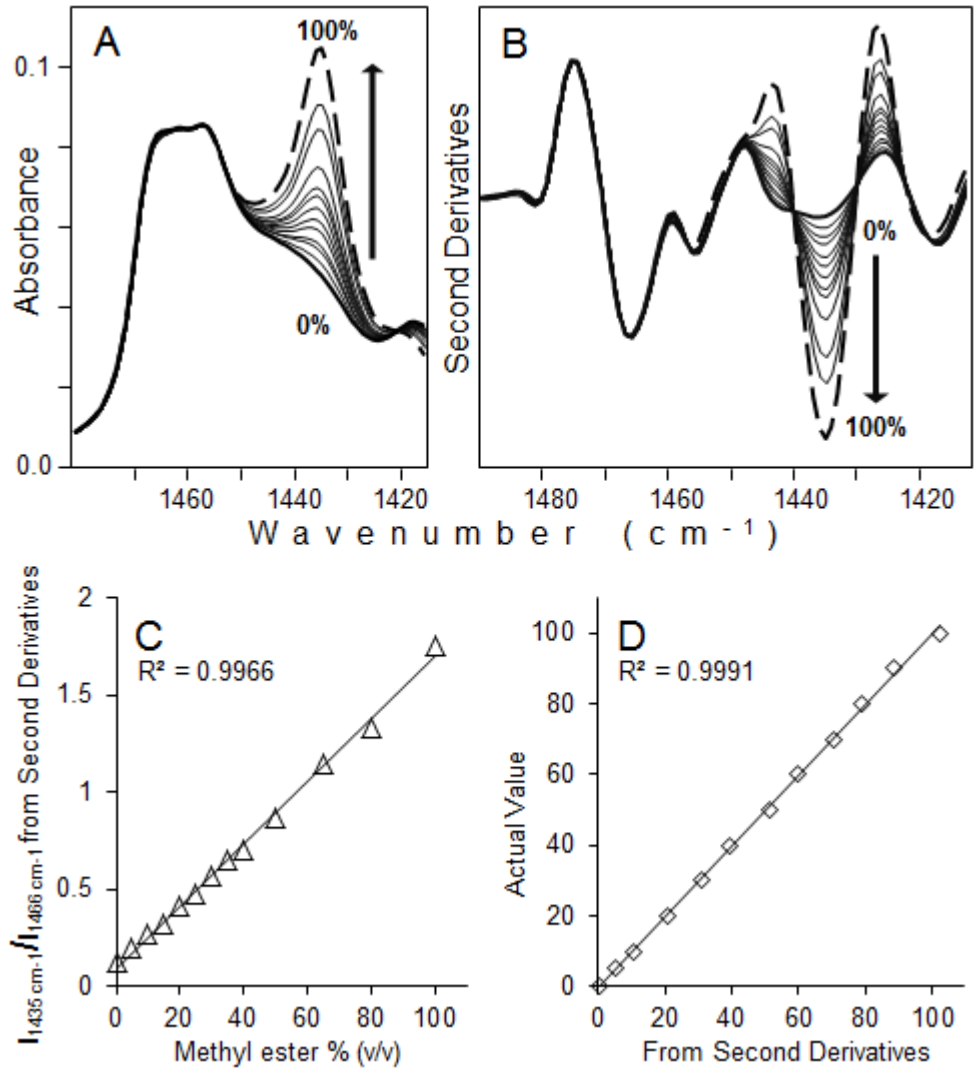

Figure 2. Methyl oleate content determined by second derivative FTIR spectra.

(A) Absorption spectra of samples of known concentrations of triglycerides (triolein ~65%) and methyl oleate from 0% (v/v) to 100 % (v/v). The arrow points to increased concentrations of methyl oleate.

(B) Second derivatives of the absorption spectra reported in (A).

(C) The intensity ratio of the 1435 cm^{-1} and 1466 cm^{-1} peak intensities, from the second derivative spectra, is reported from solutions containing increased concentrations of methyl oleate as in (A). The linear regression curve is also shown.

(D) Comparison of the methyl oleate content determined by the second derivative FTIR approach and its actual value in test solutions of known concentration, not included in the data used for the straight-line calibration curve.

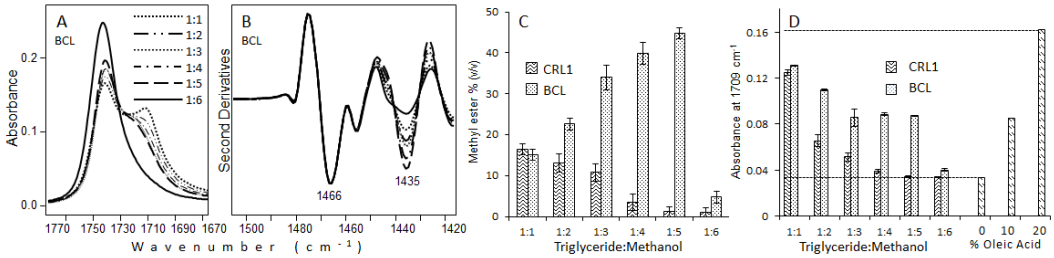

Figure 3. Lipase-catalyzed transesterification monitored by second derivative FTIR spectra.

(A) Absorption spectra in the C=O stretching region of BCL-catalyzed reaction samples obtained at different triglyceride:methanol ratios from 1:1 to 1:6. The absorption intensity around 1709 cm^{-1} has been used to evaluate the formation of free fatty acids, due to the substrate hydrolysis (see panel D).

(B) Second derivatives of the absorption spectra reported in (A) in the 1420-1500 cm^{-1} spectral region. The peak intensity at 1435 cm^{-1} has been used to evaluate the concentration of methyl esters (see panel C).

(C) Methyl ester concentration, expressed as volume percentage, in the final reaction solutions at different triglyceride:methanol ratios, from 1:1 to 1:6. The effects of triglyceride:methanol ratio on the transesterification reactions catalyzed by BCL and CRL1 are compared.

(D) Substrate hydrolysis is shown for the same samples of panel (C). The absorption at 1709 cm-1 of standard solutions containing the substrate and 0%, 10% (v/v), and 20% (v/v) of oleic acid are also reported for comparison.

Standard deviation refers to three independent experiments.

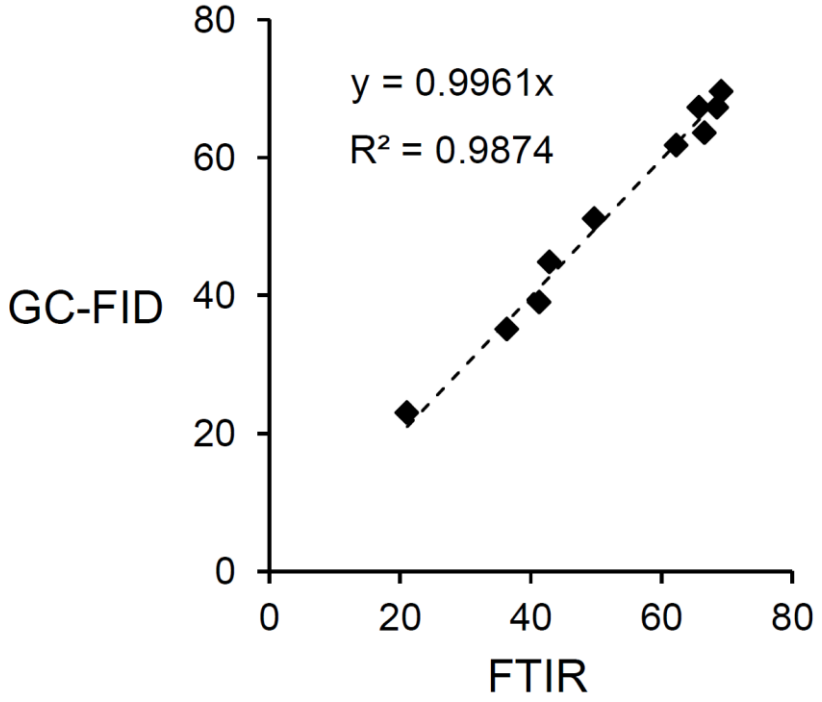

Figure S1. Comparison of the methyl ester estimation obtained by GC-FID and by the FTIR method described in text.

The reported example refers to BGL-catalyzed transesterification of pure triolein.

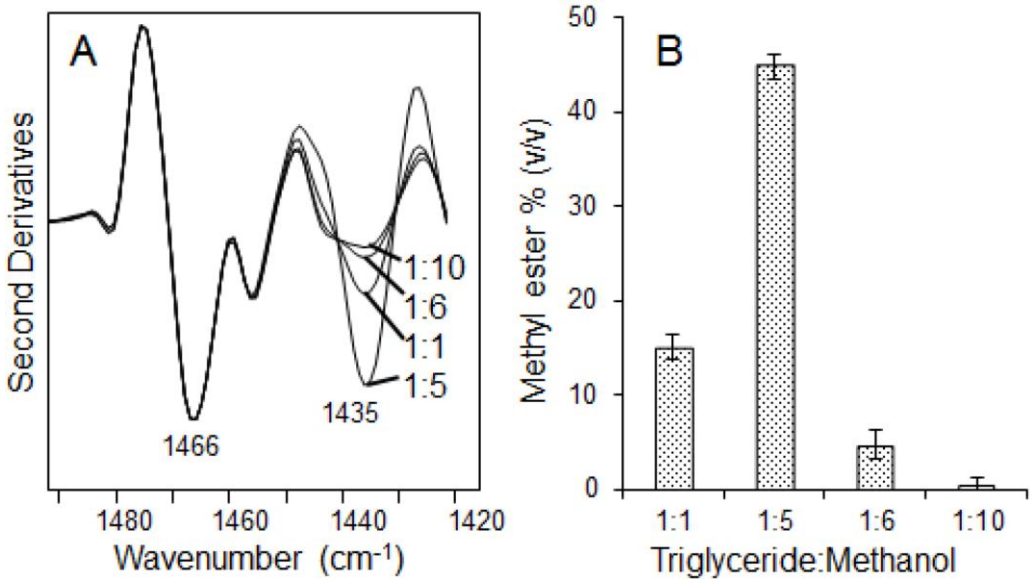

Figure S2. BCL-catalyzed transesterification at different triglyceride:methanol ratios.

(**A**) Second derivatives in the 1420-1490 cm-1 spectral region of BCL-catalyzed reaction samples, obtained at 1:1, 1:5, 1:6; and 1:10 triglyceride:methanol ratios (see text and Fig. 3 for details).

(B) The methyl ester concentrations, expressed as volume percentage, in the final reaction solutions of (A) have been determined by the peak intensity at 1435 cm-1 in the second derivative spectra.

In order to reach a triglyceride:methanol ratio of 1:10, we increased the final volume of the reaction from 550 µl (used in all the other reactions) to 622 µl.

Standard deviation refers to three independent experiments.

2.2 Effects of methanol on the activity and structure of two lipases

One of the main drawback of the enzymatic catalysis for biodiesel industrial production is the short operational life of the catalyst and this is mainly due to the inactivation exerted by methanol.

Although many scientific publications proved that the catalytic performance of both free and immobilized lipases is severely affected by methanol, none of them addresses the causes of such inhibition.

Understanding the molecular mechanism of lipase inactivation induced by methanol could be a successful key factor to make the enzymatic process compete with the well-established chemical way.

For instance, in cases structural information on lipase is available and the complicate interactions between enzyme and alcohol molecules are known, a rational engineering approach would be efficient for designing mutants which are stable in methanol.

The response to methanol and the best molar ratio oil:MeOH in the transesterification reaction of biodiesel production is characteristic for each lipase and different lipases can exhibit very different behaviors towards methanol.

In the present work we analyzed the effects of methanol on two lipases, from *Burkholderia glumae* (**sections 2.2.1 and 2.2.2**) and *Candida antarctica* (**sections 2.2.3 and 2.2.4**), in two reaction systems.

Both BGL (319 aa) and CALB (317 aa) have a molecular mass around 33 kDa and like other serine hydrolases, a serine-histidine-aspartate catalytic triad is responsible for their catalytic activity. The two lipases are widely used in many industrial applications; contrary to CALB which has already been successfully studied and employed for biodiesel production (mainly in the immobilized form as Novozym 435), BGL is a promising catalyst thanks to its tolerance to methanol.

We investigated on the effects of methanol on both activity and structure of BGL and CALB. Moreover, we chose two different reaction systems: the

transesterification of triolein and methanol to produce biodiesel and the transesterification of vinyl acetate and methanol, in presence of toluene, to produce methyl acetate. The choice of this simple system consisting of toluene, methanol and vinyl acetate was driven by the necessity to easily simulate it *in silico* by computational methods.

Interestingly, we found that BGL and CALB behave very differently when exposed to methanol (though in different reaction systems). Indeed, BGL tolerates high methanol and increases transesterification activity at higher MeOH contents. On the other side, high methanol concentrations destabilize the lipase structure inducing the protein unfolding and subsequent aggregation (**Paper II**). Moreover, in the methanolysis of vinyl acetate in the presence of toluene, the initial rate of the reaction increases dramatically with methanol concentrations up to 60% (**section 2.2.2**).

Contrary to BGL, CALB is: (i) irreversibly inactivated by oil:MeOH molar ratio higher than 1:2 in the biodiesel reaction, as demonstrated by Shimada *et al*. (2002) and (ii) in the methanolysis of vinylacetate its initial velocity steeply decreases with higher methanol content. This observations, together with the results from simulations of the enzyme in ternary toluene/methanol/vinyl acetate mixtures, suggest that methanol acts as a competitive inhibitor for CALB (**section 2.2.3**). Finally, the structural studies carried out on CALB show that methanol exposure leads to protein aggregation only at high methanol. Indeed, CALB appears only slightly affected after a 3-hours exposure at very low methanol concentration (**section 2.2.4**).

2.2.1 Paper II

Effects of methanol on a methanol-tolerant bacterial lipase

C Santambrogio, F Sasso, A Natalello, S Brocca, R Grandori, SM Doglia, M Lotti (Applied Microbiology and Biotechnology 2013, 97, 8609-8618)

Effects of methanol on a methanol- tolerant bacterial lipase

Appl Microbiol Biotechnol 2013 Oct; 97(19):8609-18

Carlo Santambrogio, Francesco Sasso, Antonino Natalello, Stefania Brocca, Rita Grandori, Silvia Maria Doglia and Marina Lotti*

Department of Biotechnology and Biosciences, State University of Milano-Bicocca, Piazza della Scienza 2, 20126 Milano, Italy

* To whom correspondence should be addressed: marina.lotti@unimib.it, tel. ++39 02 6448 3527; fax. ++ 39 02 6448 3569;

Keywords: lipase, biodiesel, methanol inhibition, denaturation, aggregation

Abstract

Methanol is often employed in biocatalysis with the purpose of increasing substrates solubility or as the acyl acceptor in transesterification reactions, but inhibitory effects are observed in several cases. We have studied the influence of methanol on the catalytic activity and on the conformation of the lipase from *Burkholderia glumae*, which is reported to be highly methanol-tolerant if compared with other lipases. We detected highest activity in the presence of 50-70% methanol. Under these conditions, however, the enzyme stability is perturbed leading to gradual protein unfolding and finally to aggregation. These results surmise that, for this lipase, methanol-induced deactivation does not depend on inhibition of catalytic activity but rather on negative effects on the conformational stability of the catalyst.

Introduction

The effect of organic solvents on the activity, stability and specificity of enzymes is a key issue in biocatalysis since it deeply impacts on their catalytic performances (Carrea and Riva, 2000; Bommarius and Riebel, 2004; Faber 2011). Very often, this topic is approached taking into account the final effect only, with the aim of defining the combination of enzyme, composition of the reaction mixture, and conditions (temperature, time of reaction, free *vs* immobilized enzyme) most effective in the process of interest. However, getting insight into the modifications induced in the enzyme by the experimental setting is of paramount interest both for application and for deepening the knowledge available about the bases of the kinetic and structural robustness (or sensitivity) of the enzyme under the conditions applied. In this work, we focus on the effect of a water-miscible solvent, methanol, on the activity and conformation of a bacterial lipase. The reaction considered is the alcoholysis of tryglicerides to alkyl esters, as commonly used for the production of biodiesel, where the substrates of the biocatalysts of choice (lipases) are short chain alcohols and oils of various origin (Fjerbaek et al., 2008; Adamczak et al., 2009; Parawira 2009). Methanol is widely used as the acyl acceptor and is often favoured over other alcohols because of its low cost. However, several lipases are reported be inhibited by methanol, which limits the possibility of increasing the alcohol:oil ratio and/or requires modified processes, for example, the stepwise addition of methanol to the reaction, the use of alcohols with longer alkyl chains, the addition of co-solvents and/or pre-treatments of the enzyme (Chen and Wu, 2003; Salis et al., 2005; Shimada et al., 1999). As the molecular mechanism of the deactivation of lipases is still poorly understood, we aimed at investigating the outcomes of exposing the lipase from *Burkholderia (Pseudomonas) glumae* (BGL) to high methanol concentrations. This enzyme, as all lipases, is organized in an alpha/beta hydrolases fold and has a catalytic center formed by a serine-histidine-glutamic acid triad embedded in a crevice covered by a mobile lid structure that regulates the access to the active site (Lang et al., 1996). BGL is relatively stable to temperature, pH and solvents (Meló et al., 2000; Invernizzi et al. 2009a and b). Also relevant for our purposes is the observation that lipases from

Pseudomonas sp. are usually methanol-tolerant (Noureddini et al., 2005) and, therefore, provide a good tool to investigate the modifications induced by this alcohol in a protein that is otherwise robust and active under the conditions considered. We show that BGL performs well in the alcoholysis of triolein with a final yield of over 90% at reactants molar ratio that correspond to ~75% methanol in the aqueous phase. Methanol, however, affects the stability and the propensity to aggregate of BGL. Inactivation is, therefore, accounted for by conformational damage, rather than by inhibition, as hypothesized for other lipases, for example, the broadly used Candida Antarctica enzyme (Shimada et al. 1999; Fjerbaek et al. 2009).

Materials and Methods

Materials

The enzyme used in this study was the lipase from *B. glumae* (*Chromobacterium viscosum*) 437707 from CalBioChem (San Diego, CA, USA). Triolein from Sigma-Aldrich (St Louis, MO, USA) was ~65% pure. An average molecular weight on 873 g/mol was calculated on the basis of the free fatty acid composition provided by the producer. Methanol, *p*-nitrophenyl laurate, Triton X-100, ammonium acetate, methyl oleate, and oleic acid of analytical grade were from Sigma-Aldrich. Recombinant *Candida rugosa* lipase was expressed in *P. pastoris* and purified as previously described (Brocca et al. 1998; Natalello et al., 2005).

Activity assays

Lipase powder (2.5 mg) was dissolved in 1 ml of de-ionized water. The mixture was vortexed and centrifuged at 11,200 x *g* for 5 min, and the supernatant was used for enzyme assays either directly or diluted by de-ionized water in the case of hydrolysis assays. One Unit *(IU)* was defined as the amount of enzyme which releases 1 μmol of *p*-nitrophenol/min in the hydrolysis reaction described below. Hydrolytic activity was determined by measuring the increase in absorbance at 410 nm produced by the release of *p*-nitrophenol during the hydrolysis of 1 mM *p*-nitrophenyl laurate (dissolved in

isopropanol) in 10 mM ammonium acetate pH 7.2 and 0.5% Triton X-100 at room temperature. To start the reaction, 0.03 IU lipase were added to 1 ml of the reaction mixture. Hydrolysis was followed for 2 min. Measurements were performed in triplicate.

Transesterification activity was assayed in mixtures with different water and methanol contents. Triolein (0.388 g) and methanol were mixed in 1.5-ml screw-cap vials and 10 IU of enzyme solution were added. The reaction mixture was incubated at 37 °C in a rotatory shaker. Methyl oleate (produced by methanolysis) and oleic acid (produced by hydrolysis) were determined by Fourier transform infrared spectroscopy (FTIR) in attenuated total reflection (ATR) mode as described (Natalello et al., 2013). Briefly, after sample centrifugation (11,200 x *g* for 5 min), 5 μL of the organic phase were deposited on the ATR device (Golden Gate, USA), and spectra were collected by a Varian 670-IR (Varian Australia, Mulgrave, Australia) spectrometer under the following conditions: 2 cm^{-1} spectral resolution, 25 kHz scan speed, 512 scan co-additions, triangular apodization, and nitrogen cooled mercury cadmium telluride detector. The second derivatives of the IR absorption spectra were obtained after the Savitsky-Golay smoothing using the Resolutions-PRO software (Varian Australia, Mulgrave, Australia).

The effect of methanol on lipase activity was studied using various amounts of methanol (14.2-85.3 mg) in order to satisfy oil:methanol molar ratios ranging from 1:1 up to 1:6. De-ionized water was added up to a final volume of 550 μl. To study the effect of water, 0-100 mg of de-ionized water were added to a mixture of 0.388 g of triolein and 42.7 mg of methanol (oil:MeOH molar ratio 1:3). The reaction was started by the addition of 10 IU enzyme solution.

Reusability of BGL previously exposed to methanol was evaluated by preparing BGL stocks in aqueous solution in presence of different methanol concentrations. In detail, the stock solutions contained 2.5 mg/ml lipase and 0, 43, 73, and 87 % (v/v) methanol. Preincubation was performed for 24 h at 37 °C in a rotary shaker, followed by centrifugation for 5 min at 11,200 × *g* to separate soluble and insoluble protein fractions. The protein amount in the soluble fraction was determined by the Bradford

assay. An equal volume, corresponding to 10 IU of enzyme in the control sample (0 % methanol), was withdrawn from each supernatant and used to catalyze transesterification in a mixture of 1:5 triglyceride/ methanol. The conversion yields were measured as already described after 24-h incubation at 37 °C.

To assess aggregation, 1.5 μM BGL (0.05 mg/ml) was incubated overnight at 37°C with 0%, 50%,75% methanol. After incubation, the samples were centrifuged at 4 °C for 10 min at 10,000 x *g* to separate soluble and insoluble protein fractions. In order to load comparable amounts of protein, the pellet was resuspended into a volume identical to the supernatant (200 μl), and 20 μl of each fraction was run in 12% SDS-PAGE and stained with SimplyBlu™ SafeStain (Life Technologies, Carlsbad, CA, USA).

Conformational analyses

Circular dichroism and fluorescence experiments were performed on a J-815 spectropolarimeter (JASCO Corporation, Tokyo, Japan) equipped with a Peltier system to control the sample temperature. Commercial BGL powder was suspended in the proper solvent and analyzed, without further purification, after equilibration of the solution for 30 minutes at 20 °C. Thermal ramps were performed in the range 20-85 °C with increments of 5 °C, collecting spectra upon 3-minute equilibration at each temperature. CD spectra were acquired in the far-UV region (190-260 nm) employing a 2-mm path-length quartz cuvette, a data pitch of 0.1 nm and a scan speed of 20 nm/min. Intrinsic fluorescence spectra were acquired employing a 1-cm path-length quartz cuvette, with excitation wavelength 295 nm and emission range 310-450 nm. Mass spectrometry measurements were performed on a hybrid quadrupole time-of-flight spectrometer (QSTAR Elite, AB-Sciex, FosterCity, CA, USA), equipped with a nano-electrospray ionization source. Protein solutions were desalted by "Zeba Spin" columns (Thermo Fisher Scientific, Waltham, MA, USA) before analysis. Metal-coated borosilicate capillaries with emitter tips of 1 μm internal diameter (Proxeon, Odense, Denmark) were used to infuse the samples. The following instrumental setting was applied: declustering potential, 80 V; ion spray voltage, 1.1–1.2 kV; and curtain

gas-pressure, 20 psi. The sample source and instrument interface were kept at room temperature.

FTIR spectra of insoluble BGL were obtained in ATR, as described above for the transesterification activity analyses.

Results

Effects of methanol on the transesterification activity of BGL

We investigated the behaviour of BGL in the reaction of transesterification between triolein and methanol at fixed triglyceride concentration and increasing methanol concentrations (triglyceride:methanol molar ratios from 1:1 up to 1:6, i.e., methanol from 3.3 to 19.6 % of the reaction mix), following by FTIR spectroscopy the formation of both methyl esters and of free fatty acids (FFAs) produced by the competing reaction of hydrolysis. FFAs are revealed directly from the IR absorption spectra in the 1770-1680 cm^{-1} region, where they display the C=O stretching band at ca. 1709 cm^{-1}. This peak can therefore be used to monitor the hydrolysis of the substrates (**Fig. 1a, d**), since it is well separated from the triglycerides and methyl-esters absorptions, occurring in both cases at about 1741 cm^{-1} (Walde and Luisi 1989; Natalello et al., 2013). In the second derivative spectra of the 1485-1425 cm^{-1} spectral region (**Fig. 1b**), the 1435 cm^{-1} peak, due to the CH_3 deformation mode, can be assumed as a marker band of methyl esters formation (see **Fig. 1c**). This is possible thanks to the lack of interference of free fatty acids that, instead, affect the direct analysis of the absorption spectra in the same spectral region (Natalello et al., 2013). **Figure 1** shows the infrared analysis of samples collected after 24-hour reaction at 37°C. We found that the yield of methyl esters increased with methanol concentration up to 1:5 molar ratio (16.4 % methanol that means ~73% methanol in the aqueous phase), converting 78% (v/v) of the substrate within the 24 h of the experiment, while at 1:6 molar ratio the yield was strongly reduced, with 41% (v/v) conversion at the end of the reaction (**Fig. 1c**). As expected, free fatty acids decreased with the triglyceride/methanol ratio from about 27% (v/v) at 1:1 to < 1% (v/v) at 1:6 (**Fig. 1d**).

To gain more detail about the process, we monitored the time course of the reaction at 37°C at triolein/methanol ratios from 1:2 to 1:5 (**Fig. 2**). Under the best performing conditions previously determined (1:5), the concentration of methyl esters increased with time reaching ~55% (v/v) in 10 h, ~78% (v/v) in 24 h (**Fig. 2a**). At suboptimal substrates ratios, the trend of transesterification was similar over the first 10 h of reaction. After this point, however, the reaction profiles diverged as the 1:2 and 1:3 reactions sharply slowed down, possibly due to the exhaustion of the methanol substrate. An interesting time-dependent behavior was observed for the free fatty acids content determined under the same conditions. During the first 2 hours of the 1:4 and 1:5 reactions, free fatty acids rapidly increased, kept almost constant during the subsequent 8 h, and decreased again with time (**Fig. 2b**). This result hints that BGL employs free fatty acids as substrates for esterification when low triglyceride levels remain in the sample solution. On the other hand, in the presence of low methanol (1:2), a progressive increase of free fatty acids was measured being methanol obviously no longer available for transesterification. The relevance of the water content was further investigated taking as a probe the 1:3 condition, where FFAs are constant over the 24 h of the experiment, and adding extra water from 2% to 20% of the total reaction volume. As expected, hydrolysis of triolein gradually increased (**Fig. 3b**), paralleled by a decrease of methyl esters yield in the presence of higher water (**Fig. 3a**). After 48 h reaction, the conversion yields obtained for each tested condition were: 50% (1:2), 72% (1:3), 88% (1:4), 94% (1:5). To evaluate the feasibility of enzyme recycling, BGL was pre-incubated for 24 h at 37°C with 0%, 43%, 73%, 87% (v/v) methanol, and the treated soluble protein was tested in transesterification at 1:5 molar ratio. (**Fig. 4**). Enzymes pre-incubated in 0%, 43%, 73% methanol performed high and comparable conversion yields of ~80% (v/v), while a ~3% conversion was obtained from BGL exposed to 87% methanol, in agreement with the formation of protein precipitate detected in this sample. Indeed, we found that the specific activity of soluble BGL (percent methyl esters produced/mg protein) remained unchanged, thus suggesting that high methanol concentration leads to protein aggregation (see also **Fig. 7**), but it does not interfere with protein activity. To summarize, these experiments

showed that, under the conditions used for analysis, BGL exerts its highest transesterification activity at 1:5 triolein:alcohol molar ratio, though the theoretical optimal balance should reflect the reaction stoichiometry (1:3). However, quantification of the competing reaction of hydrolysis accounts for the need of excess methanol to boost methanolysis and esterification of FFAs over hydrolysis. A further observation of interest is that this lipase is quite robust towards methanol, though inactivation is often reported during alcoholysis for the production of biodiesel (Fjerbaek et al., 2009; Parawira 2009). At this point it was relevant to investigate the impact of methanol on the enzyme structure.

Effects of methanol on BGL conformation and stability

To this end, we analyzed the protein secondary and tertiary structure in the presence of variable concentrations of alcohol by means of MS, CD, and intrinsic fluorescence. We focused in particular on methanol in the range 50%-75% to approximate the composition of the aqueous phase in the transesterification assays supporting highest conversion yields. The charge-state distributions obtained by nano-electrospray ionization mass spectrometry (nano-ESI-MS) under mild conditions, in the presence or absence of methanol, were very similar (**Fig. 5a, b**). Indeed both spectra were quite narrow and showed relatively low charge states (main charge state 11+). These features are typical of the compact tertiary structure of folded, globular proteins. Methanol therefore does not induce major conformational transitions in BGL at room temperature as the protein seems to maintain a compact, native-like conformation. The only noticeable difference between the two spectra was detected in the high *m/z* region, where small amounts of protein dimers were detectable in the control and disappeared in the presence of methanol, highlighting a small propensity of the folded protein to associate into dimers in aqueous solution. **Fig. 5c** shows a comparison of the far-UV CD spectra recorded under these conditions, which are well superimposable. The protein displayed the typical features of a mixed α/β fold with negative minima at 209 and 220 nm and a positive maximum at 193 nm. This set of results provided evidence that also the protein secondary structure is not affected by high methanol at room

temperature. Similar MS and CD data were obtained at lower concentrations of methanol (data not shown). For comparison, the same CD experiment has been performed on *Candida rugosa* lipase, a methanol-sensitive enzyme (Natalello et al., 2013). The results highlight that 50% methanol induces a strong change in the protein secondary structure, with an increase in β-structure content, even at 20 °C (**Figure S1**, Supplementary Material) and suggest that the response to methanol is highly protein specific. On this basis we wondered whether methanol might impact on BGL stability under transesterification conditions and, more broadly, on its stability towards heat and denaturants. Therefore, we characterized the heat denaturation of BGL in the presence of different methanol concentrations by far-UV CD and intrinsic fluorescence to monitor, respectively, changes in secondary and tertiary structure. **Fig. 6a** shows the far-UV CD spectra recorded during a temperature ramp in the absence of methanol. As the temperature increased, the ellipticity at 193 and 220 nm was progressively lost, consistently with denaturation of the protein secondary structure. The transition was characterized by an isodichroic point at 206 nm, consistent with the α/β fold of the native protein. The profile of the transition monitored by the ellipticity at 222 nm and its response to increasing methanol concentrations showed that the T_m shifts from ~65 °C at 0% methanol to ~52 °C at 50% methanol, demonstrating that the alcohol destabilizes BGL towards temperature (**Fig. 6b**). The initial and final states of the transitions in the range 15-50% methanol were similar to those observed in its absence and were characterized by the same isodichroic point (data not shown), while a peculiar behaviour was detected at 75% methanol. Indeed, the ellipticity at 222 nm changed much slower and to a lower extent during the temperature ramp, compared to the lower alcohol concentrations (**Fig. 6b**). Therefore, the raw data recorded at 75% methanol are reported separately in **Fig. 6c** where the difference with the transition displayed by the control sample (**Fig. 6a**) can be better appreciated and suggests the involvement of an α-to-β conversion. The final spectrum at 85 °C and 75% methanol was characterized by a negative minimum at 217 nm and a positive maximum at 196 nm, typical of highly β structures. We conclude that unfolded BGL in 75% methanol maintains much more ordered secondary structure than the unfolded protein at lower

methanol concentrations, with a predominance of β conformation. Thus, thermal denaturation in the presence of low or high methanol concentrations results in different denatured states. To gain information about possible structural changes, BGL denaturation by heat was monitored also by intrinsic fluorescence (**Fig. 6d**). A progressive fluorescence quenching was detected, along with a red-shift of the fluorescence emission peak. In addition, this transition was affected by methanol, with a shift of approximately 20 °C in T_m (considering both intensity and λmax) from 0% to 75% methanol (**Fig. 6e, f**). In this case, the trend of the response to methanol kept quite constant up to 75%, showing that the tryptophan environment is affected in a similar way in the denatured state at low and high methanol concentration. As the data above suggested that methanol promotes the formation of beta structures in the heat-denatured state (**Fig. 6c**), it was of interest to assess whether methanol-exposed BGL is prone to aggregation. The lipase was therefore incubated overnight (17 h) at 37°C – the temperature applied in the reactions of transesterification - in the presence of 0, 50 and 75% methanol and analysed for solubility by denaturing gel electrophoresis (**Fig. 7a**). While in the absence of methanol, the protein was almost completely soluble, at 50 and 75% methanol, a growing amount of BGL was found in the pellet containing the insoluble proteins fractions. The protein pellet collected upon incubation with 75% methanol was analyzed by FTIR (**Fig. 7b**) in order to assess its secondary-structure composition. The spectrum showed remarkable differences compared to the reference spectrum of the soluble protein. In particular, the characteristic bands of native secondary structure at 1652 and 1631 cm^{-1} (α-helices and intramolecular β-sheets) were lost and two bands at 1696 and 1623 cm^{-1}, diagnostic of intermolecular β-sheets, accumulated, becoming the only residual prominent features of the spectrum (Natalello et al., 2005; Barth 2007). These results indicated that the protein denatures and precipitates into a highly intermolecular β-sheet structures upon prolonged incubations under transesterification conditions at high methanol concentrations. Although we are aware that the conditions used for biophysical measurements cannot fully reproduce the environment to which the enzyme is exposed during the reaction (presence of a hydrophobic substrate, mixing of the two phases), we would conclude with some

confidence that methanol in the range 50-75% affects BGL stability, and that this effect can become relevant to the effeciency of transesterification at standard temperature. For the sake of completeness, we tested also how methanol impacts on the stability of BGL towards acids following the enzyme denaturation by fluorescence and far-UV CD between pH 7 and 2.5 and 0-50% methanol (**Fig. 8**). The CD spectra in the absence of methanol showed changes similar to those induced by thermal denaturation (**Fig. 8a**), even if without a clear isodichroic point. The results at 50% methanol (**Fig. 8b**) indicated that the nature of the transition already changed to an α-to-β conversion, as seen for heat denaturation at 75% methanol. The final fluorescence spectrum at pH 2.5 and 50% methanol was remarkably more red-shifted (**Fig. 8c, d**) and the residual content in ordered secondary structure revealed by CD much higher (**Fig. 8a, b**) than in the control sample without methanol. While MS cannot be used for accurate analysis of temperature effects, it can be used for measurements at variable pH. **Fig. 9** shows a comparison of nano-ESI-MS spectra acquired at 0 and 50% methanol and variable concentrations of formic acid. In the absence of methanol, protein unfolding was observed between pH 2.8 and pH 2.65, as indicated by the appearance of a new peak envelope at high charge states (25+) at pH 2.65 (**Fig. 9b**). Under these conditions also a partially folded form (18+) accumulated. In agreement with the lack of an isodichroic point in CD titrations, this result indicates that BGL acidic unfolding involves at least one intermediate (Pauwels at al., 2012). A different response was observed at 50% methanol, as the protein was already largely denatured at pH 2.8 (**Fig. 9c**) and almost completely unfolded at pH 2.65 (**Fig. 9d**). Furthermore, the denatured state was different, resulting in a more extended protein conformation in the presence of methanol (29+ instead of 25+, **Fig. 9d, b**). As in the sample without methanol, a folding intermediate accumulated during the transition (18+) (**Fig. 9c, d**).

In conclusion, as already seen for heat denaturation, methanol destabilizes BGL also against acidic denaturation, and produces denatured proteins characterized by substantial amounts of ordered, mainly β, secondary structure and therefore prone to aggregation.

Discussion

In this work, we aimed at gaining biochemical and conformational information about the behavior of a bacterial lipase in the reaction of enzymatic transesterification of triglycerides and methanol for the production of alkyl esters. This is a particular point of view from which to tackle the issue of the relationships between water miscible organic solvents and enzymes, since in this case methanol acts as a reactions substrate. In the reaction considered here, the optimal ratio between the two reactants is expected to be 1:3, i.e. 1 mole of triglyceride each 3 moles of methanol. In our case however, as reported also by others (Parawira 2009), the yield of the process is increased at a higher content of methanol (1:5). This effect might depend on two peculiarities of the process. The first one is that also free fatty acids present in triglycerides solutions contribute to transesterification. This is the standard situation observed not only in raw oils but also in the commercial triolein used in this study. The fraction of FFAs can further increase when systems also contain water, as it is the case of re-cycled waste oil (Hsu et al., 2003; Canakci 2007). Lipases, in fact, catalyze both the hydrolysis and the synthesis of ester bonds, according to the environment. While in the presence of limited water alcoholysis predominates, when enough water is available hydrolysis can compete leading to the formation of free fatty acids, besides alkyl esters.

While increasing methanol should favor transesterification, several lipases are known to undergo methanol deactivation. We have chosen to use an enzyme that belongs to the group of the *Pseudomonas/Burkholederia* lipases that are known to be relatively methanol- tolerant. Already the observation that some lipases are more sensitive than others to methanol inactivation is a challenging issue, since their robustness is apparently not related to other general properties, for example to thermal stability. At present, a systematic investigation is still lacking, neither it is possible to generalize about the biochemical effects of alcohols from the available literature, since the set up of the reactions can differ as for several parameters, for example, the starting materials used, temperature, time, co-solvents. In this study, therefore, we aimed at performing a careful analysis of the consequences of increasing methanol concentrations on the kinetics and yield of the transesterification reaction catalyzed by BGL and relating

biochemical and structural data. Since the oil component hampers spectroscopic measurements, it has been excluded from the incubation mixtures. However, we wish to point out that in an aqueous mixture of water soluble (methanol) and insoluble (triolein) components, the enzyme is dissolved in the aqueous phase and approaches the substrate at the interface between the two phases. Thus, even if the conditions applied for conformational analysis do not exactly mimic the environment to which the enzyme is exposed, they reproduce the composition of the aqueous phase where the enzyme is dissolved during the reaction. Biophysical analysis on BGL samples exposed to 0-75% methanol helped us to rule out that lipase deactivation is due to a methanol-mediated inhibition. As a matter of fact, we observed that high methanol, while boosting the rate of product formation, affects the stability of the enzyme even at a mild process temperature (37°C). Such a perturbation induces partial unfolding that in turn might cause the onset of protein aggregation.

In conclusion, our data provide evidence that the decrease in the rate of BGL-catalyzed transesterification is due to loss of the enzyme available rather than to a reduction of its activity. In this picture, the decreased rate of conversion observed in the 1:6 ratio conditions can be ascribed to the enzyme being almost fully denatured. We feel confident that information about the determinants of enzymes robustness towards methanol may be of relevance not only for this specific reaction but also in the broader context of biocatalysis, in reactions in which methanol and other water-miscible solvents added to improve substrates solubility may inactivate the enzyme instead (Secundo et al., 2010; Őztűrk et al., 2010).

Acknowledgements

This work was partly supported by a grant of the Regione Lombardia (ASTIL) to M.L.. F.S. acknowledges a PhD fellowship from the University of Milano-Bicocca.

References

Adamczak M, Bornscheuer UY, Bednarski W (2009) The application of biotechnological methods for the synthesis of biodiesel. Eur J Lipid Sci Technol 111: 808-813

Barth A (2007) Infrared spectroscopy of proteins. BBA-Bioenergetics 1767: 1073-1101

Bommarius AS, Riebel BR (2004) Biocatalysis. Fundamentals and Applications. Wiley-VCH Verlag, Weinheim

Brocca S, Schmidt-Dannert C, Lotti M, Alberghina L, Schmid R (1998) Design, total synthesis, and functional overexpression of the *Candida rugosa lipI* gene coding for a major industrial lipase. Protein Sci 7:1415-1422

Canakci M (2007) The potential of restaurant waste lipids as biodiesel feedstocks. Bioresour Technol 98: 183-190

Carrea G, Riva S (2000) Properties and synthetic applications of enzymes in organic solvents. Angew Chem Int Ed 39: 2226-2254

Chen JW, Wu WT (2003) Regeneration of immobilized *Candida Antarctica* lipase for transesterification. J Biosci Bioeng 95(5): 466-469

Faber K (2011) Biotransformations in Organic Chemistry: A Textbook. Springer-Verlag Gmbh; 6th Edition

Fjerbaek L, Christensen KV, Borddahl B (2009) A review of the current state of biodiesel production using enzymatic transesterification. Biotechnol Bioeng 102 (5): 1298-1315

Hsu A-F, Jones KC, Foglia TA, Marmer WN (2003) Optimisation of alkyl ester production from grease using a phyllosilicate sol-gel immobilised lipase. Biotechnol Lett 25: 1713-1716

Invernizzi G, Casiraghi L, Grandori R, Lotti M (2009a) Deactivation and unfolding are uncoupled in a bacterial lipase exposed to heat, low pH and organic solvents. J Biotechnol 141: 42-46

Invernizzi G, Papaleo E, Grandori R, De Gioia L, Lotti M (2009b) Relevance of metal ions for lipase stability: structural rearrangements induced in the *Burkholderia glumae* lipase by calcium depletion. J Struct Biol 168: 562-570

Lang D, Hofmann B, Haalck L, Hecht HJ, Spener F, Schmid RD, Schomburg D (1996) Crystal structure of a bacterial lipase from *Chromobacterium viscosum* ATCC6918 refined at 1.6 Angstroms resolution. J Mol Biol 259: 704-717

Meló EP, Taipa MA, Castellar MR, Costa SMB, Cabral JMS (2000) A spectroscopical analysis of thermal stability of the *Chromobacterium viscosum* lipase. Biophys Chem 87: 111–120

Natalello A, Ami D, Brocca S, Lotti M, Doglia SM (2005) Secondary structure, conformational stability and glycosylation of a recombinant *Candida rugosa* lipase studied by Fourier-transform infrared spectroscopy. Biochem. J. 385: 511-517.

Natalello A, Sasso F, Secundo F (2013) Enzymatic transesterification monitored by a new easy-to-use Fourier transform infrared spectroscopy method. Biotechnol J 8(1):133-138

Noureddini H, Gao X, Philkana RS (2005) Immobilized *Pseudomonas cepacia* lipase for biodiesel fuel production from soybean oil. Bioresour Technol 96(7):769–777

Őztűrk DC, Kazan D, Denizci AA, Grimoldi D, Secundo F, Erarslan A (2010) Water miscible mono alcohols effect on the structural conformation of *Bacillus clausii* GMBAE 42 serine alkaline protease. J Mol Catal B-Enzym 64: 184–188

Parawira W (2009) Biotechnological production of biodiesel fuel using biocatalyzed transesterification: a review. Crit Rev Biotechnol 29 (2): 82-93

Pauwels K, Sanchez del Pino MM, Feller G, Van Gelder P (2012) Decoding the folding of *Burkholderia glumae* lipase: folding intermediates *en route* to kinetic stability. PLoS ONE 7: e36999

Salis A, Pinna M, Monduzzi M, Solinas V (2005) Biodiesel production from triolein and short chain alcohols through biocatalysis. J Biotechnol 119(3): 291–299

Secundo F, Fialà S, Fraaije MW, De Gonzalo G, Meli M, Zambianchi F, Ottolina G (2011) Effects of water miscible organic solvents on the activity and conformation of the Baeyer-Villiger monooxigenases from *Thermobifida fusca* and *Acinetobacter calcoaceticus*: a comparative study. Biotechnology and Bioengineering 108 (3): 491-499

Shimada Y, Watanabe Y, Samukawa T, Sugihara A, Noda H, Fukuda H, Tominaga Y (1999) Conversion of vegetable oil to biodiesel using immobilised *Candida antarctica* lipase. J Am Oil Chem Soc 76(7): 789–793

Walde P, Luisi PL (1989) A Continuous Assay for Lipases in Reverse Micelles Based on Fourier Transform Infrared Spectroscopy Biochemistry *28*: 3353-3360

Figures and legends

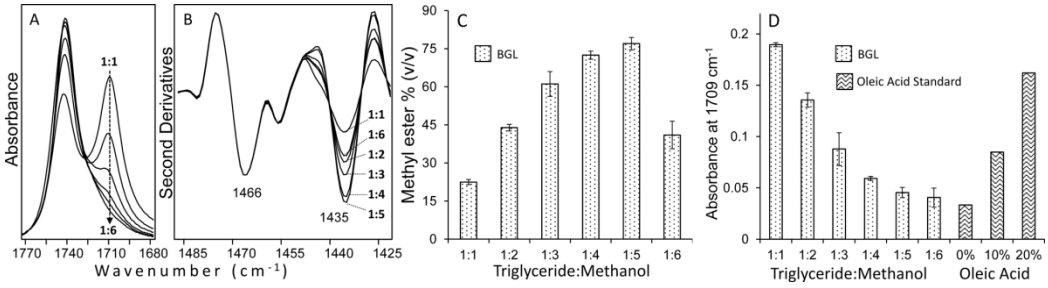

Fig. 1 Effect of methanol on BGL activity. FTIR analysis of samples collected after 24 h of reaction at 37°C. The reported molar ratios correspond to the following methanol percentages in the total volume of the reaction (1:1=3.3 % methanol; 1:2=6.5 %; 1:3=9.8 %; 1:4=13.1 %; 1:5=16.4%; 1:6=19.6 %). **a** FTIR absorption spectra in the region reporting on free fatty acids taken from samples at increasing methanol molar ratio (*dotted line*). **b** Second derivatives of the FTIR absorption spectra in the spectral region reporting on methyl esters. The different molar ratios are indicated in the spectra, which are normalized at the CH_2 peak at 1466 cm^{-1} to compensate for possible differences in the sample amount. **c** Yields of transesterification at different triglyceride/methanol ratios measured as methyl ester content (volume percentage). Values have been obtained from the 1435 cm^{-1} peak intensities in the second derivative spectra (**b**) using a linear calibration curve. **d** Substrate hydrolysis at different triglyceride/methanol ratios calculated from the IR absorption at 1709 cm^{-1} (**a**). The 1709 cm^{-1} absorbances of standard solutions, containing the substrate and 0%, 10 % (v/v) or 20% (v/v) of oleic acid, are also reported for comparison. Standard deviations refer to three independent experiments.

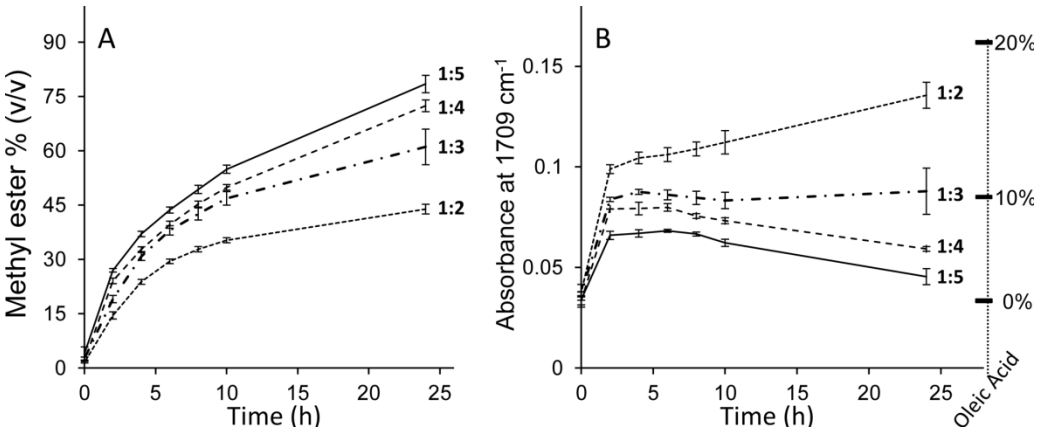

Fig. 2 Time course of transesterification and hydrolysis reactions at different triglyceride/methanol molar ratios. Samples were collected at different time points of incubation at 37°C at 1:2 to 1:5 triglyceride/methanol ratios and analyzed for methylesters (**a**) and free fatty acids (**b**) as in Fig. 1. In **b**, the 1709 cm^{-1} absorbances of standard solutions containing the substrate and 0%, 10 % (v/v) or 20% (v/v) of oleic acid, are also reported for comparison (see Y right axis). Standard deviations refer to three independent experiments.

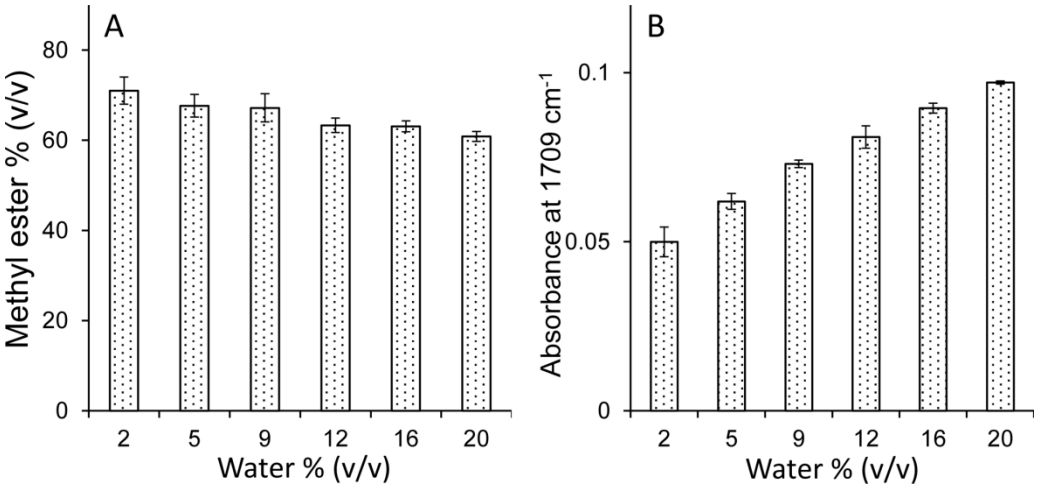

Fig. 3 Effect of water addition on transesterification and hydrolysis. Methyl esters (**a**) and free fatty acids (**b**) content in samples collected after 24 hours of reaction at 37°C

and 1:3 triglyceride/methanol molar ratio and growing percentages of water. Values are calculated as in Fig. 1 and 2. Standard deviations refer to three independent experiments.

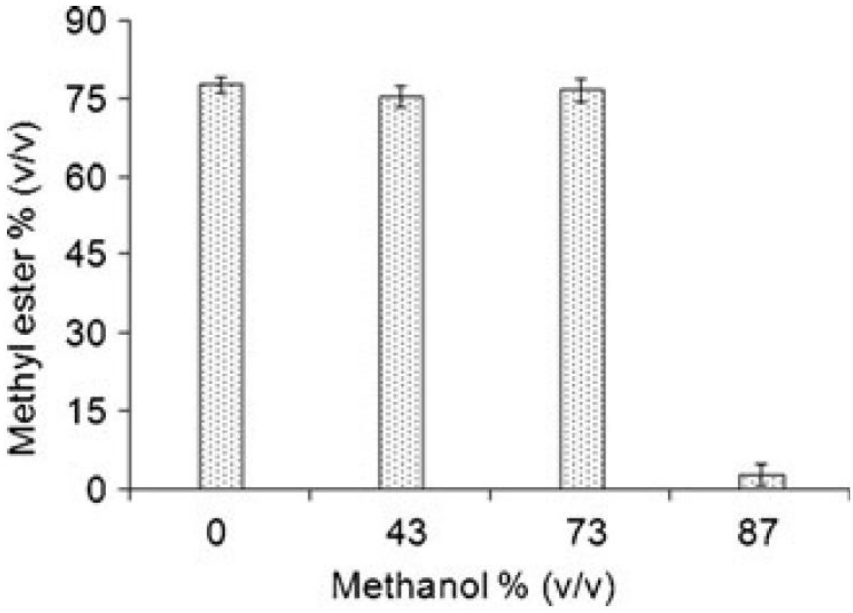

Fig. 4 Enzyme recycling. BGL samples were pre-incubated with 0%, 43%, 73%, 87% methanol (v/v). After 24 hours the soluble enzyme was recovered and assayed in transesterification at 1:5 substrates molar ratio. Standard deviations refer to three independent experiments.

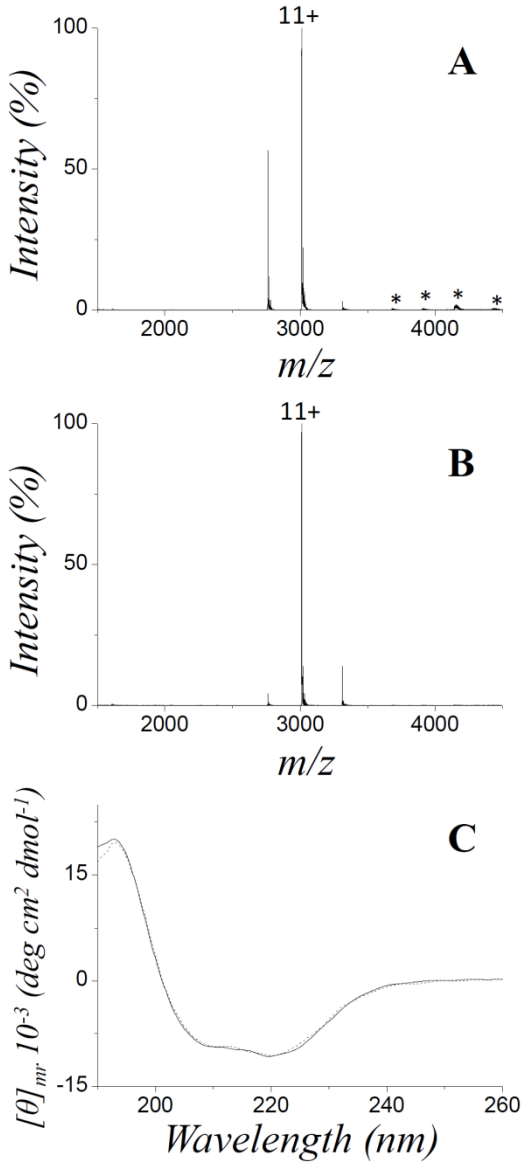

Fig. 5 Conformational analysis. **a**, **b** Nano-ESI-MS spectra of 5 µM BGL in 10 mM ammonium acetate, pH 7, in the presence of 0% (**a**) or 50% (**b**) methanol (v/v). The most intense peak is labeled by the corresponding charge state. The signals due to the dimeric form are labeled by asterisks. **c** Circular dichroism spectra of 1.5 µM BGL in 10 mM sodium phosphate buffer, pH 7, in the presence of 0% (*continuous line*) or 50% (*dotted line*) methanol. Spectra from samples incubated with 75% methanol were identical to those obtained in 50% methanol (data not shown).

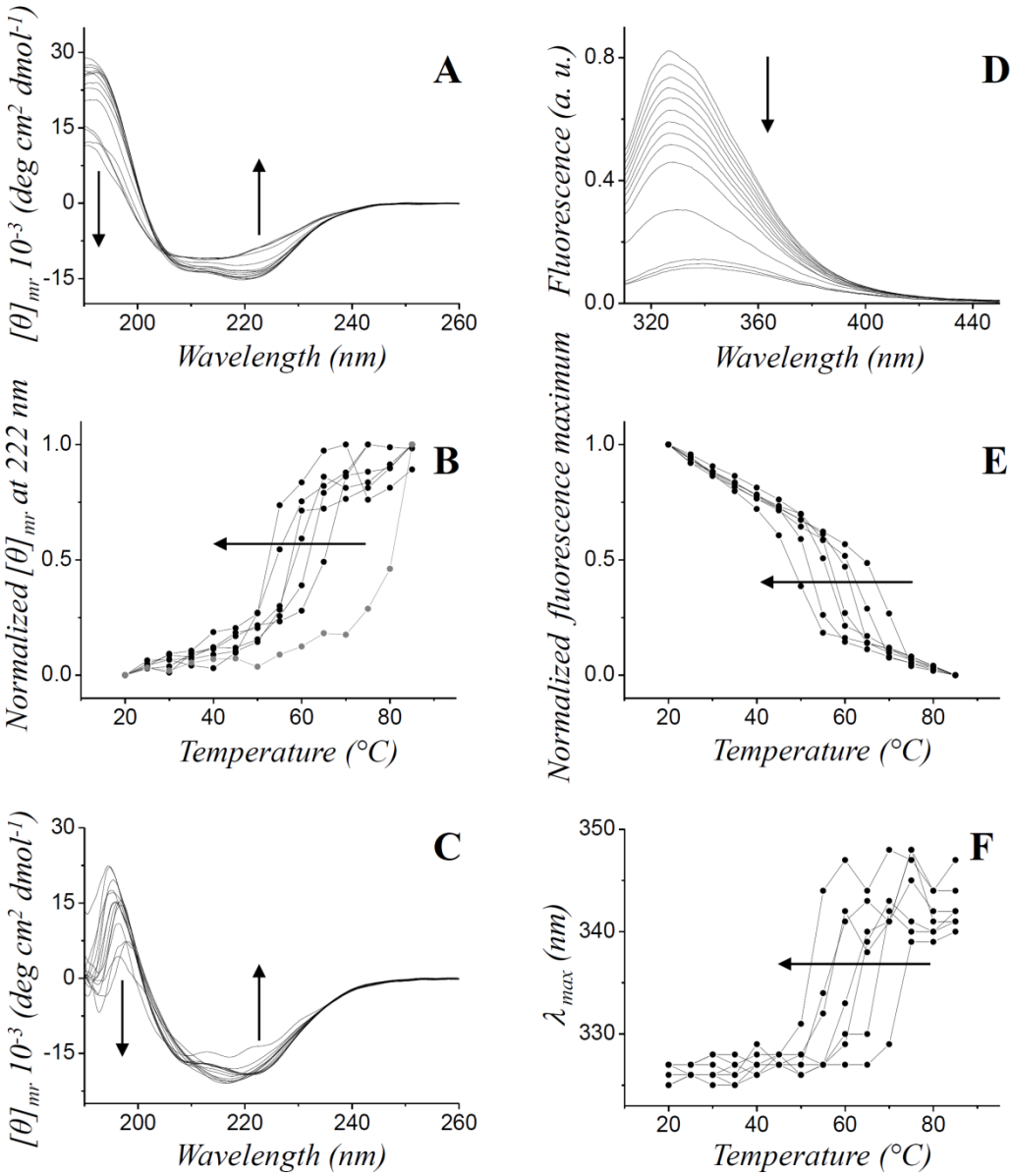

Fig. 6 Denaturation by heat. **a-c** Circular dichroism. **d-f** Intrinsic fluorescence. Samples of 1.5 µM BGL in 10 mM sodium phosphate buffer, pH 7, were analyzed in the presence of different methanol concentrations (0-75%) and temperature increasing from 20 to 85 °C, with increments of 5 °C. **a** CD spectra from a temperature ramp at 0% methanol. **b** Profiles of mean residue ellipticity at 222 nm as a function of temperature at different methanol concentrations: 0 % (*solid circles*), 15 % (*empty*

circles), 26 % (*solid squares*), 34 % (*empty squares*), 41 % (*solid triangles*), 50 % (*empty triangles*), and 75 % (*solid stars*). The profile at 75% methanol is reported in *gray*. **c** CD spectra from a temperature ramp at 75% methanol. **d** Fluorescence spectra from a temperature ramp at 0% methanol. **e** Profiles of fluorescence intensity as a function of temperature at different methanol concentrations (same symbols as in **b**). **f** Profiles of fluorescence peak position as a function of temperature at different methanol concentrations. *Arrows* indicate the direction of the effect at increasing temperature or methanol concentrations.

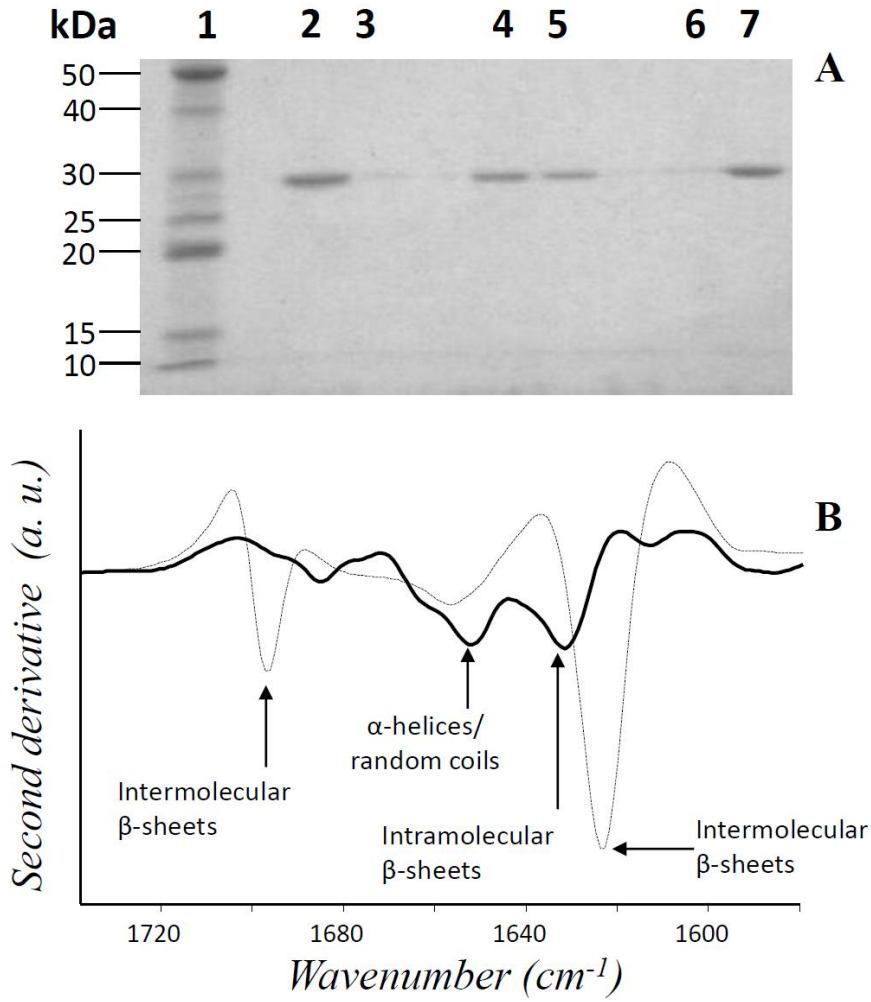

Fig. 7 Protein aggregation. **a** Coomassie Blue-stained sodium dodecyl sulfate polyacrylamide gel electrophoresis of BGL after over-night incubation at 37 °C, 1.5 µM protein concentration in 10 mM sodium phosphate buffer, pH 7, in the presence of 0% (*lanes 2* and *3*), 50% (*lanes 4* and *5*) and 75% (*lanes 6* and *7*) methanol. After incubation, the samples were centrifuged and comparable aliquots of the supernatant (*lanes 2*, *4* and *6*) and the pellet (*lanes 3*, *5* and *7*) were loaded on the gel. *Lane 1* contains the molecular-weigh markers. **b** Second-derivative FTIR spectra of BGL in water (*continuous line*) and in the pellet after overnight incubation at 37 °C, 1.5 µM protein concentration in 10 mM sodium phosphate buffer, pH 7, 75% methanol (*dashed line*). Data are normalized to the Amide-I area.

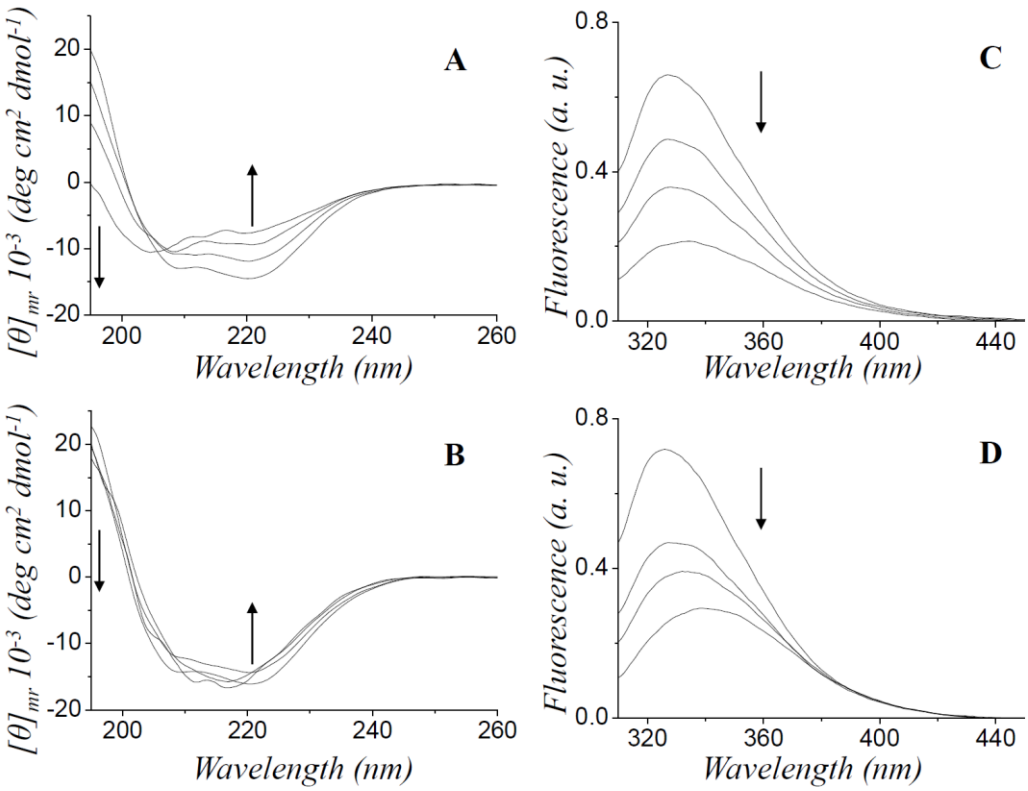

Fig. 8 Denaturation by acids. **a**, **b** Circular dichroism. **c**, **d** Intrinsic fluorescence. Samples containing 1.5 µM BGL in 10 mM sodium phosphate buffer are analyzed in the presence of 0% (**a**, **c**) and 50% (**b**, **d**) methanol at variable pH 7 (*thin continuous line*), 2.8 (*dashed line*), 2.65 (*thick continuous line*), and 2.5 (*dotted line*). *Arrows* indicate the direction of the effect at decreasing pH.

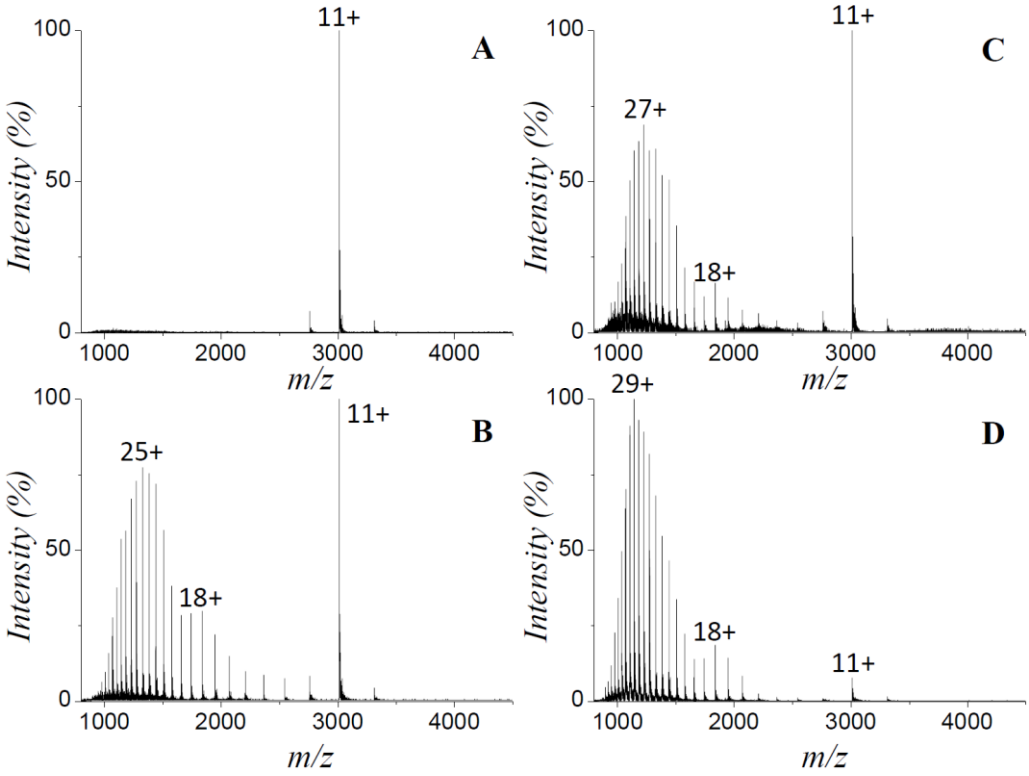

Fig. 9 Denaturation by acids. Nano-ESI-MS spectra of 5 µM BGL in 10 mM ammonium acetate in the presence of 0% (**a**, **b**) or 50% (**c**, **d**) methanol and pH 2.8 (**a, c**) or pH 2.65 (**b, d**). *Numeric labels* indicate the most intense charge state of each peak envelope.

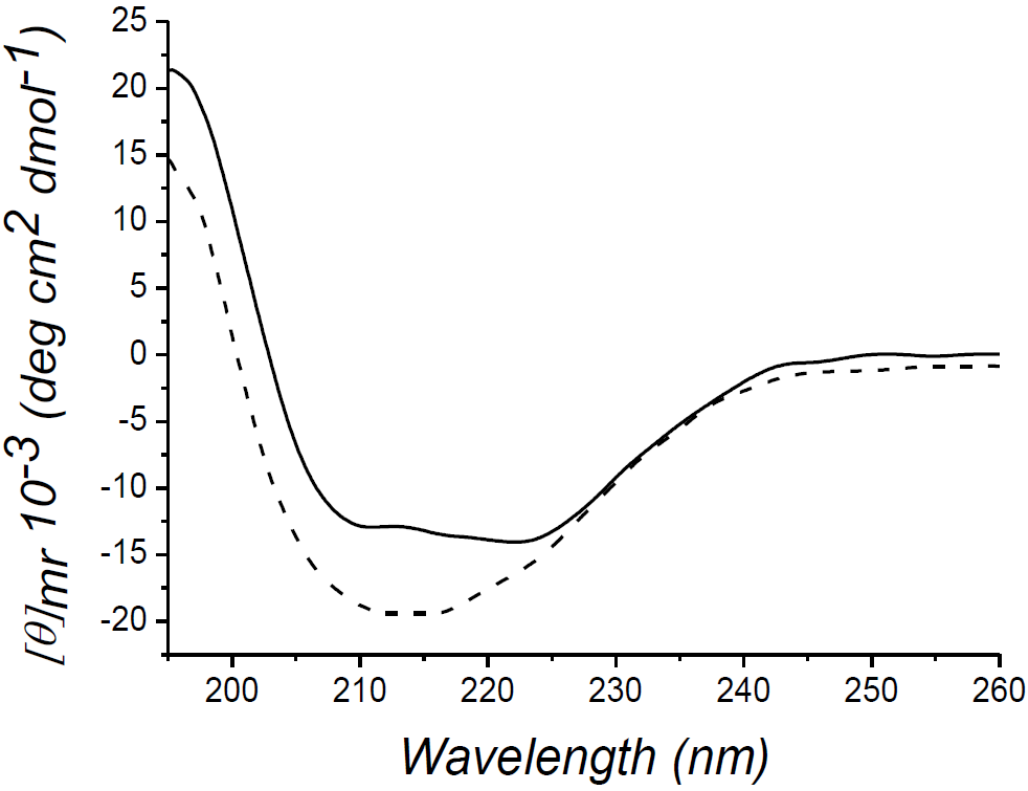

Figure S1. Circular dichroism spectra of 1.5 μM *Candida rugosa* lipase in 10 mM sodium phosphate buffer, pH 7, in the presence of 0% (*continuous line*) or 50% (*dashed line*) methanol.

2.2.2 Effects of methanol on the initial rate of methanolysis of vinyl acetate by BGL (Preliminary results)

The effect of methanol on the initial rate of BGL activity was also investigated. To this end, we chose the same system explored for CALB, i.e the transesterification of vinyl acetate and methanol in presence of toluene (see sections 2.2.3)

Materials

The lipase from *B. glumae* (*Chromobacterium viscosum*) 437707 was purchased from CalBioChem (San Diego, CA, USA). Aliquots (67 μl) containing 30 μg of BGL dissolved in 10 mM buffer phosphate pH 7, were frozen at −80 °C and lyophilized. Anhydrous toluene, vinyl acetate, methanol, cesium fluoride were purchased from Sigma–Aldrich. Before the reaction, toluene, vinyl acetate, and lipase samples were equilibrated separately at a water activity (a_w) value equal to 0.02 at least for 24 h, at 25 °C, in sealed vessels, with the vapor phase of a saturated CsF solution. Methanol was brought to the desired water activity by mixing anhydrous methanol (≤0.002% water) with a proper water amount according to Bell *et al*. (1997).

Alcoholysis reaction and analysis

The activity of commercial BGL in toluene was determined by measuring the initial rate (v_0) of alcoholysis, detecting the formation of methyl acetate. A reaction mixture made of vinyl acetate, methanol, and toluene (up to a final volume of 1 mL) was mixed to 30 μg of lipase. The reaction mixture was shaken at 125 shots per min in a horizontal shaker, at 25 °C. After 3 min from the

reaction start, the production of methyl acetate was detected by gas chromatography, as described in Paper III.

Effects of methanol on BGL activity

The effect of methanol on lipase activity was studied performing reactions at constant vinyl acetate (15.2% (vol/vol)) in the presence of the following methanol amounts: 0.2%, 0.7%, 5%, 10% and 60% v/v. All the reactions were performed at a_w value equal to 0.02.

BGL has almost no activity at methanol percentage of 0.02%, while its specific activity increases dramatically for higher concentrations of alcohol (**Figure 10).** At 60% methanol, BGL specific activity is 200-fold higher than at the lowest alcohol content assayed. This experiment clearly shows that, differently from what happens to CALB, BGL is not inhibited by methanol.

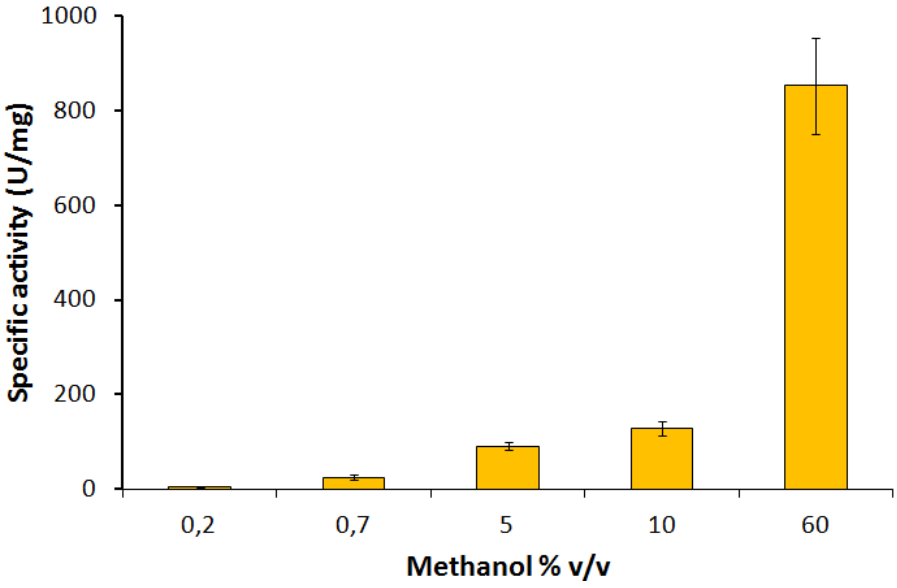

Figure 10. Initial rate (expressed as specific activity) of alcoholysis catalyzed by BGL at different methanol concentrations and a_w= 0.02. Standard deviations refer to three independent experiments.

2.2.3 Paper III

Molecular mechanism of deactivation of *C. antarctica* lipase B by methanol

T Kulschewski, F Sasso, F Secundo, M Lotti, J Pleiss, SM (Journal of Biotechnology 2013, *168*, 462-469)

Molecular mechanism of deactivation of *C. antarctica* lipase B by methanol

J Biotechnol 2013 Dec; 168(4):462-9

Tobias Kulschewski[1#], Francesco Sasso[2#], Francesco Secundo[3], Marina Lotti[2], Jürgen Pleiss[1*]

[1] Institute of Technical Biochemistry, University of Stuttgart, Allmandring 31, 70569 Stuttgart, Germany

[2] Dept. Biotechnology and Biosciences – University of Milano-Bicocca, Piazza della Scienza 2, 20126 Milan, Italy

[3] Institute of Chemistry of Molecular Recognition, National Research Council, Via Mario Bianco 9, 20131 Milan, Italy

[#] contributed equally

[*] Corresponding author:

Prof. Dr. Jürgen Pleiss
Institute of Technical Biochemistry
University of Stuttgart
Allmandring 31
D-70569 Stuttgart
Germany
Phone: (+49) 711-68563191
E-mail: Juergen.Pleiss@itb.uni-stuttgart.de

Short title: Molecular mechanism of deactivation of CALB by methanol

Keywords: model; thermodynamic activity; toluene; vinyl acetate

Abstract

The catalytic activity of *C. antarctica* lipase B upon alcoholysis of a constant concentration of 15.2% vinyl acetate (vol/vol) and varying concentrations of methanol (0.7-60%) in toluene was determined experimentally by measuring the initial reaction velocity. The molecular mechanism of the deactivation of the enzyme by methanol was investigated by fitting the experimental data to a kinetic model and by molecular dynamics simulations of *C. antarctica* lipase B in toluene-methanol-water mixtures.

The highest catalytic activity (280 U/mg) was observed at methanol concentrations as low as 0.7 % methanol (vol/vol), followed by a sharp decrease at higher methanol concentrations. For methanol concentrations above 10 % (vol/vol), catalytic activity was at 30 % of the maximum activity. A variation of water activity in the range 0.02 - 0.09 had only minor effects. These experimental observations are described by a simple kinetic model using three assumptions: (1) a ping-pong bi-bi mechanism of the enzyme, (2) competitive inhibition by the substrate methanol, and (3) by describing enzyme kinetics by the thermodynamic activities of the substrates rather than by their concentrations. Two equilibrium constants of methanol ($K_{M,MeOH}$ = 0.05 and $K_{i,MeOH}$ = 0.23) were derived by modeling methanol binding to the substrate binding site of the lipase in molecular dynamics simulations of protein-solvent systems at atomic resolution.

Thus, the sharp maximum of catalytic activity of *C. antarctica* lipase B at 0.7 % methanol is a direct consequence of the fact that methanol-toluene mixtures are far from ideal. Understanding the thermodynamics of solvent mixtures is prerequisite to a quantitative model of enzymatic activity in organic solvents.

1. Introduction

Since the first systematic studies on the catalytic activity of enzymes in organic solvents (Sym, 1936; Zaks et al., 1988), it was recognized that in non-aqueous solvents catalytic activity and substrate specificity depend not only on the structure and concentration of the substrates, but also on the choice of the organic solvent and the water content (Degn et al., 2001; Laane et al., 1987). Thus, solvent engineering served as a promising strategy to improve the performance of biocatalysts in synthetic applications (Castillo et al., 2003; Edmundo et al., 1998). There are four factors on how organic solvents might mediate the enzyme-catalyzed reaction: by changing the structure or dynamics of the enzyme's binding site, by competitive binding of the organic solvent molecules, by removal of protein-bound water, or by improved solubility of hydrophobic substrates. Careful modeling studies have been performed to investigate the molecular mechanisms of these factors.

The effect of solvent to structure and dynamics of enzymes have been studied thoroughly. It was suggested that the effect of organic solvents on an enzyme is primarily caused by the interactions between the organic solvent and the enzyme-bound water, and that a low amount of water is required to provide sufficient conformational flexibility to the enzyme (Zaks et al., 1988). At least two types of mechanisms how solvent interacts with an enzyme have been suggested: the dielectric constant (logP, hydrophobicity) of the organic solvent (Affleck et al., 1992) and its molecular volume (Ottosson et al., 2002b). It was shown that changing the solvent and increasing the pressure can substantially change the structure of the active site. While in most cases enthalpy (and thus the shape of the binding site) drives enantioselectivity, sometimes entropy is driving enantioselectivity, such as the experimentally observed preference of *C. antarctica* lipase B for the (*R*)-enantiomer of 3-hexanol. Molecular dynamics simulations concluded that the preference towards the (*R*)-enantiomer is caused by the fact that it accessed a larger volume within the active site than the non-preferred enantiomer, which is in agreement with the higher entropy of (*R*)-3-hexanol in its transition state (Ottosson et al., 2002a). It has been shown that organic solvents affect the flexibility of enzymes, therefore it might be a second mechanism of how

catalytic activity and enantioselectivity are changed by organic solvents. The correlation between the internal protein mobility and the enantioselectivity was noted (Broos et al., 1995). Similarly, the conformational flexibility of subtilisin affected its ability to discriminate between enantiomeric amino acid and ester substrates for the subtilisin-catalyzed reaction in an organic solvent (Watanabe et al., 2004). As a third mechanism how organic solvents might affect catalytic activity, it has been proposed that solvent molecules could block the substrate binding site. When the effect of six solvents to the catalytic activity of *C. antarctica* lipase B was studied in a solid/gas reactor (Graber et al., 2007), it was shown that two ketones reduced the enzyme activity whereas two tertiary alcohols and two hydrocarbons did not. Molecular modeling of three solvents predicted that a ketone and a tertiary alcohol bound to the active site, but one of the hydrocarbons did not. Thus, competitive inhibition by organic solvent molecules might contribute to the effect of solvents.

By varying the thermodynamic activity of water in organic solvents, it has been shown that residual water has a major impact on stability, catalytic activity, and selectivity (Lee et al., 1995). Molecular dynamics simulations of *C.rugosa* lipase in organic solvent at a low water content demonstrated that water molecules might change the shape of the active site (Kahlow et al., 2001). For cutinase, the enantioselectivity in hexane under varying hydration conditions was studied by free energy simulations which were in accordance with experimental data (Micaelo et al., 2005). By analysing solvent-free reactions in a gas/solid reactor, protein hydration was studied without the interference of organic solvent. Gas-phase simulations confirmed a two-phase behaviour of water binding forming patches at low thermodynamic activity and a layer at high activity (Branco et al., 2009). Apart from unspecific binding, water molecules might also bind specifically to the substrate binding site of an enzyme, thus mediating catalytic activity and enantioselectivity (Léonard et al., 2007).

While most reports focus to the effect of solvent to structure and dynamics of the enzyme, the effect of substrate solubility is not yet widely recognized. In the pioneering work of Jongejans it was demonstrated that the kinetic performance of two lipases became independent of the choice of solvent, if substrate concentration was

replaced by thermodynamic activity in the equations of enzyme kinetics (van Tol et al., 1995a; van Tol et al., 1995b). This was confirmed for lipase-catalyzed alcoholysis reactions in solvent-free systems, assuming a ping-pong bi-bi mechanism and competitive inhibition by the alcohol substrate (Sandoval et al., 2002; Sandoval et al., 2001; Strompen et al., 2012). However, in some cases, using activities instead of concentrations was not sufficient to explain the observed kinetics (Janssen et al., 1996). For lipase-catalyzed alcoholysis of esters, the concentration dependency of the catalytic activity on the alcohol concentrations showed a steep increase at low alcohol concentrations and a slow decrease for higher concentrations (Sandoval et al., 2002; Sandoval et al., 2001; Strompen et al., 2012).

Adverse effects of methanol on lipase activity are a major limitation in enzyme-catalyzed alcoholysis reactions, for example in the enzymatic production of biodiesel. Lipases are reported to differ from each other in their sensitivity towards methanol what is of relevance in the development of the biodiesel production process (Fjerbaek et al., 2009; Santambrogio et al., 2013). For example, one of the broadly exploited biocatalysts, the *C. antarctica* lipase B is deactivated at high methanol concentrations (Shimada et al., 1999; Virsu et al., 2001; Watanabe et al., 2000), while it is stable and catalytically active in a broad range of organic solvents (Anderson et al., 1998), and methanol has therefore to be added stepwise (Shimada et al., 1999; Watanabe et al., 2000). Although this avoids deactivation, it results in longer production times. Availability of efficient and cost-effective biocatalysts and processes is a key factor for the competitiveness of the biocatalytic process. In this frame it is of relevance to study and understand the mechanisms leading to enzyme deactivation. We have performed a careful computational and experimental analysis of a model reaction system with *C. antarctica* lipase B, the substrates vinyl acetate and methanol, and toluene as organic solvent to describe the effect of increasing alcohol concentration on the specific activity of the lipase. The observed methanol-dependency of activity could be explained by three simple assumptions: a ping-ping bi-bi reaction mechanism, competitive substrate inhibition by methanol, and using thermodynamic activities of the two substrates instead of concentrations.

2. Materials and methods

2.1 Modeling methods

2.1.1 Calculation of thermodynamic activities of methanol and vinyl acetate

Mixtures of methanol and vinyl acetate in toluene were analyzed. For all mixtures, the concentration c_{VA} of vinyl acetate was constant (15.2 % (vol/vol)), while the concentration c_{MeOH} of methanol was varied from 0.7 to 60 % (vol/vol) (Table S1). The molar fractions χ_{MeOH}, χ_{VA}, and χ_{Tol} of methanol and vinyl acetate were derived as

$$\chi_{MeOH} = n_{MeOH} / (n_{MeOH} + n_{VA} + n_{Tol})$$
$$\chi_{VA} = n_{VA} / (n_{MeOH} + n_{VA} + n_{Tol})$$
$$\chi_{Tol} = 1 - \chi_{MeOH} - \chi_{VA} \qquad \text{(eq. 1)}$$

with $n_{MeOH} = c_{MeOH} \cdot \rho_{MeOH} / M_{MeOH}$

$n_{VA} = c_{VA} \cdot \rho_{VA} / M_{VA}$

$n_{Tol} = (1-c_{MeOH}-c_{VA}) \cdot \rho_{Tol} / M_{Tol}$

and densities ρ_{MeOH} = 0.7918 g/cm^3, ρ_{VA} = 0.934 g/cm3, ρ_{Tol} = 0.87 g/ml and molar weights M_{MeOH} = 32.04 g/mol, M_{VA} = 86.09 g/mol and M_{Tol} = 92.14 g/mol

From the mole fractions χ_{MeOH} and χ_{VA}, thermodynamic activity coefficients γ_{MeOH} and γ_{VA} were evaluated using the UNIFAC model (Fredenslund et al., 1975), and the thermodynamic activities of methanol and vinyl acetate (a_{MeOH} and a_{VA}, respectively) (Table S3 – S6) were calculated by

$$a_{MeOH} = \gamma_{MeOH} \cdot \chi_{MeOH}$$
$$a_{VA} = \gamma_{VA} \cdot \chi_{VA} \qquad \text{(eq. 2)}$$

2.1.2 Modeling enzyme kinetics

The initial velocity of CALB-catalyzed methanolysis of vinyl acetate in toluene as solvent was evaluated based on a ping-pong bi-bi mechanism with competitive inhibition by methanol (Fig. 1). To account for solvation of methanol, the thermodynamic activities a_{MeOH} and a_{VA} of methanol and vinyl acetate rather than their concentrations were used (Sandoval et al., 2001), and the reaction velocity was calculated by:

$$v = v_{max} \cdot a_{MeOH} \cdot a_{VA} / (K_{M,VA} \cdot a_{MeOH} + K_{M,MeOH} \cdot a_{VA} + a_{MeOH} \cdot a_{VA} + K_{M,VA} \cdot a_{MeOH}^2 / K_{i,MeOH}) \quad \text{(eq. 3)}$$

The four kinetic parameters are the maximum reaction velocity v_{max} , the Michaelis constants $K_{M,VA}$ and $K_{M,MeOH}$ of vinyl acetate and methanol, respectively, and the inhibition constant $K_{i,MeOH}$ of methanol. The model was fitted to the experimental data using the solver tool of Microsoft Excel by minimizing the squared deviation between experimental and modeled data.

2.1.3 Molecular dynamics simulations

2.1.3.1 Simulation of CALB in ternary mixtures of methanol, vinyl acetate, and toluene

The simulation systems were set up using mutant N74S of *Candida antarctica* lipase B (CALB), a nonglycosylated form of CALB (Larsen et al., 2008). The enzyme was neutral and no counter ions were added. The protein was solved in binary mixtures of methanol and toluene, with methanol concentrations between 0% (vol/vol) and 43.4% (vol/vol). To each methanol-toluene mixture, 5 different numbers of water molecules (10,...,400) were added and molecular dynamics simulations were performed. The SPC/E water model was used, for toluene and vinyl acetate the OPLS all-atom model was used (Jorgensen et al., 1988). For methanol, a modified OPLS all-atom model was used (Kulschewski et al., 2013).

Each simulation was repeated 3 times using different initial placements of the water molecules and different starting velocities. In total, 74 simulations were performed. The simulation started with an energy minimization using *steepest decent* and *conjugate gradient*. After this, equilibration was performed by heating the system from 10 K to 298 K within 1 ns. Subsequently, a molecular dynamics simulation of 50 ns was performed for each system. All simulations were performed at the BWGrid Cluster (bwGRiD (http://www.bw-grid.de)) of the HLRS in Stuttgart and the computational cluster at the Institute of Technical Biochemistry, Stuttgart.

After the simulation, the data was analyzed by calculating the flexibility and the root mean square fluctuation (rmsd) using the tools g_msd and and g_rmsf, which were supplied with the GROMACS (Hess et al., 2008) package. The number of water, methanol and toluene molecules on the surface of the protein was counted using the "Visual Molecular Dynamics" (VMD) (Humphrey et al., 1996) package. The solvent accessible surface was calculated using both the tools of the GROMACS package and VMD.

For the analysis, the last 10 ns of the 50 ns simulation were used. A long simulation time was chosen to make sure that the system was properly equilibrated. The 10 ns of analysing time were chosen to make sure, that the slow movement of water molecules was properly analysed. Each simulation was repeated three times with different starting conditions for better statistics.

Binding of methanol molecules to the alcohol binding site (Asp134, Thr138 and Gln157) and the acetate binding site (Gly39, Thr40, Ser105, Gln106, Ile189, Val190, His224, Leu278, Ala281 and Ala282) of CALB was studied by averaging the number of methanol molecules at a distance of 0.3 nm from the respective amino acids. The number of bound methanol molecules N_{MeOH} as a function of methanol activity a_{MeOH} was fitted by the law of mass action

$$N_{MeOH} = N_{max} \cdot a_{MeOH} / (K_{MeOH} + a_{MeOH}) \qquad \text{(eq. 4)}$$

resulting in two parameters, the number of N_{max} binding sites for methanol and a binding constant K_{MeOH}.

To calculate the activity of water and methanol, a bulk phase was defined. All water, methanol and toluene molecules beyond 0.3 nm from the protein were assigned to this bulk phase. The number of water and methanol molecules was calculated for each simulation.

The mole fraction of water was calculated by

$$\chi_{Wat} = N_{Wat}^{bulk} / (N_{Wat}^{bulk} + N_{MeOH}^{bulk} + N_{Tol}^{bulk}) \quad \text{(eq. 5)}$$

The methanol concentration (in % (vol/vol)) was calculated from the number of methanol and toluene molecules in the bulk phase, N_{MeOH}^{bulk} and $N_{toluene}^{bulk}$, respectively by

$$c_{MeOH} = 1/(V_{Tol}/V_{MeOH} + 1) \text{ and}$$

$$V_{Tol}/V_{MeOH} = M_{Tol} \cdot N_{Tol}^{bulk} \cdot \rho_{MeOH} / M_{MeOH} \cdot N_{MeOH}^{bulk} \cdot \rho_{Tol}$$

with molecular masses M (32 and 92.14 g/mol) and densities ρ (0.775 and 0.894 g/cm^3 at 298 K) of methanol and toluene, respectively.

The mole fraction of methanol in the bulk was calculated by

$$\chi_{MeOH} = N_{MeOH}^{bulk} / (N_{Wat}^{bulk} + N_{MeOH}^{bulk} + N_{Tol}^{bulk}) \quad \text{(eq. 6)}$$

From the mole fractions χ_{MeOH} and χ_{Wat}, thermodynamic activity coefficients γ_{MeOH} and γ_{Wat} were evaluated using the UNIFAC model (Fredenslund et al., 1975). The thermodynamic activities of methanol and water (a_{MeOH} and a_w, respectively) were calculated according to eq. 2.

2.2 Experimental methods

2.2.1 Materials

The recombinant, non-glycosylated *Candida antarctica* lipase B (CALB), was prepared and purified to homogeneity as described previously (Loegering et al., 2011)

and kindly provided by Kai Lögering and Reiner Luttmann, Hamburg University of Applied Sciences. Toluene, vinyl acetate, methanol, lithium chloride, lithium bromide, cesium fluoride were purchased from Sigma-Aldrich. All other reagents and compounds were of analytical grade. The protein concentration of CALB preparations was determined by Bradford method (Bio-Rad Protein Assay).

2.2.2 Alcoholysis reaction and gas chromatography analysis

The activity of recombinant CALB in organic solvent was determined by measuring the initial rate (v_0) of formation of methyl acetate from the alcoholysis of vinyl acetate by methanol in toluene. To this end, a reaction mixture made of vinyl acetate, methanol, and toluene (up to a final volume of 1 mL) was added to 20 µg of lipase.

Aliquots (67 µl) containing 20 µg of CALB dissolved in 10 mM buffer phosphate, pH 7, were frozen at -80°C and lyophilized. Before reaction, toluene, vinyl acetate, and lipase samples were equilibrated separately at the desired water activity (a_w) value for at least 24 h, at 25°C, in sealed vessels, with the vapour phase of a saturated CsF (a_w 0.02), LiBr (a_w 0.05) or LiCl (a_w 0.09) solution. Methanol was brought to the desired water activity by mixing anhydrous methanol ($\leq$ 0.002% water) with a proper water amount according to Bell et al. (Bell et al., 1997).

The reaction mixture was shaken at 125 shots per min in a horizontal shaker, at 25°C. After 3 minutes from the reaction start, the production of methyl acetate was measured by means of a gas chromatograph equipped with a HP-1 column (Crosslinked Methyl Silicone Gum, 25m, 0.32 mm ID, Agilent Technologies Milan) and a Flame Ionization Detector (FID). The oven temperature was initially held at 35 °C for 3 min and then increased to 120 °C at 25 °C/min and held for 0.5 min at the final temperature. Split ratio was 40:1 and column flow 0.7 ml/min. Quantitative data were extracted from peak areas and used to calculate conversion, initial rate and specific activity (U/mg). The retention times for methanol, methylacetate and vinylacetate, were 3.9, 4.4, 4.8 minutes, respectively (Fig. S1). No acetic acid was detected (instrumental limit of detection 0.1 µg). Therefore the formation of the hydrolysis product can be neglected.

2.2.3 Effects of methanol on CALB activity

The effect of methanol on lipase activity was studied performing reactions at constant vinyl acetate (15.2 % (vol/vol)) and various methanol amounts (0.7–60 % (vol/vol)) in order to satisfy methanol: vinyl acetate molar ratios ranging from 0.1:1 up to 9:1. Toluene was added up to a final volume of 1 ml. Reagents were added to 20 µg lipase in the following order: toluene, vinyl acetate and methanol, the latter started the reaction. Specific activity was measured after 3 minutes. The reactions were performed at a_w values of 0.02, 0.05 and 0.09.

The effect of methanol on kinetic stability was evaluated by measuring the initial rate of reaction after pre-incubation of the lipase in a mixture methanol/toluene. Three different methanol percentages (0.7%, 10% and 60% (vol/vol)) and two a_w values (0.02 and 0.09) were assayed. After the selected time of incubation, the reaction was triggered by the addition of vinyl acetate.

3. Results

3.1 Experimental results

3.1.1 Methanol concentration and catalytic activity

The specific activity of CALB at increasing methanol concentrations was measured at three different a_w values (0.02, 0.05, 0.09). For each of the a_w values tested, the specific activity decreased dramatically from 0.7% to 10 % (vol/vol) methanol (loss of about 60% of activity) and then kept almost constant (Fig. 2). Even at the highest methanol concentration employed, CALB maintained about 30% of the highest activity. The curves corresponding to the three different a_w values were almost superimposable, suggesting a negligible effect of water activity on the decrease of v_o produced by methanol. While the activity curves follow the same trend independently on a_w, we observed minor differences in that at low methanol highest catalytic activity decreases

with a_w and at high methanol it slightly increases with a_w (notice the small increase in specific activity between methanol 50% and 60%).

With the aim of shedding some light on the reasons of the dramatic deactivation exerted by methanol on this lipase, we investigated about the effects of the alcohol on the enzyme kinetic stability. To this end, CALB was first incubated up to 24 hours in the appropriate methanol/toluene mixture before starting alcoholysis by the addition of vinyl acetate. The initial reaction rates were measured for three different methanol concentrations (0.7 % (vol/vol), 10 % (vol/vol) and 60 % (vol/vol)) and two water activities (a_w = 0.02 and a_w = 0.09) (Fig.3, Fig. S2 and Fig. S3). At both a_w, pre-incubation in the mixture methanol/toluene with 0.7 % and 10% (vol/vol) methanol had almost no effect on the activity of CALB that was comparable with that of the control On the contrary, pre-incubation in 60 % (vol/vol) methanol induced deactivation and the effect was higher at low water activity value (Fig. S2). Notably after 180 minutes preincubation at a_w 0.02 the initial rate was reduced by 70% while at a_w 0.09 reduction was 30% only (Fig. 3).

3.2 Modeling of ternary mixtures of methanol, vinyl acetate, and toluene

30 different ternary mixtures of methanol, vinyl acetate, and toluene were analyzed and the thermodynamic activities of methanol and vinyl acetate were evaluated (Tab. S1 and Tab.S3 – Tab. S6). In all mixtures, the concentration of vinyl acetate was 15.2 % (vol/vol), while the concentration of methanol was increased from 0 to 80 % (vol/vol). For ideal mixtures, it would be expected that the thermodynamic activity of methanol was proportional to the mole fraction of methanol in the mixtures, and that the thermodynamic activity of vinyl acetate was constant. However, ternary mixtures of methanol, vinyl acetate, and toluene are far from ideal. The thermodynamic activity of methanol as a function of the mole fraction of methanol has a sigmoidal shape (Fig. S4). As a consequence, it depends sensitively on the methanol concentration for low methanol concentrations (Fig. 4). Between 0 and 10 % (vol/vol), it increases steeply to 0.75. Beyond 10 % it increases only gradually. Similarly, the thermodynamic activity of vinyl acetate varies, despite its concentration being constant (Fig. 4). The

thermodynamic activity of vinyl acetate decreases to a minimum at 11 – 19 % methanol (vol/vol) and increased for higher methanol concentrations, due to an increase of the thermodynamic activity coefficient at high methanol concentrations (Tab.S3-S6). Varying the thermodynamic activity of water between 0.02 and 0.09 had only a negligible effect to the thermodynamic activities of methanol and vinyl acetate (Fig. S4 – S6).

3.3 Modeling of the reaction velocity

The lipase-catalyzed methanolysis of vinyl acetate in toluene was modeled by a ping-pong bi-bi mechanism (Fig. 1) with competitive inhibition by methanol according to (eq. 1).

In total four parameters were necessary to model the catalytic activity: the Michaelis constant of methanol ($K_{M,MeOH}$), the inhibition constant of methanol ($K_{i,MeOH}$), the Michaelis constant of vinyl acetate ($K_{M,VA}$), and the maximum reaction velocity (v_{max}). Because of the limited number of data points for very low methanol concentrations, the error bars of the peak, and the constant vinyl acetate concentration used in the experiment, an independent determination of all four parameters by fitting the experimental data by eq. 3 was not possible, but the parameters were coupled. Therefore, two parameters ($K_{M,MeOH}$ and $K_{i,MeOH}$) were evaluated from the simulation data: The binding of methanol to the alcohol binding site (Asp134, Thr138 and Gln157) and to the acetate binding site (Gly39, Thr40, Ser105, Gln106, Ile189, Val190, His224, Leu278, Ala281, Ala282) was used to model $K_{M,MeOH}$ and $K_{i,MeOH}$, respectively. The two parameters v_{max} and $K_{M,VA}$ were fitted to the experimental data by minimizing the root mean square deviation. Because of the constant concentration of vinyl acetate, these two parameters were also coupled. As a consequence, the quality of the fit to experimental data was insensitive to small changes of the parameters. Even for a change of a single parameter by a factor of two and a subsequent fit of v_{max} and $K_{M,VA}$, the shape of the curve was robust and the root mean square deviation only changed slightly.

By modeling catalytic activity by eq. 3, using two parameters from simulation and two by fitting the experimental data, the experimentally observed catalytic activity as a function of the concentration of methanol was reproduced: a peak of catalytic activity at methanol concentrations as low as 0.7 % (vol/vol) and a subsequent decrease at higher methanol concentrations activities to a constant value (Fig. 5a-c). For the first 5 data points (0.7 to 20 % (vol/vol) methanol), the experimental data and the model were in good agreement. However, for methanol concentrations above 20 % (vol/vol), the modeled data overestimated the experimental data for water activities of a_w = 0.02 and a_w = 0.05 (Fig. 5a,b). However, for a_w = 0.09 the experimentally measured and the predicted catalytic activities were in good agreement (Fig 5c), and a slight increase of catalytic activity at high methanol concentration was observed.

3.4 Molecular dynamics simulations of CALB in ternary mixtures

To study the molecular basis of the experimentally observed deactivation of CALB by methanol, molecular dynamics (MD) simulations were performed. CALB was simulated in an environment, which was comparable to the experimental setup in both water and methanol activity. During the 50 ns simulation time, no change in the flexibility and the structure of the enzyme was observed (data not shown). In total 5 simulations were extended to a total of 300 ns. In one simulation with 40% (vol/vol) methanol and a water activity of a_w = 0.01, unfolding of the N-terminus was observed. The flexibility of the enzyme was neither dependent of the water activity nor of the methanol activity. No conformational changes were observed.

The binding of methanol molecules to the alcohol binding site (Asp134, Thr138 and Gln157) of CALB was studied for three water activities (0.02, 0.05, 0.09) (Fig. S7a, Fig. 6, Fig. S7b). Assuming a simple law of mass action (eq. 4 in 2.1.3.1) to describe binding of methanol molecules to a limited number of methanol binding sites in the alcohol binding site of CALB as a function of methanol activity resulted in maximum number N_{max} of bound methanol molecules of 6.6, 5.8, and 6.6 (a_w =0.02, 0.05, 0.09, respectively) and binding constants $K_{M,MeOH}$ of 0.05, 0.05 and 0.06, respectively (Fig. S7a, Fig. 6, Fig. S7b, respectively).

The binding of methanol molecules to the acetate binding site (Gly39, Thr40, Ser105, Gln106, Ile189, Val190, His224, Leu278, Ala281 and Ala282) was studied accordingly, resulting in a maximum number N_{max} of bound methanol molecules of 37.6, 35.2, and 38.4 (a_w =0.02, 0.05, 0.09, respectively) and binding constants $K_{i,MeOH}$ of 0.22, 0.23 and 0.25, respectively (Fig. S8a, Fig. 8b, Fig. S8c, respectively). The water activity had only a minor effect on the binding of methanol to the alcohol and acetate binding site.

4. Discussion

Lipase-catalyzed alcoholysis reactions are widely applied in a broad range of organic solvents as well as in solvent-free systems (for a review see (Tan et al., 2010; Vyas et al., 2010)). Although the catalytic mechanism of alcoholysis (ping-pong bi-bi) is well understood (Bousquet-Dubouch et al., 2001) and the reaction system contains only five different compounds (the enzyme, the two substrates methanol and ester, residual water, and an organic solvent), the reaction kinetics under different conditions still cause surprises. The complexity of the reaction kinetics arises from the fact that all compounds interact, and therefore it is often difficult to discern effects, to identify their molecular mechanism, and to predict the system behavior. To study lipase-catalyzed alcoholysis in organic solvent, a model reaction was investigated which incorporates a sufficient amount of complexity. The initial velocities of CALB-catalyzed alcoholysis of a constant concentration of 15.2% (vol/vol) vinyl acetate were determined for different concentrations of methanol in toluene.

A three phase behavior was observed: for low methanol concentrations of 0.7 % (vol/vol) a high reaction velocity was observed (vol/vol) (phase I), the velocity decreases until a methanol concentration of 10 % (vol/vol) is reached (phase II). For higher methanol concentrations, the reaction velocity was nearly constant up to a methanol concentration of 60 % (vol/vol) (phase III). While concentration-dependent reaction velocity according to phase I and II has been observed previously and modeled by a ping-pong bi-bi mechanism and inhibition by methanol (Sandoval et al., 2002; Sandoval et al., 2001; Strompen et al., 2012), the nearly constant reaction

velocity for high methanol concentrations in phase III has not been observed before and seems to be in contrast to substrate inhibition by methanol.

4.1 Phase I (c_{MeOH} < 1%)

The highest reaction rate was determined for very low methanol concentrations below 1% (vol/vol) which has been observed previously for CALB-catalyzed alcoholysis and aminolysis reactions (Sandoval et al., 2001; Strompen et al., 2012). Under the assumption of an ideal methanol-toluene mixture, the steep increase of catalytic activity between 0 and 0.7% methanol (vol/vol) would be interpreted as an apparent very high affinity of the lipase to methanol. However, if the thermodynamic activity of methanol rather than its concentration is used to calculate the reaction velocity (Sandoval et al., 2001), the calculated $K_{m,MeOH}$ value is 0.2, a value which corresponds to moderate binding affinity. The observed steep increase between 0 and 1 % (vol/vol), therefore, is not a consequence of tight binding of methanol to CALB, but of non-ideal mixing of methanol and the solvent, toluene. For low methanol concentrations (mole fraction of methanol below 0.1, concentration below 4 % (vol/vol)), the activity coefficient and the thermodynamic activity is up to 9 times higher than expected from an ideal mixture. Although methanol and toluene are completely miscible, the activity coefficient corresponds to a compound with a limited solubility of only 6 % (vol/vol) (χ_{MeOH}= 0.15) in toluene (Fig. 4).

The molecular mechanism that leads to this non-ideal behavior is reflected in the large difference between the polarity of methanol and toluene (logP = -0.82 and 2.6, respectively). As a consequence of its high polarity, methanol tends to separate from the nonpolar toluene, resulting in a high activity coefficient and a steep increase of thermodynamic activity at increasing methanol concentrations. For 29 % (vol/vol) methanol the percolation threshold is reached (Lorenz et al., 2001), and a bicontinuous microemulsion (De Gennes et al., 1982) is formed, as observed previously for water-methanol mixtures (Benson et al., 2013).

4.2 Phase II (1% < c_{MeOH} < 10%)

The observed dependency of reaction velocity on methanol was successfully modeled by a ping-pong bi-bi mechanism with substrate inhibition (Sandoval et al., 2002; Sandoval et al., 2001; Strompen et al., 2012), because methanol is acting both as a substrate and a competitive inhibitor. The reaction kinetics in phase II are dominated by the inhibition by the substrate methanol with a $K_{i,MeOH}$ value of 0.2. Between χ_{MeOH} = 0.025 and 0.222 (corresponding to 1 and 10 % (vol/vol), respectively), the activity coefficient of methanol ranges between 8.9 and 3.1. In phase II, the increase of thermodynamic activity with methanol concentration is larger than expected for an ideal mixture, but smaller than in phase I. The molecular mechanism of substrate inhibition is reflected by the binding of methanol molecules into the acetate binding site of CALB, thus competing with the substrate vinyl acetate. This mechanism is supported by molecular dynamics simulations of CALB in ternary mixtures. The binding constant of methanol to the acetate binding site ($K_{i,MeOH}$ = 0.22-0.25) as derived by simulations agrees well with the substrate inhibition constant $K_{i,MeOH}$ as deduced from the experiments.

4.3 Phase III (10% < c_{MeOH} < 60%)

Between χ_{MeOH} = 0.22 and 0.78 (corresponding to 10 and 60 % (vol/vol), respectively) the activity coefficient of methanol decreases from 3.1 to 1.1, therefore the thermodynamic activity increases only gradually. Thus, the concentration effect of substrate inhibition is damped and therefore much smaller than expected from an ideal mixture.

For inhibition of an enzyme by ideally soluble substrates, a decrease of reaction velocity to zero is expected. In contrast, a constant reaction velocity is observed for high methanol concentrations. This is a consequence of the thermodynamics of the non-ideal ternary mixture. Three factors contribute to the reaction velocity:

(1) In an ideal mixture, upon increasing the methanol concentration, the inhibitory effect of methanol is expected to increase and the reaction velocity to decrease.

However, because the ternary mixture is far from ideal and the thermodynamic coefficient is very low, the increase in thermodynamic activity is less than expected from the increase in concentration, and thus the reaction velocity is expected to decrease less than expected in an ideal mixture.
(2) Because of the different molecular weight of methanol and toluene, the total number of molecules in a given volume increases as the methanol : toluene ratio increases. As a consequence, the molar ratio of the second substrate vinyl acetate drops and thus the reaction velocity is expected to decrease.
(3) The thermodynamic activity of vinyl acetate increases as the methanol concentration increases as a consequence of the non-ideal ternary mixture, although the concentration of vinyl acetate is constant: Therefore, the thermodynamic activity of vinyl acetate also increases and thus the reaction velocity is expected to increase.

A loss of catalytic activity of CALB upon incubation in methanol was observed only at a high methanol concentration of 60 % (vol/vol) and a low water activity of 0.02 (Fig. 3; Fig. S2 and S3), while at high water activities or low methanol concentrations the enzyme was stable. Accordingly, a slight increase of catalytic activity for high methanol concentrations was observed for a high water activity of 0.09 as predicted by the model, while for low water activities the catalytic activity was lower than predicted by the model due deactivation of the enzyme.

5. Conclusion

The methanol concentration dependency of the reaction velocity of CALB-catalyzed methanolysis of vinyl acetate in toluene was modeled using three simple assumptions:

1. A ping-ping bi-bi reaction mechanism
2. Competitive inhibition by binding of methanol to the substrate binding site of CALB
3. Using thermodynamic activities of the substrates instead of concentrations

As a consequence, highest catalytic activity was observed at very low methanol concentration of 0.7% (vol/vol). Due to substrate inhibition, the catalytic activity

decreased for increasing methanol concentrations between 1 and 10%. For higher methanol concentrations, the catalytic activity did not further decrease, due to the low thermodynamic activity coefficient of methanol and the increase of the thermodynamic activity of vinyl acetate. Thus, for high methanol concentrations, even a slight increase of catalytic activity was expected. The experimentally observed inhibition constant of methanol was confirmed by molecular modeling. Additional effects are expected to play only a minor role. Non-competitive inhibition by methanol was only observed for high methanol concentration and low water activity. Product inhibition could be excluded, because vinyl acetate was used as a substrate and the initial reaction velocity was measured.

Thus, two major factors contribute to the observed concentration dependency of the catalytic activity of CALB: the thermodynamic properties of the non-ideal substrate-solvent mixture and the molecular interactions between substrate and enzyme. Therefore, our model can be applied to optimize reaction parameters for methanolysis reactions and to improve the enzyme by protein engineering.

Acknowledgements

We are grateful for constructive discussions with Peter Halling (University of Strathclyde) and with Joachim Gross (University of Stuttgart), and for recombinant, non-glycosylated *Candida antarctica* lipase B provided by Kai Lögering and Reiner Luttmann (Hamburg University of Applied Sciences). The authors acknowledge the German Science Foundation DFG ("Sonderforschungsbereich 716"), the German Academic Exchange Service and the Italian Ministry of Education, University and Research ("German-Italian Exchange Program VIGONI") for financial support. ML acknowledges a grant by Regione Lombardia ("Biotechnological production of biodiesel").

References

Affleck, R., Haynes, C.A., Clark, D.S., 1992. Solvent dielectric effects on protein dynamics. Proceedings of the National Academy of Sciences of the United States of America 89, 5167-5170.

Anderson, E.M., Larsson, K.M., Kirk, O., 1998. One biocatalyst-many applications: the use of Candida antarctica B-lipase in organic synthesis. Biocatalysis and Biotransformation 16, 181-204.

Bell, G., Janssen, A.E.M., Halling, P.J., 1997. Water activity fails to predict critical hydration level for enzyme activity in polar organic solvents: Interconversion of water concentrations and activities. Enzyme and Microbial Technology 20, 471-477.

Benson, S.P., Pleiss, J., 2013. Incomplete mixing versus clathrate-like structures: A molecular view on hydrophobicity in methanol-water mixtures. Journal of Molecular Modeling 1-10.

Bousquet-Dubouch, M.-P., Graber, M., Sousa, N., Lamare, S., Legoy, M.-D., 2001. Alcoholysis catalyzed by Candida antarctica lipase B in a gas/solid system obeys a Ping Pong Bi Bi mechanism with competitive inhibition by the alcohol substrate and water. Biochimica et Biophysica Acta (BBA) - Protein Structure and Molecular Enzymology 1550, 90-99.

Branco, R.J.F., Graber, M., Denis, V., Pleiss, J., 2009. Molecular mechanism of the hydration of Candida antarctica lipase B in the gas phase: Water adsorption isotherms and molecular dynamics simulations. ChemBioChem 10, 2913-2919.

Broos, J., Visser, A.J.W.G., Engbersen, J.F.J., Verboom, W., van Hoek, A., Reinhoudt, D.N., 1995. Flexibility of enzymes suspended in organic solvents probed by time-resolved fluorescence anisotropy. Evidence that enzyme activity and enantioselectivity are directly related to enzyme flexibility. Journal of the American Chemical Society 117, 12657-12663.

bwGRiD (http://www.bw-grid.de), member of the German D-Grid initiative, funded by the Ministry for Education and Research (Bundesministerium für Bildung und Forschung) and the Ministry for Science, Research and Arts Baden-Wuerttemberg (Ministerium für Wissenschaft, Forschung und Kunst Baden-Württemberg).

Castillo, E., Pezzotti, F., Navarro, A., Lopez-Munguia, A., 2003. Lipase-catalyzed synthesis of xylitol monoesters: solvent engineering approach. Journal of Biotechnology 102, 251-259.

De Gennes, P.G., Taupin, C., 1982. Microemulsions and the flexibility of oil/water interfaces. The Journal of Physical Chemistry 86, 2294-2304.

Degn, P., Zimmermann, W., 2001. Optimization of carbohydrate fatty acid ester synthesis in organic media by a lipase from Candida antarctica. Biotechnology and Bioengineering 74, 483-491.

Edmundo, C., Valerie, D., Didier, C., Alain, M., 1998. Efficient lipase-catalyzed production of tailor-made emulsifiers using solvent engineering coupled to

extractive processing. Journal of the American Oil Chemists' Society 75, 309-313.
Fjerbaek, L., Christensen, K.V., Norddahl, B., 2009. A review of the current state of biodiesel production using enzymatic transesterification. Biotechnology and Bioengineering 102, 1298-1315.
Fredenslund, A., Jones, R.L., Prausnitz, J.M., 1975. Group-contribution estimation of activity coefficients in nonideal liquid mixtures. AIChE Journal 21, 1086-1099.
Graber, M., Irague, R., Rosenfeld, E., Lamare, S., Franson, L., Hult, K., 2007. Solvent as a competitive inhibitor for Candida antarctica lipase B. Biochimica et Biophysica Acta (BBA) - Proteins & Proteomics 1774, 1052-1057.
Hess, B., Kutzner, C., van der Spoel, D., Lindahl, E., 2008. GROMACS 4: Algorithms for highly efficient, load-balanced, and scalable molecular simulation. Journal of Chemical Theory and Computation 4, 435-447.
Humphrey, W., Dalke, A., Schulten, K., 1996. VMD: Visual molecular dynamics. Journal of Molecular Graphics 14, 33-38.
Janssen, A.E.M., Vaidya, A.M., Halling, P.J., 1996. Substrate specificity and kinetics of Candida rugosa lipase in organic media. Enzyme and Microbial Technology 18, 340-346.
Jorgensen, W.L., Tirado-Rives, J., 1988. The OPLS [optimized potentials for liquid simulations] potential functions for proteins, energy minimizations for crystals of cyclic peptides and crambin. Journal of the American Chemical Society 110, 1657-1666.
Kahlow, U.H., Schmid, R.D., Pleiss, J., 2001. A model of the pressure dependence of the enantioselectivity of Candida rugosalipase towards (+/-)-menthol. Protein Sci 10, 1942-1952.
Kulschewski, T., Pleiss, J., 2013. A molecular dynamics study of liquid aliphatic alcohols: simulation of density and self-diffusion coefficient using a modified OPLS force field. Molecular Simulation 1-14.
Laane, C., Boeren, S., Vos, K., Veeger, C., 1987. Rules for optimization of biocatalysis in organic solvents. Biotechnology and Bioengineering 30, 81-87.
Larsen, M.W., Bornscheuer, U.T., Hult, K., 2008. Expression of Candida antarctica lipase B in Pichia pastoris and various Escherichia coli systems. Protein Expression and Purification 62, 90-97.
Lee, S.B., Kim, K.-J., 1995. Effect of water activity on enzyme hydration and enzyme reaction rate in organic solvents. Journal of Fermentation and Bioengineering 79, 473-478.
Léonard, V., Fransson, L., Lamare, S., Hult, K., Graber, M., 2007. A water molecule in the stereospecificity pocket of Candida Antarctica lipase B enhances enantioselectivity towards pentan-2-ol. ChemBioChem 8, 662-667.
Loegering, K., Mueller, C., Voss, J.-P., Wagenfuehrer, C., Zahn, D., Bertelsen, H.-P., Scheffler, U., Luttmann, R., 2011. An integrated scale-down plant for optimal recombinant enzyme production by Pichia pastoris. Biotechnology Journal 6, 428-436.

Lorenz, C.D., Ziff, R.M., 2001. Precise determination of the critical percolation threshold for the three-dimensional ``Swiss cheese" model using a growth algorithm. The Journal of Chemical Physics 114, 3659-3661.

Micaelo, N.M., Teixeira, V.H., Baptista, A.M., Soares, C.M., 2005. Water dependent properties of cutinase in nonaqueous solvents: A computational study of enantioselectivity. Biophysical Journal 89, 999-1008.

Ottosson, J., Fransson, L., Hult, K., 2002a. Substrate entropy in enzyme enantioselectivity: An experimental and molecular modeling study of a lipase. Protein Science 11, 1462-1471.

Ottosson, J., Fransson, L., King, J.W., Hult, K., 2002b. Size as a parameter for solvent effects on Candida antarctica lipase B enantioselectivity. Biochimica et Biophysica Acta (BBA) - Protein Structure and Molecular Enzymology 1594, 325-334.

Sandoval, G., Condoret, J.S., Monsan, P., Marty, A., 2002. Esterification by immobilized lipase in solvent-free media: Kinetic and thermodynamic arguments. Biotechnology and Bioengineering 78, 313-320.

Sandoval, G.C., Marty, A., Condoret, J.-S., 2001. Thermodynamic activity-based enzyme kinetics: Efficient tool for nonaqueous enzymology. AIChE Journal 47, 718-726.

Santambrogio, C., Sasso, F., Natalello, A., Brocca, S., Grandori, R., Doglia, S., Lotti, M., 2013. Effects of methanol on a methanol-tolerant bacterial lipase. Applied Microbiology and Biotechnology 1-10.

Shimada, Y., Watanabe, Y., Samukawa, T., Sugihara, A., Noda, H., Fukuda, H., Tominaga, Y., 1999. Conversion of vegetable oil to biodiesel using immobilized Candida antarctica lipase. Journal of the American Oil Chemists' Society 76, 789-793-793.

Strompen, S., Weiß, M., Ingram, T., Smirnova, I., Gröger, H., Hilterhaus, L., Liese, A., 2012. Kinetic investigation of a solvent-free, chemoenzymatic reaction sequence towards enantioselective synthesis of a β-amino acid ester. Biotechnology and Bioengineering 109, 1479-1489.

Sym, E.A., 1936. Action of esterase in the presence of organic solvents. Biochemical Journal 30, 609-617.

Tan, T., Lu, J., Nie, K., Deng, L., Wang, F., 2010. Biodiesel production with immobilized lipase: A review. Biotechnology Advances 28, 628-634.

van Tol, J.B.A., Jongejan, J.A., Duine, J.A., Kierkels, H.G.T., Geladé, E.F.T., Mosterd, F., van der Tweel, W.J.J., Kamphuis, J., 1995a. Thermodynamic and kinetic parameters of lipase-catalyzed ester hydrolysis in biphasic systems with varying organic solvents. Biotechnology and Bioengineering 48, 179-189.

van Tol, J.B.A., Stevens, R.M.M., Veldhuizen, W.J., Jongejan, J.A., Duine, J.A., 1995b. Do organic solvents affect the catalytic properties of lipase? Intrinsic kinetic parameters of lipases in ester hydrolysis and formation in various organic solvents. Biotechnology and Bioengineering 47, 71-81.

Virsu, P., Liljeblad, A., Kanerva, A., Kanerva, L.T., 2001. Preparation of the enantiomers of 1-phenylethan-1,2-diol. Regio- and enantioselectivity of

acylase I and Candida antarctica lipases A and B. Tetrahedron: Asymmetry 12, 2447-2455.

Vyas, A.P., Verma, J.L., Subrahmanyam, N., 2010. A review on FAME production processes. Fuel 89, 1-9.

Watanabe, K., Yoshida, T., Ueji, S.-i., 2004. The role of conformational flexibility of enzymes in the discrimination between amino acid and ester substrates for the subtilisin-catalyzed reaction in organic solvents. Bioorganic Chemistry 32, 504-515.

Watanabe, Y., Shimada, Y., Sugihara, A., Noda, H., Fukuda, H., Tominaga, Y., 2000. Continuous production of biodiesel fuel from vegetable oil using immobilized Candida antarctica lipase. Journal of the American Oil Chemists' Society 77, 355-360.

Zaks, A., Klibanov, A.M., 1988. The effect of water on enzyme action in organic media. Journal of Biological Chemistry 263, 8017-8021.

Figures and legends

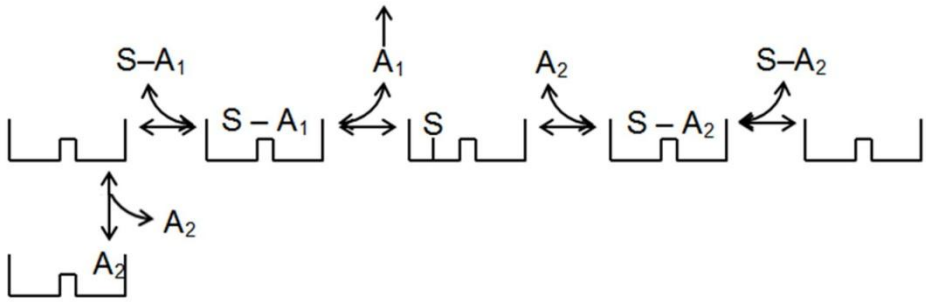

Fig. 1: Ping-pong bi-bi mechanisms of enzyme-catalyzed alcoholysis of ester S-A_1 by alcohol A_2 and substrate inhibition by alcohol A_2. S = acetic acid, A_1 = vinyl alcohol, A_2 = methanol, S-A_1, S-A_2 = esters

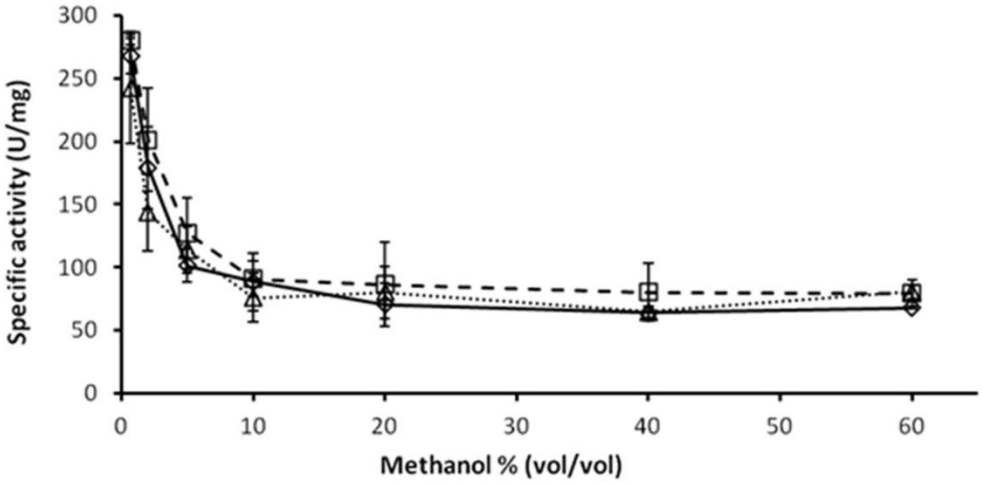

Fig. 2: Initial rate (expressed as specific activity) of alcoholysis reaction catalyzed by CALB at different methanol concentrations and different a_w values: a_w = 0.02 (diamonds; full line), a_w = 0.05 (squares, dashed line) and a_w = 0.09 (triangles, dotted line). Standard deviations refer to three independent experiments.

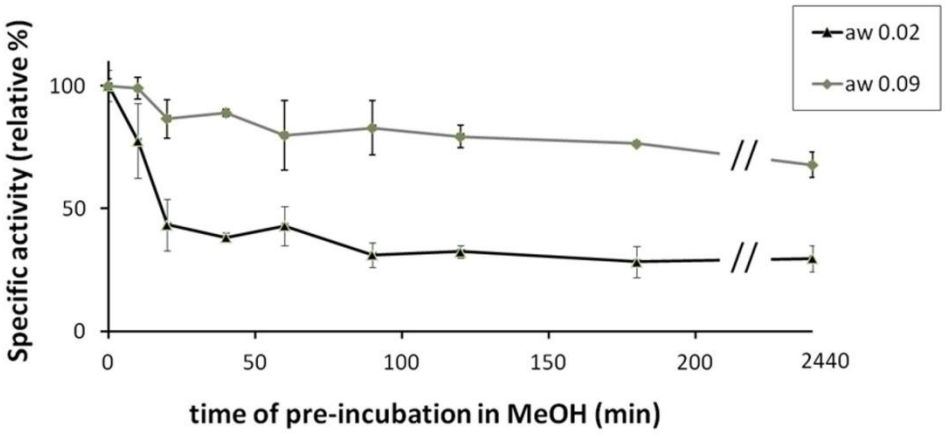

Fig. 3: Comparison of CALB specific activity (relative percentage) after different times of pre-incubation in 60% (vol/vol) methanol at a_w 0.02 (triangles, grey line) and a_w 0.09 (diamonds, black line). Standard deviations refer to three independent experiments.

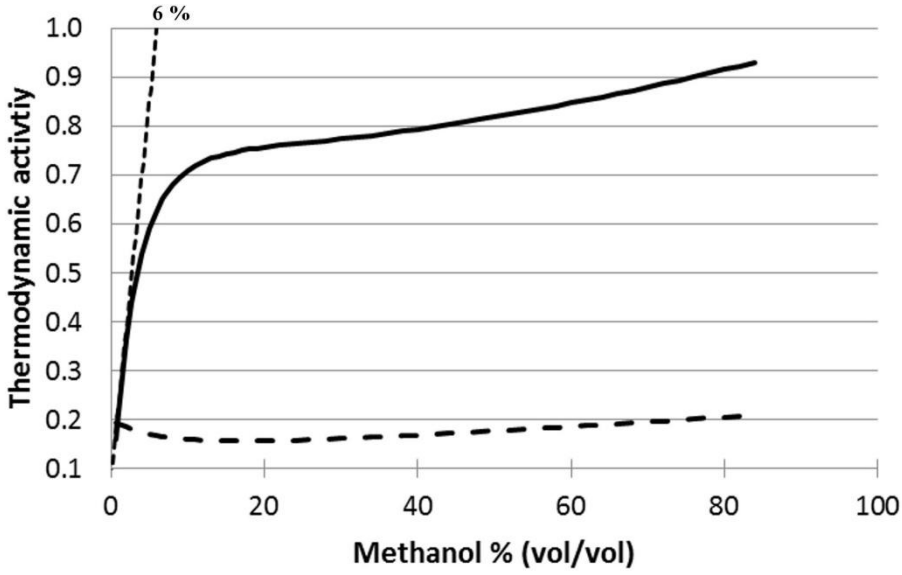

Fig. 4: Thermodynamic activity of methanol (full line) and vinyl acetate (long dashed line) in a ternary mixture of methanol, toluene and vinyl acetate. A straight line with

the slope of 0.132 (short dashed line) was fitted through the first 5 data points, which achieves the thermodynamic activity of 1.0 at 6 % (vol/vol) methanol.

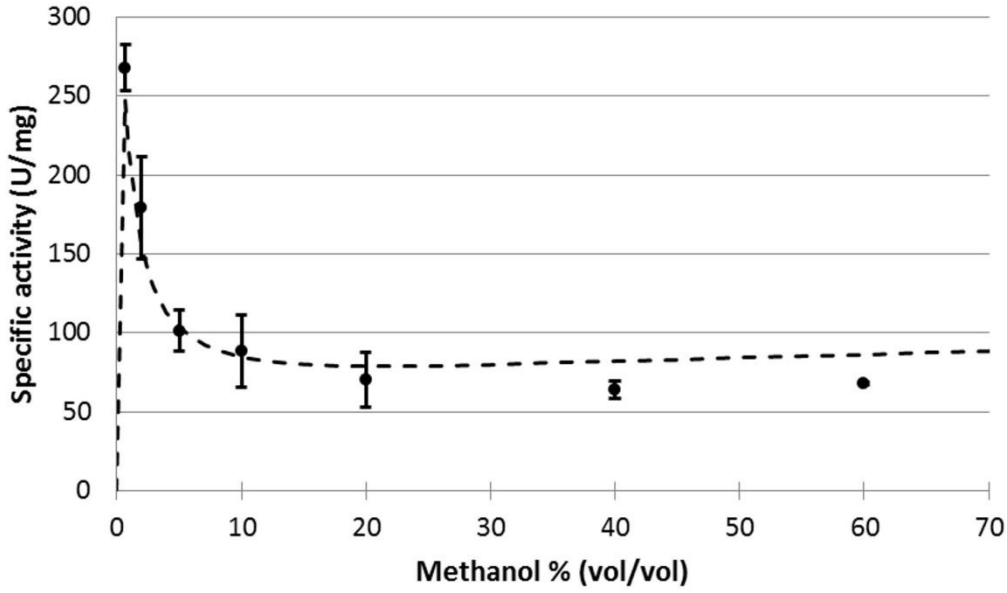

Fig. 5a: Experimentally determined catalytic activity (circles) and predicted modeled activity (dashed line) at a water activity of $a_w = 0.02$

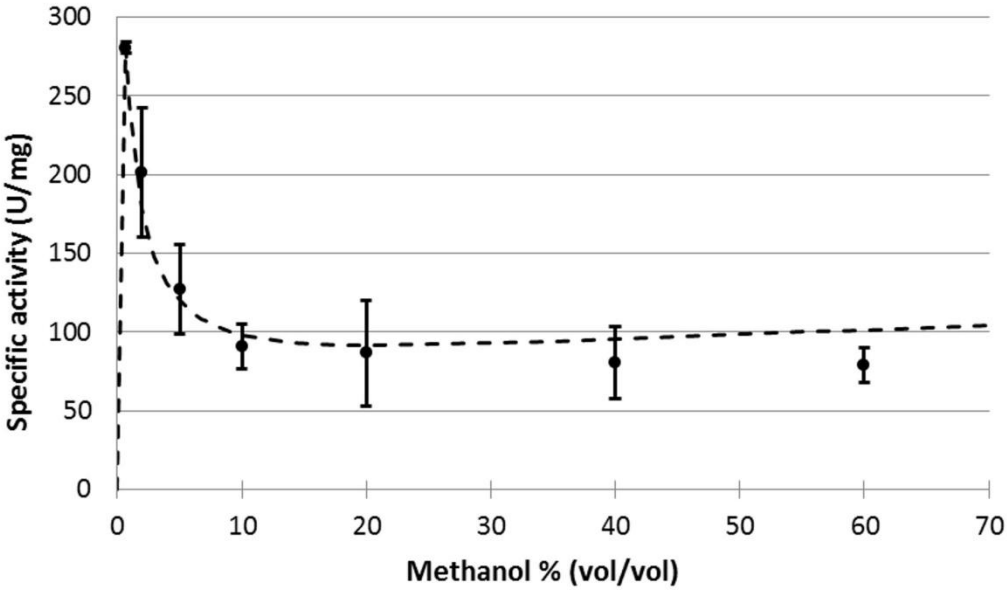

Fig. 5b: Experimentally determined catalytic activity (circles) and predicted modeled activity (dashed line) at a water activity of $a_w = 0.05$

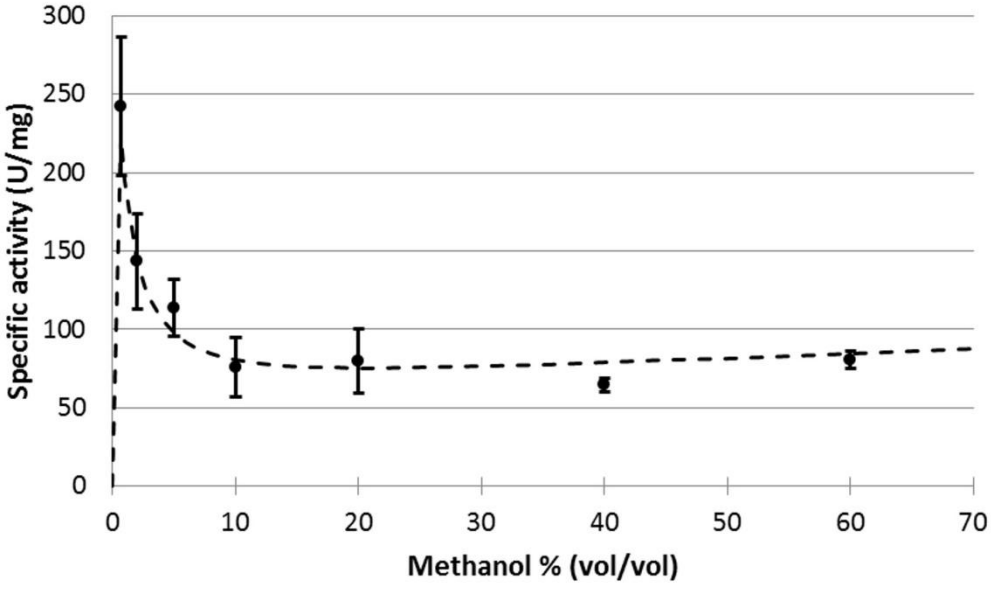

Fig. 5c: Experimentally determined catalytic activity (circles) and predicted modeled activity (dashed line) at a water activity of $a_w = 0.09$

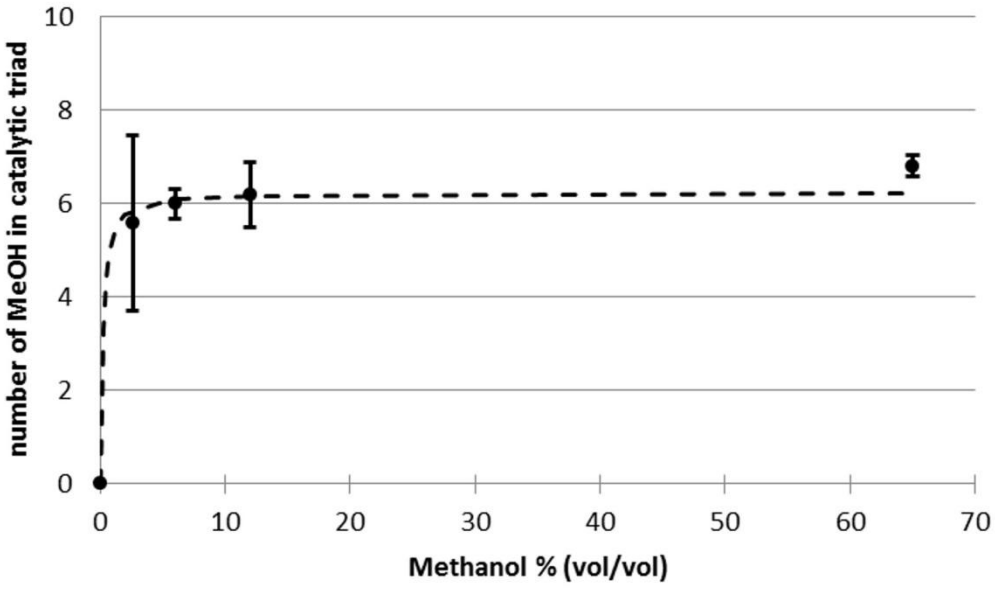

Fig. 6: Number of methanol molecules in the alcohol binding site (a_w = 0.05)

Tables

Table S1: composition of the systems:

Methanol		Vinyl acetate		Toluene	
c_{MeOH} (V/V)	χ_{MeOH}	c_{VAC} (V/V)	χ_{VAC}	c_{TOL} (V/V)	χ_{TOL}
0.7	0.02	0.152	0.19	0.82	0.79
2	0.05	0.152	0.18	0.82	0.77
5	0.12	0.152	0.17	0.79	0.71
10	0.22	0.152	0.16	0.75	0.62
20	0.37	0.152	0.14	0.66	0.49
40	0.62	0.152	0.11	0.46	0.27
60	0.78	0.152	0.1	0.25	0.12

Table S2: (specific) catalytic activity of CALB for 3 different water activities including error bars.

MeOH % (V/V)	a_w = 0.02	+/-	a_w = 0.05	+/-	a_w = 0.07	+/-
0.7	267.95	14.33	280.54	3.72	242.70	44.20
2	179.23	32.55	201.28	40.90	143.42	30.46
5	101.31	13.14	127.22	28.35	113.91	18.17
10	88.56	23.03	90.71	14.09	75.84	19.24
20	70.48	17.27	86.57	33.28	80.04	20.62
40	64.07	5.40	80.44	22.96	64.65	4.29
60	68.00	0.97	79.19	10.88	80.65	5.25

Table S3: thermodynamic activity of the a tertiary mixture containing methanol, toluene and vinyl acetate

Table S4: thermodynamic activity of the a mixture containing methanol, toluene, vinyl acetate and water at aw = 0.02

Table S5: thermodynamic activity of the a mixture containing methanol, toluene, vinyl acetate and water at aw = 0.05

Table S6: thermodynamic activity of the a mixture containing methanol, toluene, vinyl acetate and water at aw = 0.09

Table S3 to S6 are submitted as separate xls-file.

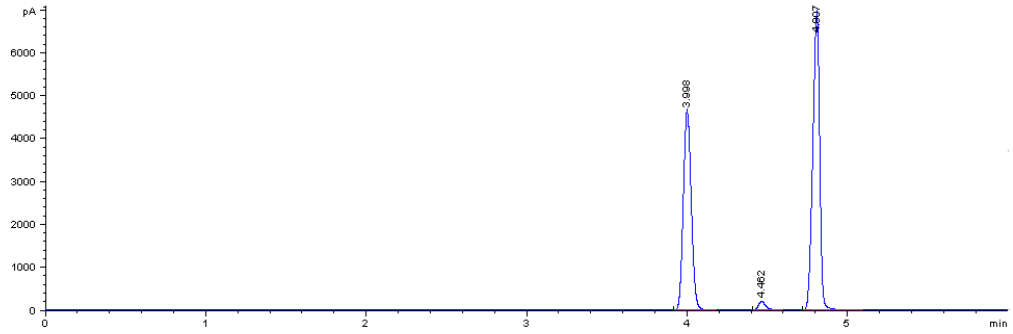

Fig. S1 Chromatogram of a 3 minutes alcoholysis reaction catalyzed by CALB. Peaks of methanol, methyl acetate and vinyl acetate are well separated and their retention times are 3.9, 4.2, and 4.8 min, respectively.

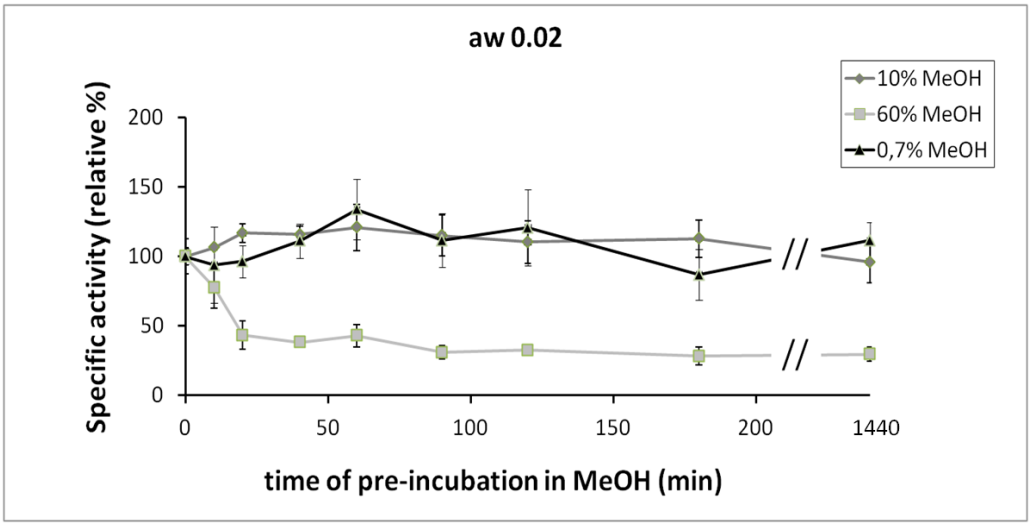

Fig. S2 Specific activity (as relative percentage) of the alcoholysis reaction catalyzed by CALB, at a_w 0.02, after different times of pre-incubation in methanol. Standard deviations refer to three independent experiments.

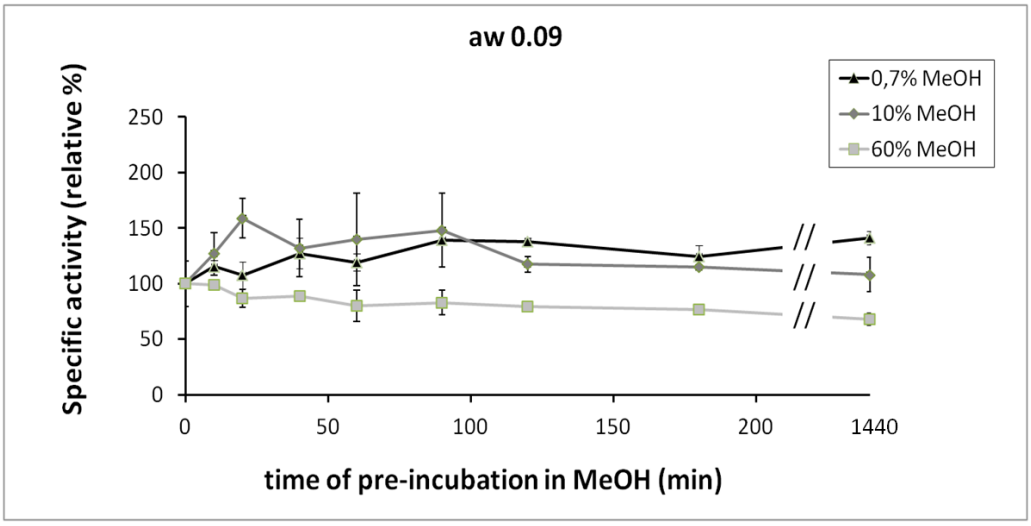

Fig. S3 Specific activity (as relative percentage) of the alcoholysis reaction catalyzed by CALB, at a_w 0.09, after different times of pre-incubation in methanol. Standard deviations refer to three independent experiments.

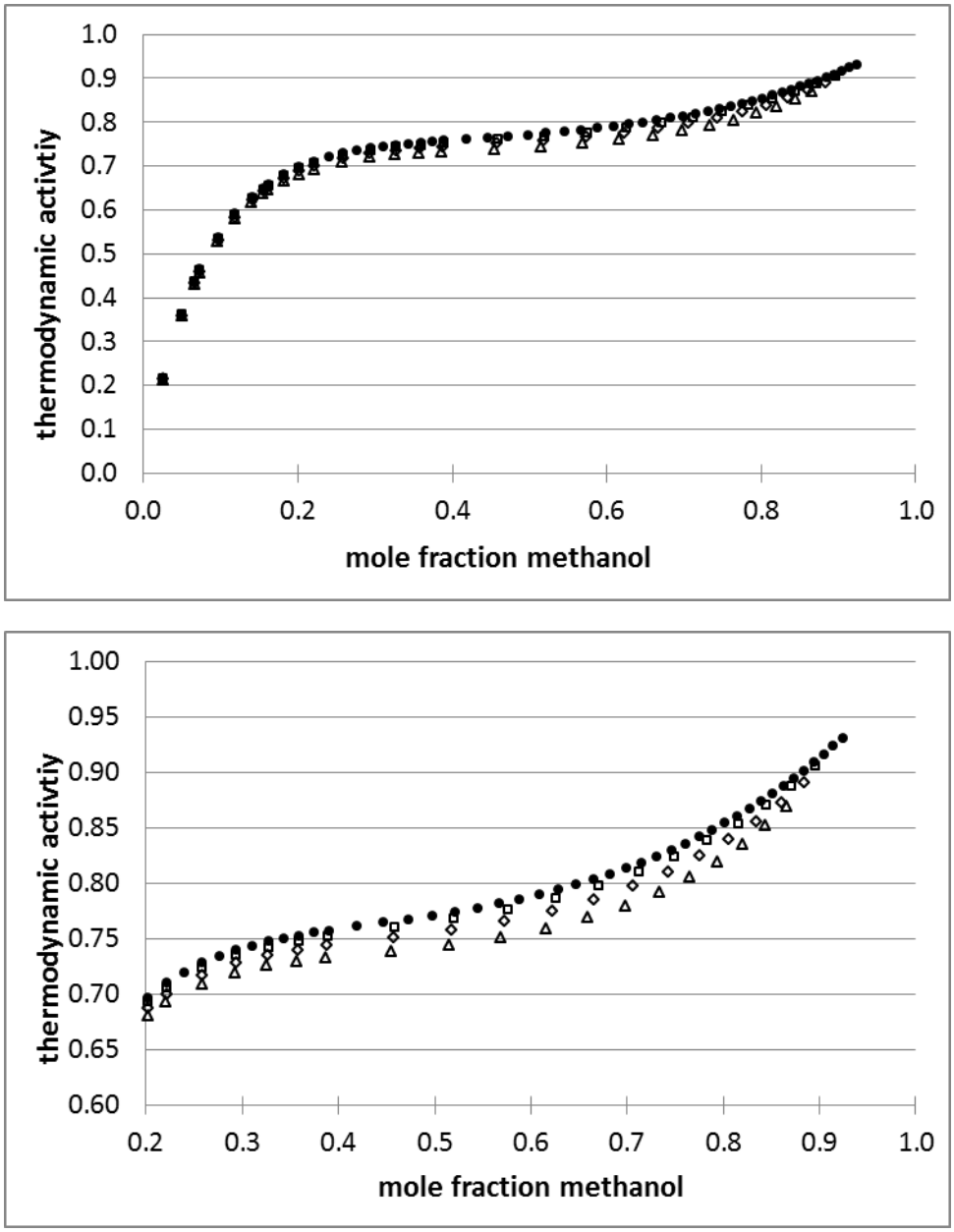

Fig. S4: Thermodynamic activity of methanol in a mixture of methanol, toluene, vinyl-acetate and water with a_w=0.00 (circle), a_w=0.02 (square), a_w=0.05 (diamond) and a_w=0.09 (triangle)

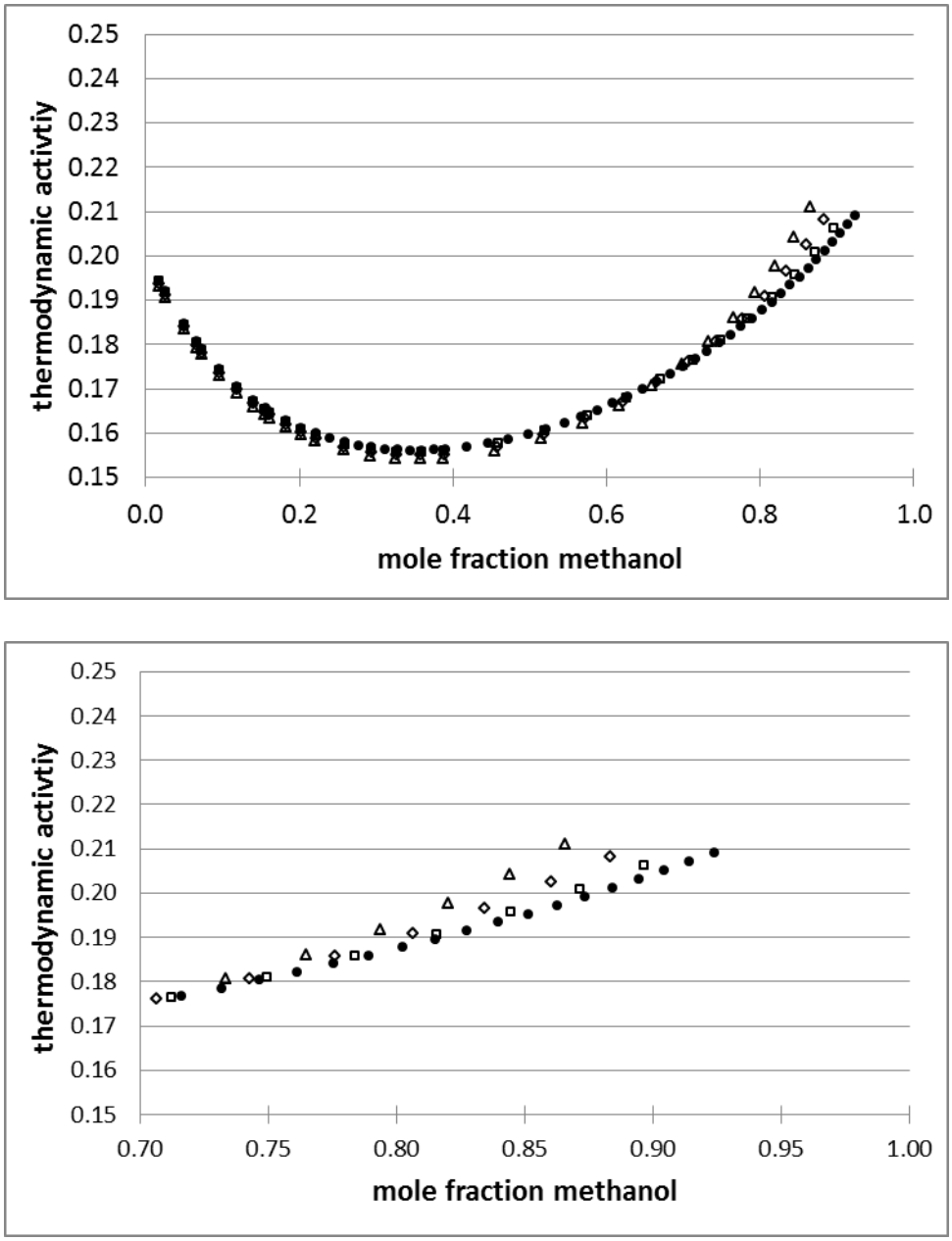

Fig. S5: Thermodynamic activity of vinyl acetate in a mixture of methanol, toluene, vinyl-acetate and water with a_w=0.00 (circle), a_w=0.02 (square), a_w=0.05 (diamond) and a_w=0.09 (triangle)

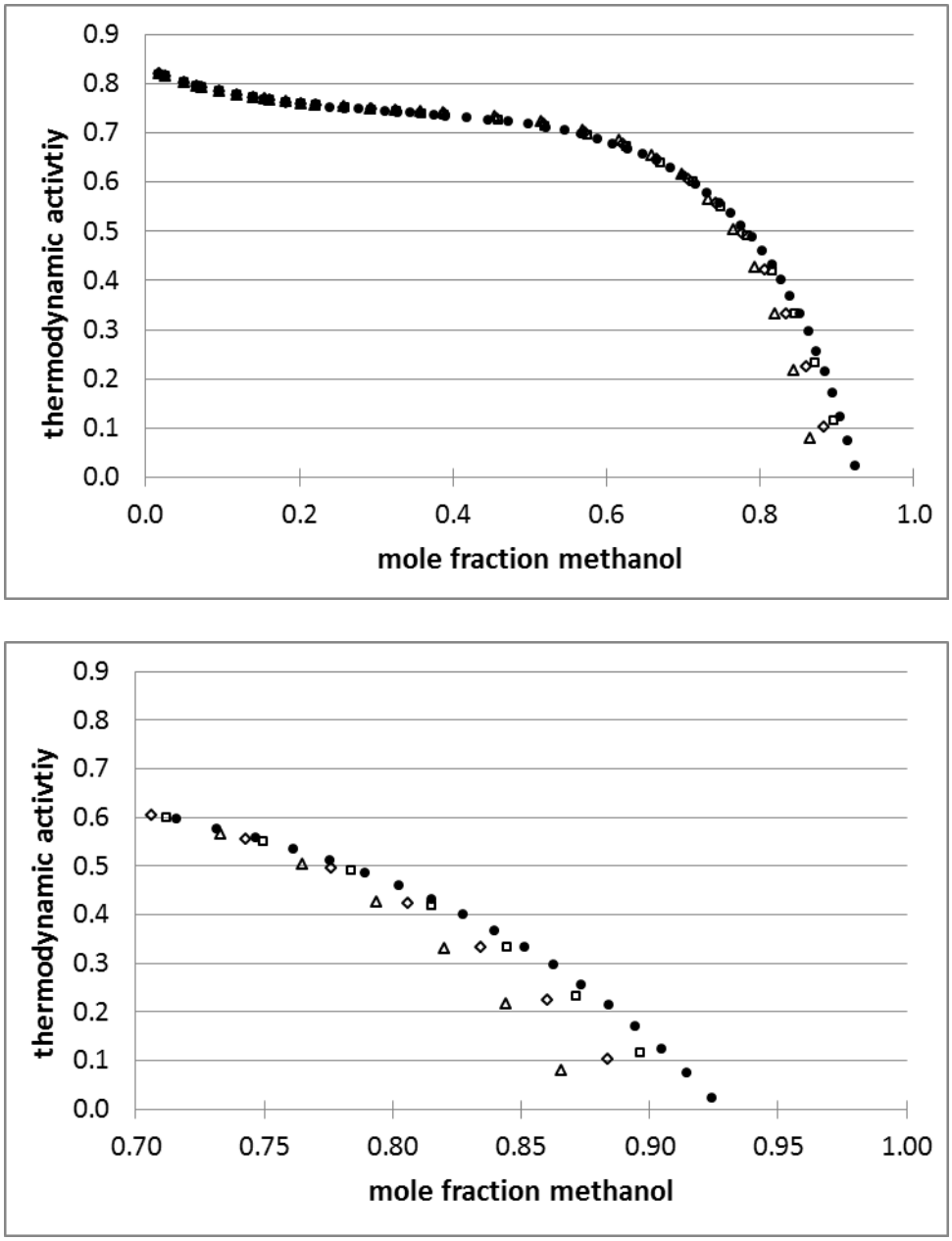

Fig. S6: Thermodynamic activity of toluene in a mixture of methanol, toluene, vinyl-acetate and water with a_w=0.00 (circle), a_w=0.02 (square), a_w=0.05 (diamond) and a_w=0.09 (triangle)

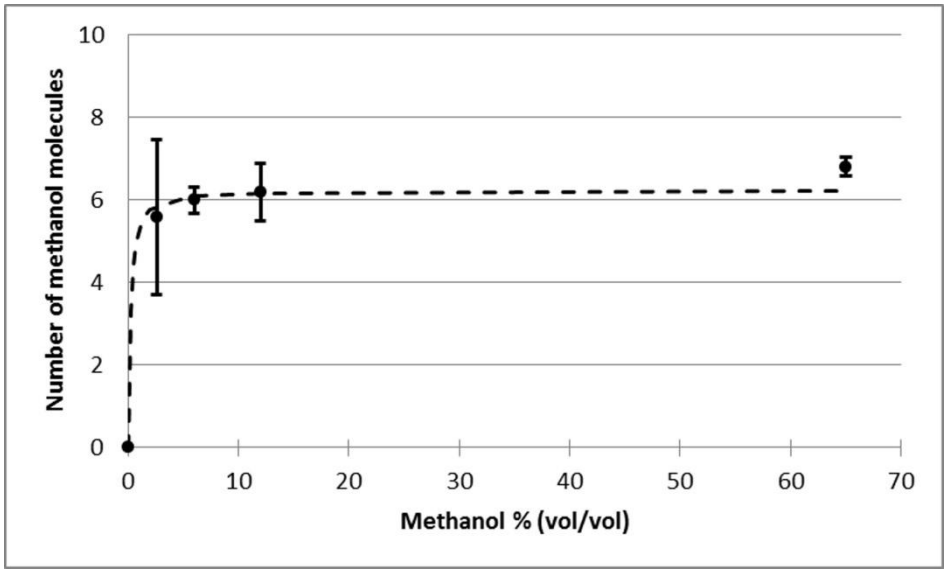

Fig. S7a: Number of methanol molecules in the alcohol binding site (a_w = 0.02)

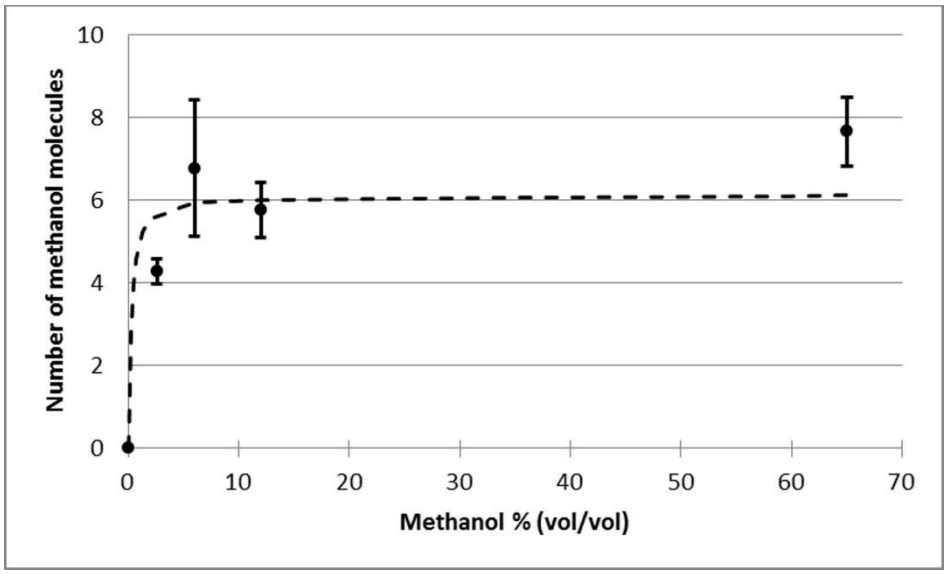

Fig. S7b: Number of methanol molecules in the alcohol binding site (a_w = 0.09)

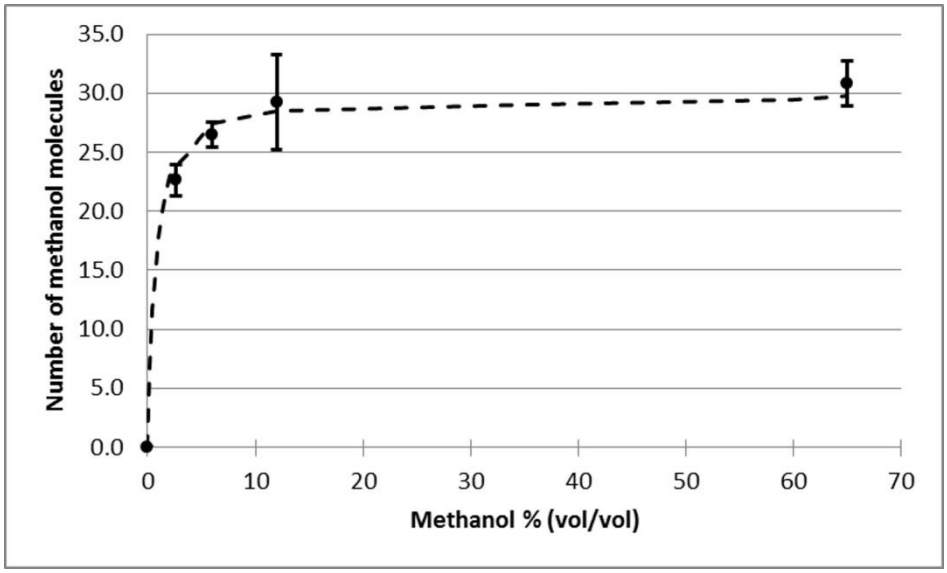

Fig. S8a: Number of methanol molecules in the acetate binding site (a_w = 0.02)

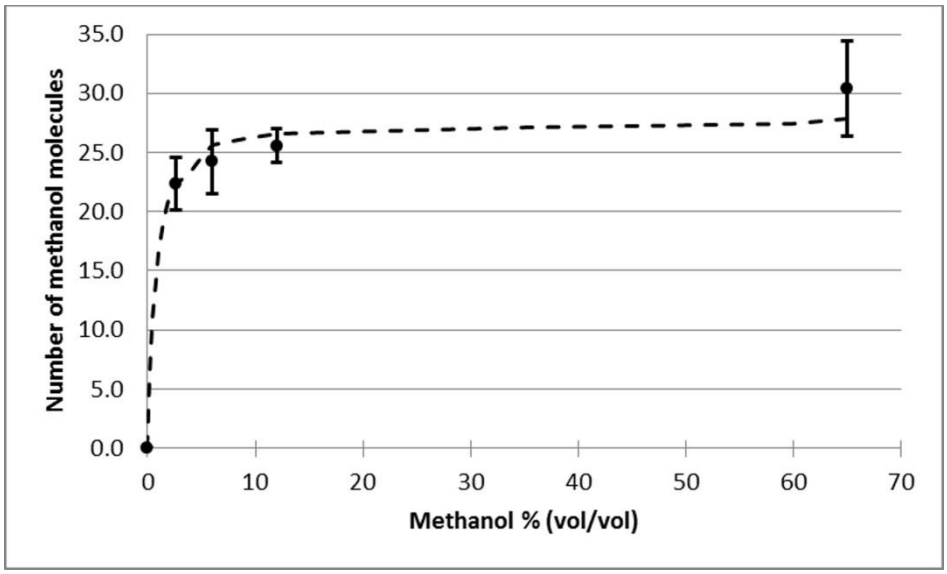

Fig. S8b: Number of methanol molecules in the acetate binding site (a_w = 0.05)

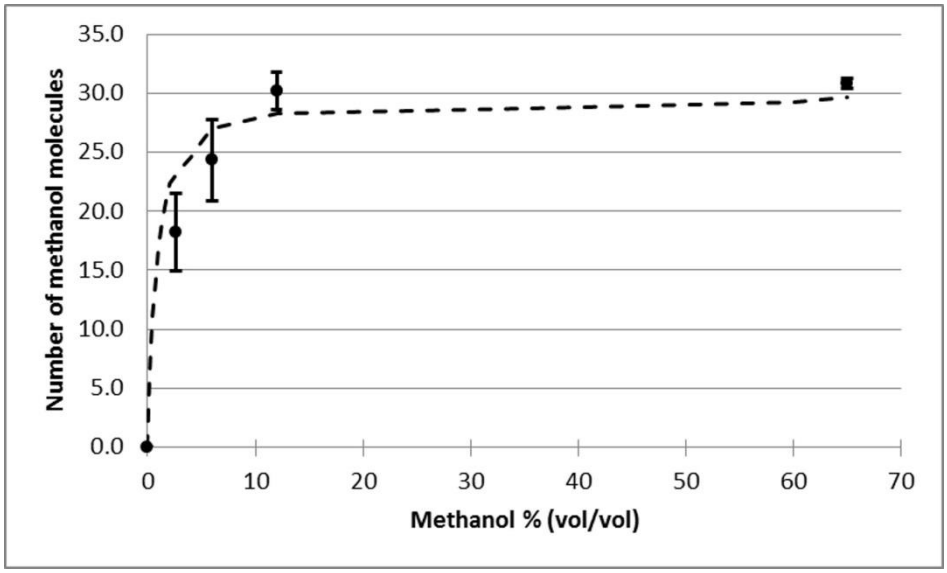

Fig. S8c: Number of methanol molecules in the acetate binding site (a_w = 0.09)

2.2.4 Effects of methanol on CALB structure in presence of toluene (Preliminary results)

For a sake of completeness, we studied the
in Paper III. We used FTIR analysis to study the secondary structure of CALB when exposed to different methanol concentrations. Since toluene showed a strong absorbance in the far-UV region, it was not possible to register "conventional" CD spectra.

Materials

The recombinant non-glycosylated *C. antarctica* lipase B was kindly provided by Kai Lögering and Reiner Luttmann, Hamburg University of Applied Sciences. Toluene and methanol were purchased from Sigma–Aldrich.

Experimental results

FTIR spectra of insoluble CALB were obtained in ATR as described in Paper II. Since CALB is not soluble in toluene/MeOH mixtures, a new approach consisting in collecting the FTIR spectrum of a "protein film" was set up. A 5 mg/ml solution of protein was prepared, centrifuged and the supernatant collected and deposited (3 μl) on ATR plate. After water evaporation, protein formed a film on the ATR plate and 25 μl of an appropriate toluene/MeOH mixture were deposited on the film. Protein spectra were collected at different times upon incubation at room temperature (RT) (**Figure 11**).

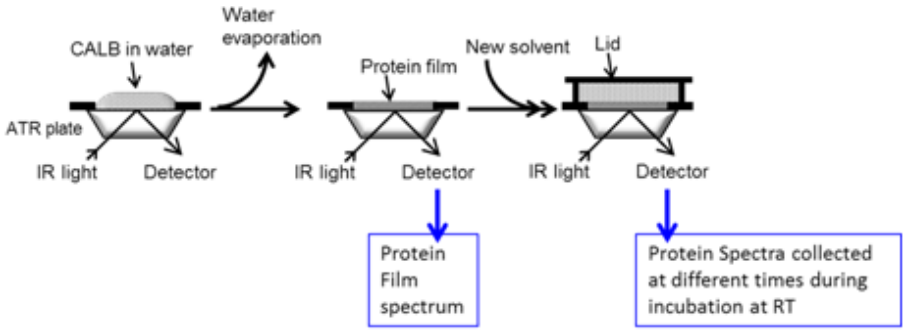

Figure 11. Experimental approach to collect FTIR spectrum of protein film.

The following mixtures were assayed: toluene 100%; toluene and MeOH 0.7%; toluene and MeOH 10%; toluene e MeOH 60%; D_2O; D_2O and MeOH 60%.

Figure 12 and **Figure 13** show the second derivatives of the FTIR spectra, in the amide I absorption region, of CALB film exposed to different mixtures.

The spectrum of protein film shows the following peaks in the amide I region **Figure 12A**: 1633.5 cm^{-1} (β-sheets), 1656.5 cm^{-1} (α-helices and random coil), 1680 cm^{-1} and 1690 cm^{-1} (turns e β-sheets). The protein film in D_2O 100 % has the same characteristics **Figure 13A**. The spectral variations before and after adding D_2O to the protein film can be ascribable to the hydrogen/deuterium exchange.

During the three-hours incubation in toluene 100%, the secondary structure of CALB doesn't change significantly (**Figure 12A**), thus indicating that toluene doesn't induce major conformational changes on the protein structure. The incubation in toluene/MeOH 0.7% causes very limited initial aggregation of the protein: in fact, the native beta peak at 1633.5 cm^{-1} shifts slightly towards lower wavelength values after 3 h incubation (**Figure 12B**).

The mixture toluene/MeOH 10% induces a consistent aggregation of the protein, which is particularly evident after 3-h incubation: two peaks (1695 and 1626 cm^{-1}) diagnostic of intermolecular β-sheet structures appear and the peak 1633.5 cm^{-1} decreases its intensity (**Figure 12C**).

The protein aggregation is more evident in the presence of highest assayed MeOH concentrations, i.e. 60% (**Figure 12D**).

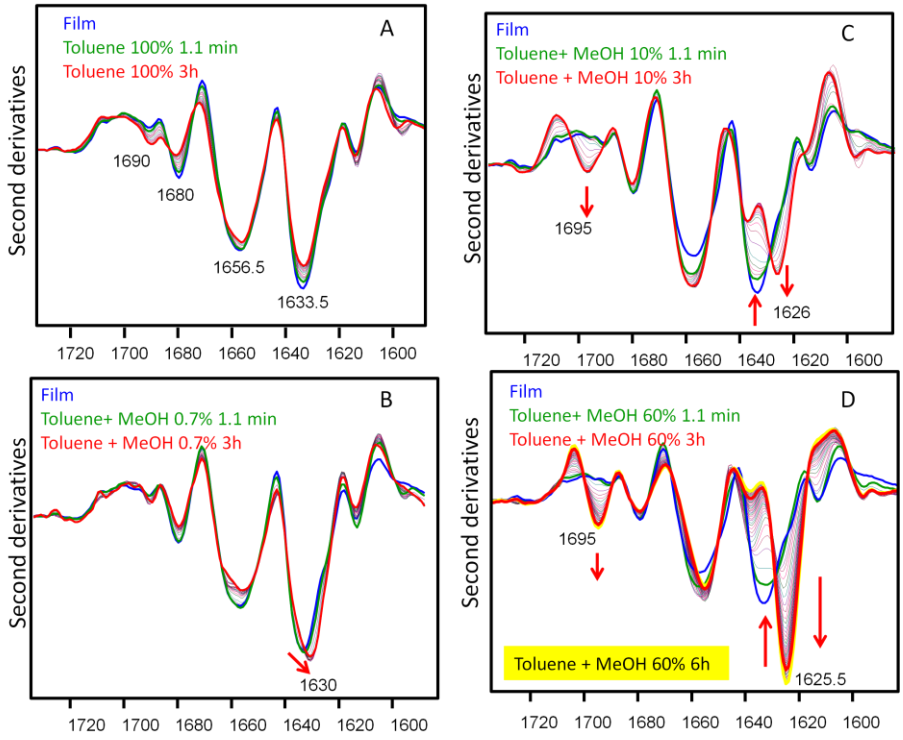

Figure 12. Second derivatives of FTIR spectra, in the amide I region, of the CALB protein film exposed to different toluene/MeOH mixtures.

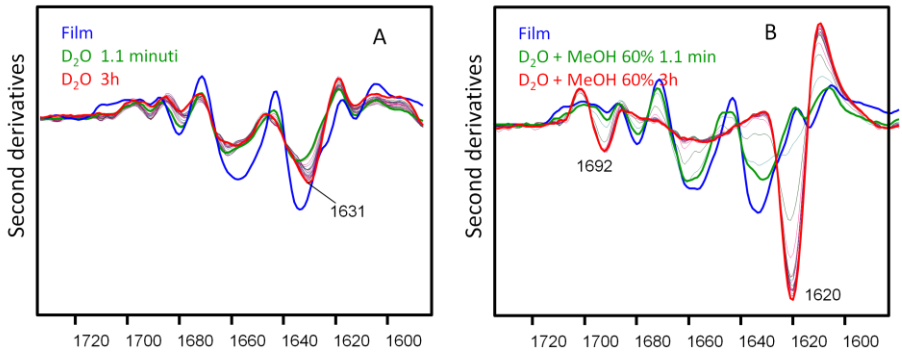

Figure 13. Second derivatives of FTIR spectra, in the amide I region, of the CALB protein film exposed to D_2O and D_2O/MeOH 60% mixture.

In order to exclude the contribution of toluene on the protein aggregation, we also investigated the behavior of CALB in the mixture D_2O/MeOH. Even in D_2O/MeOH 60% the protein suddenly loses its native secondary structures and aggregates (**Figure 13B**).

The FTIR spectra indicate that very low methanol content (i.e. 0.7% v/v) doesn't affect CALB structure while 3-hours exposure at higher methanol percentages (10% v/v or more) induces the protein aggregation.
However, the protein concentration, much higher than that used in the transesterification assay (Paper III), and the state of lipase, as solid film, may contribute to amplify the effect of aggregation induced by methanol.

2.3 Immobilization of BGL on polypropylene membranes treated with oxygen plasma (Preliminary results)

Most enzymes are not stable in organic solvents or suffer a tremendous loss of activity, which often renders processes economically less feasible. To overcome these obstacles, many studies on enzyme immobilization have been performed in the last decades. In contrast to free enzymes, immobilized biocatalysts offer major advantages, such as enhanced long-term stability, ease of recovery, and facilitated application in continuous processes without contamination of the product by the catalyst itself. Different strategies can be applied to immobilize enzymes such as adsorption or deposition onto hydrophobic materials, covalent binding via a spacer molecule or encapsulation of the enzyme. However, any enzyme immobilization does not follow a generally applicable protocol, since they differ in immobilization behavior. Besides the protein properties, another crucial factor for efficient immobilization is the microenvironment of the support, for example, hydrophobicity/ hydrophilicity, surface charge, surface area, and the particle or pore size. Hence, the best combination of support and enzyme properties is decisive for efficient immobilization.

In this part of the work, we studied the immobilization of lipase BGL on polypropylene membrane treated with oxygen plasma. Plasma techniques have frequently been used to provide materials with functional groups on the surface. Low pressure plasma contains many radicals, ions, and metastable species dependent on the type of gas used in the process. Oxygen plasma, for instance, can create reactive groups on the surface, such as peroxides or hydroxides without changing the bulk characteristics of the material. In addition, these reactive groups shift the support properties from hydrophobic to hydrophilic making the material more feasible for enzyme immobilization.

Materials

The lipase from *Burkholderia glumae* 437707 was purchased from CalBioChem (San Diego, CA, USA). Polypropilene membrane not treated (PP) and treated with plasma oxygen (pPP) were kindly provided by Prof. Claudia Riccardi and Dott. Andrea Zanini (Department of Physics, University Milano-Bicocca)

Immobilization procedure and washings

400 μl of a solution of BGL dissolved in deionized water at the desired concentration and a circular disk of polypropylene membrane, with surface area equal to 0.196 cm^2, were shaked in a termomixer at 1400 rpm, at room temperature. The enzyme was absorbed onto the PP membrane thanks to aspecific hydrophobic interactions.
After immobilization, three washings with 2 L deionized water, 30 minutes each, were carried out.

Hydrolysis assay to determine the activity of the PP membrane-immobilized lipase

PP Membrane disks with the absorbed lipase were incubated in 2.5 ml reaction mix containing buffer ammonium acetate 10 mM pH 7.2, triton-X 0.5% v/v and *p*-nitrophenyl laurate 1mM dissolved in isopropanol. The hydrolysis of *p*-nitrophenol was followed by collecting an aliquot of reaction mix every 30 seconds and by spectrophotometrical measures of the absorbance at 410 nm.

Results

The immobilization of BGL on polypropylene membrane, treated and not-treated with plasma oxygen, was valuated indirectly by measuring the enzymatic activity of the membrane. The activity was expressed as enzymatic units (U) per cm^2 of the membrane surface area. Both PP and pPP membranes without enzyme (negative control) had no activity. Moreover, the contribution of the auto-hydrolysis of *p*-nitrophenyl laurate present in the reaction mix was negligible and was not taken into consideration for the determination of the enzymatic activity.

Regarding the PP membrane, we calculated the efficiency of lipase immobilization at three different BGL concentrations, 0.1, 0.5 and 0.025 mg/ml and three different immobilization times, 3, 5 and 24 h. We found that (i) all the enzyme was absorbed to the membrane in the first 3 hours and (ii) higher lipase concentrations gave higher efficiency of immobilization (**Figure 14**).

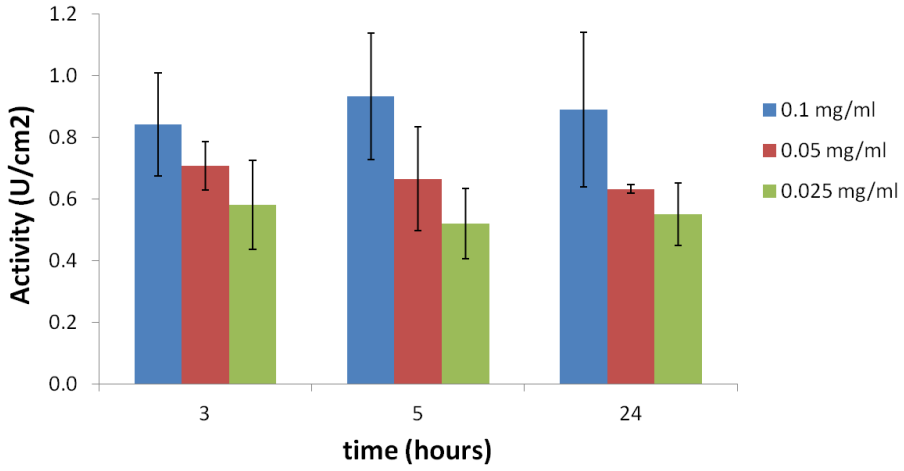

Figure 14. Efficiency of BGL immobilization, expressed as enzymatic activity (U/cm^2) of PP membrane, at three different enzymatic concentrations, 0.1, 0.05 and 0.025 mg/ml and three different immobilization times, 3, 5 and 24 h, Standard deviations refer to three independent experiments.

Finally, the efficiency of immobilization on PP membrane was compared to that on pPP one **Figure 15**. At the enzymatic concentration of 0.1 mg/ml, the pPP membrane exhibited an activity ~5 fold higher than PP. Moreover, even for pPP membrane, the extent of lipase absorbed didn't increase through longer immobilization times.

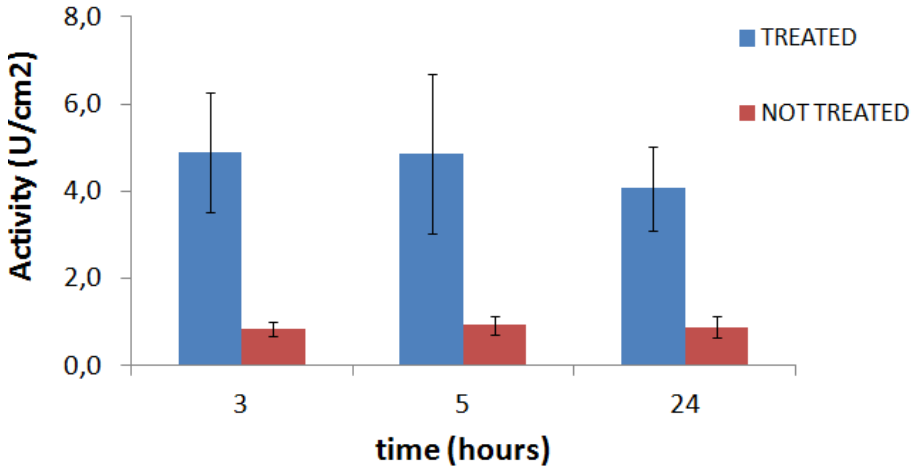

Figure 15. Comparison of BGL immobilization on polypropylene membrane treated and not treated with oxygen plasma, at the enzymatic concentration of 0.1 mg/ml and at three different immobilization times, 3, 5 and 24 hours. Standard deviations refer to three independent experiments.

The results clearly demonstrate that oxygen plasma-modified surfaces more efficiently bind the enzyme, compared to untreated material.
Further experiments should be carried out to verify whether the lipase immobilization on polypropylene membranes can improve the tolerance to the reaction conditions, in particular to the organic solvents like methanol.

References

- Aires-Barros MR *et al*. (1994) Lipases: their structure, biochemistry and application. Cambridge University Press, Cambridge, 243–270.
- Akoh CC *et al*. (2007) Agric Food Chem *55*, 8995–9005.
- Al-Zuhair S (2007) Biofuel Bioprod Biorefin *1*, 57–66.
- Antczak MS *et al*. (2009). Renew Energ *34*, 1185-1194.
- Arzamendi G *et al*. (2006) Chem Eng J *122*, 31–40.
- Barnwal BK and Sharma MP (2005) Renew Sust Energy 9, 363–378.
- Bell G *et al*. (1997) Enzym Microb Technol *20*, 471–477.
- Bornscheuer UT and Kazlauskas RJ (1999) Hydrolases in Organic Synthesis: Regio- and Stereoselective Biotransformations, Second Edition. Chapter 5
- Bozbas K (2008) Renew Sustain Energy Rev *12*, 542–52.
- Chen JW and Wu WT (2003) J Biosci Bioeng *95*, 466–469.
- Chisti Y (2007) Biotechnol Adv *25*, 294–306.
- Chisti Y (2008) Trends Biotechnol 26, 126–31.
- Colombo M *et al*. (2012) Angew Chem Int Ed *51*, 9272–9275.
- Cvengros J and Cvengrosova Z (1999) J Am Oil Chem Soc *71*, 1349–1352.
- Da Cunha ME *et al*. (2009) Fuel Process Technol *90*, 570–575.
- Darnoko D *et al*. (2000) J Liq Chromatogr Relat Technol *23*, 2327–2335.
- De Filippis P *et al*. (1995) J Am Oil Chem Soc *72*, 1399–1404.
- Demirbas A (2007) Energy Convers Manag *48*, 937–941.
- Demirbas A (2008) Energy Convers Manag *49*, 125–130.
- Dizge N *et al*. (2009a) Bioresour Technol *100*, 1983–1991.
- Dizge N *et al*. (2009b) Biochem Eng J *44*, 220–225.
- Dror A *et al*. (2013) Appl Environm Microbiol. Published ahead of print.
- Du W *et al*. (2008) Appl Microbiol Biotechnol *79*, 331–337.
- Freedman B et al. (1984) JAOCS *61*, 1638–1643.

- Freedman B *et al*. (1986) J. Am Oil Chem Soc *63*, 1370–1375.
- Fukuda H *et al*. (2001) J Biosci Bioeng *92*, 405–416.
- Gelbard G *et al*. (1995) J Am Oil Chem Soc *72*, 1239–1241.
- Haag AL (2007) Nature *447*, 520–521.
- Haas MJ *et al*. (2006) Technol *97*, 671–678.
- Halim SFA *et al*. (2009) Bioresour Technol *100*, 710–716.
- Henniges O and Zeddies J (2006) Bioenergy in Europe: experiences and prospects. Washington: International Food Policy Research Institute.
- Holcapek M *et al*. (1999) J Chromatogr *858*, 13–31.
- Iso M *et al*. (2001) J Mol Catal B: Enzym *16*, 53–58.
- Jaeger KE and Eggert T (2002) Curr Opin Biotechnol *13*, 390–397.
- Jegannathan KR *et al*. (2008) Crit Rev Biotechnol *28*, 253–264.
- Kaieda M *et al*. (1999)J Biosci Bioeng *88*, 627–631.
- Kaieda M *et al*. (2001) J Biosci Bioeng *91*, 12–15.
- Knothe G (1999) J Am Oil Chem Soc *76*, 795–800.
- Knothe GJ (2006) Am Oil Chem Soc *83*, 823–833.
- Korbitz W (1999) Renew Energy *16*,1078–1083.
- Korman TP *et al*. (2013) Biotechnol Biofuels 6, 70.
- Kose O *et al*. (2002) Bioresour Technol *83*, 125–129.
- Kumari V *et al*. (2007) Energ Fuel *21*, 368–372.
- Lai CC *et al*. (2005) J Chem Technol Biotechnol *80*, 331–337.
- Lapinskienė A *et al*. (2006) Environ Pollut *142*, 432–437.
- Lara Pizarro AV and Park EY (2003) Process Biochem *38*, 1077–1082.
- Lara PV and Park EY (2004) Enzyme Microb Technol *34*, 270–277.
- Lee JH *et al*. (2010) Appl Biochem Biotechnol *161*, 365–71.
- Lee K-T *et al*. (2002)J Am Oil Chem Soc *79*, 191–195.
- Li L *et al*. (2006) J Mol Catal B: Enzym *43*, 58–62.
- Li X *et al.* (2007) Biotechnol Bioeng *98*, 764–771.
- Linko YY *et al*. (1995) J Am Oil Chem Soc *72*, 1293–1299.
- Lu J *et al*. (2008) Bioresour Technol 99, 6070–6074.
- Lu J *et al*. (2009) J Mol Catal B Enzym *56*, 122–125.

- Lv P *et al*. (2008) Energ Source Part A *30*, 872–9.
- Ma F and Hanna MA (1999) Bioresour Technol *79*, 1-15.
- Marangoni AG (2002) Lipid biotechnology. New York: Marcel Dekker Inc 357–84.
- Marchetti JM *et al*. (2007) Renew Sustain Energy Rev *11*, 300–311.
- Meher LC *et al*. (2006) Renew Sustain Energ Rev *10*, 248–268.
- Miller C *et al*. (1988) J Am Oil Chem Soc *65*, 927–931.
- Min E and Zhang L (2006) Beijing: China petrochemical press.
- Mittelbach M (1990) J Am Oil Chem Soc *67*, 168–170.
- Mittelbach M (1993) Chromatographia *37*, 623–626.
- Monteiro M *et al*. (2008) Talanta *77*, 593–605.
- Nelson LA *et al*. (1996) J Am Oil Chem Soc *73*, 1191–1195.
- Ngo HLN *et al*. (2008) Energ Fuel *22*, 626–634.
- Nie K *et al*. (2006) J Mol Catal B: Enzym *43*, 142–147.
- Noureddini H *et al*. (2005) Bioresour Technol 96, 769-777.
- Park *et al*. (2012) Biotechnol Bioprocess Eng *17*, 722–728.
- Ranganathan SV *et al*. (2008) Bioresour Technol 99, 3975-3981.
- Richard R *et al*. (2011) Bioresour Technol *102*, 6702–6709.
- Röttig A et al. (2010) Appl Microbiol Biotechnol *85*, 1713-1733.
- Royon D *et al*. (2007) Bioresour Technol *98*, 648–653.
- Salis A *et al*. (2005) J Biotechnol *119*, 291–299.
- Shah S and Gupta MN (2007) Process Biochem *42*, 409–414.
- Shah S *et al*. (2004) Energ Fuel *18*, 154–159.
- Shimada Y *et al*. (1999) J Am Oil Chem Soc *76*, 789–793.
- Shimada Y *et al*. (2002) J Mol Catal B: Enzym *17*, 133-142.
- Silva C *et al*. (2007) Ind Eng Chem Res *46*, 5304–9.
- Sim JH *et al*. (2009) Energ Fuel *23*, 4651–4658.
- Sims B (2007) Biodiesel: A global perspective. Biodiesel Magazine http://www.biodieselmagazine.com/article.jsp?article_id=1961
- Soumanou MM and Bornscheuer UT (2003) Enzyme Microb Technol *33*, 97-103.

- Soumanou MM and Bornscheuer UT (2003) Enzyme Microb Technol 33, 97–103.
- Suehara K *et al*. (2005) J Biosci Bioeng *100*, 437–442.
- Talukder MMR *et al*. (2006) Biocatal Biotransform 24, 257–262.
- Tamalampudi S *et al*. (2008) Biochem Eng J 39, 185–189.
- Um B-H and Kim Y-S (2009) J Ind Eng Chem *15*, 1–7.
- US National Biodiesel Board. http://www.biodiesel.org/pdf_files/fuelfactsheets/BDSpec.pdf2008.
- Vasudevan PT and Briggs M (2008) J Ind Microbiol Biotechnol *35*, 421-430.
- Verger (1997) Trends Biotechnol *15*, 32-38.
- Vorhaben T *et al*. (2010) Chem Cat Chem 2, 992-996.
- Watanabe Y *et al*. (1999)J Biosci Bioeng *88*, 622–626.
- Wu Q *et al*. (2007) Ind Eng Chem Res 46, 7955–7960.
- Xie W and Ma N (2009) Energy & Fuels 23, 1347–1353.
- Xu H *et al*. (2006) J Biotechnol *126*, 499–507.
- Xue F *et al*. (2006) Process Biochem *41*, 1699–1702.
- Xue F *et al*. (2008) Bioresour Technol 99, 5923–5927.
- Yamane T (1987) J Am Oil Chem Soc 64, 1657–1662.
- Zagonel GF *et al*. (2004) Talanta 63, 1021–1025.
- Zhang B *et al*. (2012) Appl Microbiol Biotechnol 93, 61-70.
- Zhang TZ *et al*. (2002) J Mol Catal B: Enzym *18*, 315–323.
- Zhang TZ *et al*. (2005) Enzyme Microb Technol 36, 203–209.
- Zhang Y *et al*. (2003) Bioresour Technol 89, 1–16.

Acknowledgements

First of all, I would like to acknowledge prof. Marina Lotti, my tutor, a person who I esteem not only as scientist but also from the "human" point of view: she can be strict, assertive, joking and funny but always in the fullness of time.

A special thank goes to Stefania, my "second" tutor and "life mentor": she always had the patience to help me in the lab, to give me precious advices....and I always had the feeling I could count on her for everything.

Thanks to Lorenzo, Cristian, Mattia, Giorgio, Simone & Simone, Antonino, Carlo, Marco Falc, Roberto Cighetti, Federico, Fede, Chiara, Giusy, Susy, Alessandra: they are much more than simple work-collegues.

Thanks to Prof. Rajni Hatti Kaul and Prof. Juergen Pleiss who gave me the possibility to try the experience of working abroad and all the guys of their "equipe".

Thanks to Prof. Doglia, Prof. Grandori and Dott. Secundo for our profitable collaborations which gave me the possibility to publish three works!!

Thanks to my family and, in particular, to my mother who called me every day during these 1095 days of PhD.....: Mom, I'm fine, don't worry!

Thanks to all the guys of Residence U22; thanks to them I spent the most beautiful years of my life.